

**Mechanisms for the Formation of Rhythmic Topography in the
Nearshore Region**

by

Giovanni Coco

A thesis submitted to the University of Plymouth in partial fulfilment for the degree of

DOCTOR OF PHILOSOPHY

Institute of Marine Studies

Faculty of Science

October 1999

LIBRARY STORE

REFERENCE ONLY

UNIVERSITY OF PLYMOUTH	
Item No.	900 4061319
Date	29 FEB 2000 S
Class No.	T 551.457 COC
Contl: No.	X704072156
LIBRARY SERVICES	

90 0406131 9



Mechanisms for the Formation of Rhythmic Topography in the Nearshore Region

Giovanni Coco

Abstract

The possibility that the periodic features observed in the nearshore region are the result of self-organisational processes is investigated in this work. The behaviour of two numerical models, based on different techniques, has been analysed in order to describe the formation of periodic features in the surf and swash zone respectively. The appearance of periodic patterns in the nearshore region has been traditionally linked to the presence of standing edge waves with the topographic changes passively driven by the flow patterns. A more recent approach indicates the possibility that periodic patterns appear because of feedback processes between beach morphology and flow. In the first model, the coupling between topographic irregularities and wave driven mean water motion in the surf zone is examined. This coupling occurs due to the fact that the topographic perturbations produce excess gradients in the wave radiation stress that cause a steady circulation. To investigate this mechanism, the linearised stability problem in the case of an originally plane sloping beach and normal wave incidence is solved. It is shown that the basic topography can be unstable with respect to two different modes: a giant cusp pattern with shore attached transverse bars that extend across the whole surf zone and a crescentic pattern with alternate shoals and pools at both sides of the breaking line showing a mirroring effect. For the swash zone, the formation of beach cusps has been investigated. The several theories proposed in the past have been analysed and all the field and laboratory measurements available in the literature collected in order to test such theories. It is suggested that, with the available measurements it is not possible to distinguish between the standing edge wave model and the self-organisation approach. A numerical model based on self-organisation has been here developed and tested in order to understand the processes occurring during beach cusp formation and development, to evaluate the sensitivity towards the parameters used and to look at how the model might relate to field observations. Results obtained confirm the validity of the self-organisation approach and its capacity to predict beach cusp spacing with values in fair agreement with the available field measurements and with most of the input parameters primarily affecting the rate of the process rather than the final spacing. However, changes in the random seed and runs for large numbers of swash cycles reveal a dynamical system with significant unpredictable behaviour. A qualitative comparison between the model results and field measurements collected by Masselink et al. (1997) during beach cusp formation and development has also been performed on the basis of a non-linear fractal technique. Results indicate beach locations and time-scales where non-linearities are more important and self-organisation can play a fundamental role.

TABLE OF CONTENTS

Abstract

List of Figures

List of Plates

List of Tables

Acknowledgements

Author's Declaration

1. INTRODUCTION	1
2. MORPHODYNAMIC MODELLING	4
2.1 Introduction	4
2.2 Complex dynamics	5
2.3 Complexity in coastal processes	6
2.4 Stability theory	7
2.4.1 Linear stability analysis	7
2.4.2 Non-linear stability and bifurcation theory	9
2.4.3 On stability models in coastal morphodynamics	10
2.4.4 Stability models applied to coastal morphodynamics: a review	12
2.4.4.1 Ripples	12
2.4.4.2 Cuspate features	14
2.4.4.3 Transverse and welded bars	16
2.4.4.4 Crescentic bars	18
2.5 Self-organisation and cellular automata models	21
2.5.1 Basic theory of cellular automata	21
2.5.2 Self-organisation models applied to morphodynamics: a review	22
2.5.2.1 River dynamics	23
2.5.2.2 Eolian ripples	25
2.6 Comparison between stability theory and self-organisation models	26
3. A STABILITY MODEL FOR THE FORMATION OF RHYTHMIC PATTERNS IN THE SURF ZONE	28
3.1 Introduction	28
3.2 Governing equations and stability analysis	29
3.2.1 Governing equations	29

3.2.2	Basic state	31
3.2.3	Linear stability equation	31
3.2.4	Sediment transport parameterisation	35
3.3	Analysis of the instability mechanism	36
3.3.1	Bottom evolution equation	37
3.3.2	Flow over topography (FOT) problem	38
3.3.3	The instability mechanism in a simple case	40
3.4	Numerical simulation	42
3.5	Discussion	52
4.	BEACH CUSPS: A COMPARISON OF DATA AND THEORIES FOR THEIR FORMATION	56
4.1	Introduction	56
4.2	Field and laboratory observations	57
4.2.1	Beach cusp occurrence and nature	63
4.2.2	The sediment properties of beach cusps	65
4.2.3	Current patterns	67
4.3	Beach cusp formation theories	68
4.3.1	Instabilities in the breaking waves or in the swash	68
4.3.2	Instability of the littoral drift	69
4.3.3	Rip currents	70
4.3.4	Intersecting wave trains	70
4.3.5	Edge wave theory	71
4.3.6	Theories related to swash dynamics	78
4.4	Compatibility between the edge wave and the self-organisational approach	79
4.5	Discussion	82
5.	A SELF-ORGANISATION MODEL FOR THE SWASH ZONE	83
5.1	Introduction	83
5.2	Model description	84
5.2.1	Hydrodynamics	84
5.2.2	Sediment dynamics	85
5.2.2.1	Morphological smoothing	86
5.2.2.2	Angle of repose	87
5.2.3	Boundary conditions	87
5.2.4	Random features of the model	89

5.2.5	Model simulation	89
5.2.6	Physical mechanism	92
5.3	Sensitivity to model parameterisation	92
5.4	Tests of model behaviour	96
5.5	Long-term model behaviour	101
5.6	Results over a non-planar topography	104
5.7	Numerical simulations of edge wave and self-organisation compatibility	108
5.8	Discussion	113
6. COMPARISON BETWEEN MODELS AND FIELD MEASUREMENTS: THE FRACTAL APPROACH		115
6.1	Introduction	115
6.2	Analysis of time series through non-linear techniques	116
6.3	The fractal approach	118
6.4	Data available	121
6.5	Results	125
6.6	Discussion	133
7. CONCLUSIONS AND FUTURE DIRECTIONS		135
REFERENCES		139

LIST OF FIGURES

CHAPTER 2

Figure 2.1 Sketch of morphodynamic instability

CHAPTER 3

Figure 3.1 Sketch of the geometry and co-ordinate system

Figure 3.2 Sketch of the bed-surf instability mechanism in the idealised case on a monotonically increasing α/D_0 function

Figure 3.3 The sum of the squares of the cross-shore velocities for the first seven edge wave modes on a linear slope (arbitrary units)

Figure 3.4 Instability curves for different values of r , $N=0.01$, $\gamma=0.02$, $\alpha(0)=0.1$

Figure 3.5 Instability curves for different values of γ , $r=0.5$, $N=0.01$, $\alpha(0)=0.1$

Figure 3.6 Instability curves for different values of N , $r=0.5$, $\gamma=0.02$, $\alpha(0)=0.1$

Figure 3.7 Contour lines of the topographic perturbation for $k=3.0$, $r=0.5$, $N=0.01$, $\gamma=0.02$, $\alpha(0)=0.1$. For these plots the alongshore direction is on the horizontal axis while the vertical axis indicates the cross-shore direction; darker areas correspond to greater depths

Figure 3.8 Topographic perturbation and relative flow pattern for $k=3.0$, $r=0.5$, $N=0.01$, $\gamma=0.02$, $\alpha(0)=0.1$

Figure 3.9 3d-view of the topographic perturbation (basic slope and perturbation amplitude have been chosen arbitrarily) for $k=3.0$, $r=0.5$, $N=0.01$, $\gamma=0.02$, $\alpha(0)=0.1$

Figure 3.10 Instability curves for different values of $N=0.01$, $r=0.5$, $\gamma=0.02$, $\alpha(0)=0.0$

Figure 3.11 Contour lines of the topographic perturbation for mode $n=2$ and $k=1$ ($r=0.5$, $N=0.01$, $\gamma=0.02$, $\alpha(0)=0.0$)

Figure 3.12 Topographic perturbation and relative flow pattern for mode $n=2$ and $k=1$ ($r=0.5$, $N=0.01$, $\gamma=0.02$, $\alpha(0)=0.0$)

Figure 3.13 3d-view of the topographic perturbation (basic slope and perturbation amplitude have been chosen arbitrarily) for mode $n=2$ and $k=1$ ($r=0.5$, $N=0.01$, $\gamma=0.02$, $\alpha(0)=0.0$)

Figure 3.14 Instability curves for different values of ϵ , $r=0.5$, $N=0.01$, $\gamma=0.02$, $\alpha(0)=0.1$

Figure 3.15 Instability curves for different values of r , $N=0.01$, $\gamma=0.02$, $\alpha(x)=\text{constant}$

Figure 3.16 Instability curves for different values of γ , $r=0.5$, $N=0.01$, $\alpha(x)=\text{constant}$

Figure 3.17 Instability curves for different values of N , $r=0.5$, $\gamma=0.02$, $\alpha(x)=\text{constant}$

Figure 3.18 Contour lines of the topographic perturbation for $k=4.0$ ($r=0.5$, $N=0.01$,

$\gamma=0.02, \alpha(x)=\text{constant}$)

Figure 3.19 Topographic perturbation and relative flow pattern for mode for $k=4.0$ ($r=0.5, N=0.01, \gamma=0.02, \alpha(x)=\text{constant}$)

Figure 3.20 3d-view of the topographic perturbation (basic slope and perturbation amplitude have been chosen arbitrarily) for $k=4.0$ ($r=0.5, N=0.01, \gamma=0.02, \alpha(x)=\text{constant}$)

Figure 3.21 Contour lines of the topographic perturbation for $k=4.0$ ($r=0.5, N=0.01, \gamma=0.02, \alpha(0)=0.3$)

Figure 3.22 Contour lines of the topographic perturbation for $k=4.0$ ($r=0.5, N=0.01, \gamma=0.02, \alpha(0)=0.5$)

Figure 3.23 Contour lines of the topographic perturbation for $k=4.0$ ($r=0.5, N=0.01, \gamma=0.02, \alpha(0)=0.7$)

CHAPTER 4

Figure 4.1 Planar and profile view of a cusped system

Figure 4.2 Variation of measured cusp spacing and mean diameter

Figure 4.3 Swash circulation pattern over a cusped beach

Figure 4.4 Variation of measured cusp spacing and wave height

Figure 4.5 Cross-shore variations in the amplitude of edge waves ($n = 0-3$)

Figure 4.6 3D view of an edge wave of mode $n = 2$

Figure 4.7 Maximum runup and cusp spacing for subharmonic edge waves

Figure 4.8 Maximum runup and cusp spacing for synchronous edge waves

Figure 4.9 Comparison of measured cusp spacing with subharmonic and synchronous mode zero edge wavelength.

Figure 4.10 Breaker type and cusp existence

Figure 4.11 Observed cusp amplitude (η_c) versus cusp steepness ($\lambda \tan\beta$)

Figure 4.12 Variation of measured cusp spacing with swash excursion

CHAPTER 5

Figure 5.1 Different regions of the grid field as related to the boundary conditions

Figure 5.2 Formation and evolution of a cusped beach (see text)

Figure 5.3 Relationship between cusp spacing and swash excursion for numerical simulations

Figure 5.4 Relationship between the number of water particles representing the swash front and the number of cycles required to reach a quasi-equilibrium spacing

Figure 5.5 Variation of the cusp spacing with the sediment flux exponent

- Figure 5.6** Relationship between the “ α ” coefficient (see equation 5.6) and the number of cycles required to reach a quasi-equilibrium spacing
- Figure 5.7** Relationship between the angle of repose and the number of cycles required to reach a quasi-equilibrium spacing
- Figure 5.8** Flow pattern over a cusped beach
- Figure 5.9** Average cross-shore profile at the beginning of the simulation (planar slope) and after 100 cycles (developed cusped morphology)
- Figure 5.10** Variation of the peakedness (Q_p) for different values of the angle of approach. The first 100 cycles were run with $\theta = \pm 2^\circ$
- Figure 5.11** Cusp existence and randomness in swash excursion
- Figure 5.12** Comparison between contour spectra of an alongshore grid-line inside the swash region during cusp formation and development (swash excursion is around 1.8m). The two samples differ only in the random seed used
- Figure 5.13** Variation in the peakedness factor (Q_p) for the runs considered in Figure 5.13.a and 5.13.b
- Figure 5.14** Formation and long-term evolution of a cusped beach
- Figure 5.15** Cross-shore profile of an initially barred topography (a) and beach cusp formation after 200 cycles (b)
- Figure 5.16** Formation of beach cusps on a topography initially characterised by the presence of a bump (a). Figure (b) shows the topography developed after 200 cycles
- Figure 5.17** Self-organisation process over an initially cusped shoreline
- Figure 5.18** Formation and evolution of a cusped beach under sub-harmonic standing edge wave forcing
- Figure 5.19** Formation and evolution of a cusped beach under synchronous standing edge wave forcing
- Figure 5.20** Formation and evolution of a cusped beach under sub-harmonic standing edge wave forcing
- Figure 5.21** Formation and evolution of a cusped beach under synchronous standing edge wave forcing (see text)
- Figure 5.22** Development of a cusped beach over a pre-existing topography
- Figure 5.23** Development of a cusped beach over a pre-existing topography
- Figure 5.24** Variation in the peakedness under different hydrodynamic inputs

CHAPTER 6

- Figure 6.1** Cusp evolution during the field experiment (T=1 indicates the initial topography while T=145 corresponds to the last survey)
- Figure 6.2** Actual and cumulative beach levels at the top of the swash zone (location 4-7)
- Figure 6.3** Actual and cumulative beach levels at the centre of the swash zone (location 10-3)
- Figure 6.4** Actual and cumulative beach levels at the bottom of the swash zone (location 14-5)
- Figure 6.5** Actual and cumulative bed elevations for a model simulation (bottom of the swash zone)
- Figure 6.6** Actual and cumulative bed elevations for a model simulation (inside the swash zone)
- Figure 6.7** Growth of variance at the top of the swash zone (Location 4-7)
- Figure 6.8** Growth of variance at the centre of the swash zone (Location 10-3)
- Figure 6.9** Growth of variance at the bottom of the swash zone (Location 14-5)
- Figure 6.10** Growth of range at the top of the swash zone (Location 4-7)
- Figure 6.11** Growth of range at the centre of the swash zone (Location 10-3)
- Figure 6.12** Growth of range at the bottom of the swash zone (Location 14-5)
- Figure 6.13** Local Hurst exponent at the top of the swash zone (Location 4-7)
- Figure 6.14** Local Hurst exponent at the centre of the swash zone (Location 10-3)
- Figure 6.15** Local Hurst exponent at the bottom of the swash zone (Location 14-5)
- Figure 6.16** Growth of variance for a model simulation (bottom of the swash zone)
- Figure 6.17** Growth of variance for a model simulation (inside the swash zone)
- Figure 6.18** Growth of range for a model simulation (bottom of the swash zone)
- Figure 6.19** Growth of range for a model simulation (inside the swash zone)
- Figure 6.20** Local Hurst exponent for model simulation (bottom of the swash zone)
- Figure 6.21** Local Hurst exponent for model simulation (inside the swash zone)

LIST OF PLATES

CHAPTER 2

- Plate 2.1** Ripple field on Teignmouth, U.K. (courtesy of Andy Saulter, Plumouth University, U.K.)
- Plate 2.2** Beach cusps system (courtesy of Tony Bowen, Dalhousie University, Canada)
- Plate 2.3** Giant cusps at Cape Hatteras, North Carolina, U.S.A. (taken from Dolan, 1971)
- Plate 2.4** Transverse bars on Trabucador Beach on the Ebro Delta, Spain (courtesy of the “Laboratorio de Investigacion Maritima”, Barcelona, Spain)
- Plate 2.5** Welded bars on Cape Cod, Massachusettes, U.S.A. (taken from Komar, 1998)
- Plate 2.6** Crescentic bar system at Duck, North Carolina, U.S.A. (taken from Lippmann and Holman, 1990)
- Plate 2.7** Multiple crescentic bar system (courtesy of Tony Bowen, Dalhousie University, Canada)
- Plate 2.8** Meandering river.
- Plate 2.9** Braided river in Alaska (courtesy of Jim Apriletti, University of California, U.S.A.)
- Plate 2.10** Eolian ripple field

CHAPTER 4

- Plate 4.1** Beach cusps (courtesy of Tony Bowen, Dalhousie University, Canada)
- Plate 4.2** Beach cusps (courtesy of Tony Bowen, Dalhousie University, Canada)
- Plate 4.3** Sediment sorting on a cusped beach (taken from Darbyshire, 1977).

CHAPTER 5

- Plate 5.1** Cusp formation with a non-uniform spacing (courtesy of Gerd Masselink, Loughborough University, U.K.)

LIST OF TABLES

CHAPTER 4

Table I Summary of parameters for field data

Table II Summary of parameters for laboratory data

CHAPTER 6

Table III Value of the Hurst exponent for field data using the growth of variance method (offshore direction goes from top to bottom of the table)

Table IV Value of the Hurst exponent for field data using the growth of range method (offshore direction goes from top to bottom of the table)

ACKNOWLEDGEMENTS

The author would like to thank his two supervisors, **Prof. David Huntley** and **Dr. Tim O'Hare** for their help and assistance in the past 3 years. In particular, my gratitude and admiration goes to **David** for his continuous support, encouragement, patience and passion for research.

I couldn't find in the dictionary any word to describe how indebted I am to **Dr. Andy Saulter**. His help is in every page of this thesis and in every day of the past 3 years (not to mention, he also bought my first pint of Guinness ...)

Moltes gràcies al **Dr. Albert Falqués** per iniciar-me en el món dels problemes d'anàlisi d'estabilitat i per convidar-me a colaborar a la UPC compartint els seus coneixements i el model MORFO13. Una abraçada al **Dr. Daniel Calvete**, a la **I(Y)olanda** (la "chica" catalana), a la **Cesca**, a l'**Amador** i al **Dr. Miquel Caballeria** per fer de la meua visita a Barcelona una agradable experiència.

Thanks to **Dr. Gerd Masselink** and **Dr. Chari Pattiaratchi** for letting me use the field measurements shown in Chapter 6.

Il capitolo sui "fractals" deve molto all'aiuto e ai consigli di **Dr. Howard Southgate** a alle lunghe "non-linear dinners" con **Ken Kingston** (thanks also for reading some of the chapters' drafts) Bedankt voor alle references und discussies over "self-organisation" to the IMS adopted **Dr. Gerben Ruessink**. Merci à **Dr. Philippe Gleizon** pour tous les précieux conseils sur le Fortran.

Thanks to **Darren Stevens** because I'm a pain and he's been very patient sorting out some of the figures and the never ending computer problems.

Grazie infine al **Dr. Enrico Foti** senza l'aiuto del quale non avrei trovato la strada per Plymouth.

Completing a PhD is a complicated thing and certainly involves more than sitting in front of the computer. For this reason I feel I want to thank a number of people who have been close in the last three years and that have certainly contributed to this work even without knowing what a "beach cusp" is ...

A huge hug to "little" **Andy** and "my neighbour" **Sophie** because they have been and they are true friends.

Grazie a **Barbara, Giuseppe, Enrico e Salvatore** che ci si vede poco ma si e' vicini assai.

Merci à **Sandrine** et **Sophie** qui ont été vachement sympas et qui m'ont cuisiné des plats hyperbons. Je tiens particulièrement à remercier **Sandrine** (bisous!) pour son soutien quotidien, notamment lors de mes mauvais jours.

Rispetto per **Claudia, Antonio e Marcello** (omo e coco) che le loro visite non si possono dimenticare ...

Muito obrigado a **Elisa e Gilberto** (nos encontramos novamente na Bahia ou na Sicilia?), **Ana** (a melhor guia turística no Rio), **Eleine** ("my flatmate") e **Fernanda** (por organizar a minha visita a Wood-Hole).

Big thanks to **Malcolm** (always there for advice), **Mr P.** (always there for a pint), **Manuela** (always there for an Italian chat), **Mark W.** (such a help when I started!), **Suzanne** (always there for coffee, chats, salsa ...) and to all the other suspicious characters who have been (drinking) part of the "Coffee Club".

Ai miei genitori

AUTHOR'S DECLARATION

At no time during the registration for the degree of Doctor of Philosophy has the author been registered for any other University award.

This study was financed with the aid of studentships from Fondazione Bonino-Pulejo (Messina, Italy), Opera Universitaria (Catania, Italy) and University of Plymouth (U.K.).

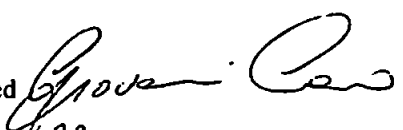
A programme of advanced study was undertaken, which included attendance at one Advanced Study Course, one Short Course and a one month sabbatical to the Universitat Politècnica de Catalunya, Barcelona, Spain, as a visitor researcher. IMS seminars and three conferences detailed below were attended.

Courses attended: Hydro- and morphodynamic processes in coastal seas, Renesse, The Netherlands, 28/6-11/7/1998 (EC/MAST Advanced Study Course).
Mechanics of coastal sediment-transport processes (Madsen, O.S.), Coastal Sediments '99, Long Island, U.S.A., June 1999.

Conferences attended: Coastal Dynamics '97, Plymouth, U.K.
UK Oceanography '98, Southampton, U.K.
Euromech 395, Twente, The Netherlands
Coastal Sediments '99, Long Island, U.S.A.

Oral presentations: Coco, G., Huntley, D.A., and O'Hare, T.J., 1998. "A possible mechanism for the formation of rhythmic patterns". Renesse, The Netherlands.
Coco, G., Huntley, D.A., and O'Hare, T.J., 1998. Sensitivity analysis of a model for beach cusp formation. UK Oceanography '98, Southampton (presentation was nominated for best talk).
Coco, G., Huntley, D.A., and O'Hare, T.J., 1998. "The mystery of beach cusp formation". As visiting researcher Department de Fisica Aplicada, UPC, Barcelona, Spain.
Huntley, D.A., and Coco, G., 1999. "Beach cusps: self-organisation or response to hydrodynamics?", Euromech 395, Twente, The Netherlands.
Coco, G., Huntley, D.A., and O'Hare, T.J., 1999. "Beach cusp formation: analysis of a self-organisation model". Coastal Sediments '99, Long Island, USA.
Coco, G., and Huntley, D.A., 1999. "Evidence for fractal behaviour in nearshore processes", NICOP meeting, Long Island, U.S.A.
Coco, G., Huntley, D.A., and O'Hare, T.J., 1999. "The mystery of beach cusp formation". As guest speaker to Department of Applied Ocean Physics and Engineering, Woods Hole Oceanographic Institution, USA.

Publications: Coco, G., Huntley, D.A., and O'Hare, T.J., 1999. "Beach cusp formation: analysis of a self-organisation model". Proceedings of Coastal Sediments '99, Long Island, USA: 2190-2205.
Coco, G., O'Hare, T.J., and Huntley, D.A., 1999. "Beach cusps: a comparison of data and theories for their formation". Journal of Coastal Research, vol. 15 (3): 741-749.
Falqués, A., Coco, G., and Huntley, D.A., 1999. "A mechanism for the generation of wave driven rhythmic patterns in the surf zone" (submitted for publication on the Journal of Geophysical Research).

Signed 
Date 28-01-2000

Chapter 1: Introduction

Although in the last decades our understanding of the physical processes governing the nearshore region has consistently improved, finding an answer to the question “why are beaches different?” is still a difficult task. Furthermore, if the question is changed to “will beaches be different in ... years?”, an even less confident answer can be given. Our knowledge of hydrodynamics and sediment transport is still not conclusive. Improvements in the quality of the field and laboratory measurements made in the last 20 years are considerable but usually require “further” developments. The number of physical processes that should be included in a “perfect” numerical simulation of beach evolution are far beyond any computer capacity and, probably, some physical processes are still unknown. In this scenario, studying the formation and development of simple, regular features appearing in the nearshore region is undoubtedly a very useful tool. It is in fact possible to argue that, understanding how periodicity is possible in systems that exhibit a variety of longshore and offshore shapes at different length scales, would improve our knowledge of nearshore processes.

Interest has always been shown in the formation and development of the variety of three-dimensional morphological features appearing on the inner part of the nearshore region (beach cusps), stretching from the shoreline offshore across the surf zone (giant cusps, transverse and welded bars) or entirely confined around the breaking area (crescentic bars). A broad number of theories have been formulated in order to explain the reason(s) for morphological changes resulting in features characterised by a distinct longshore periodicity. Until recently some of these theories were widely accepted (Bowen and Inman, 1971; Guza and Inman, 1975; Holman and Bowen, 1982) and it was generally agreed that longshore patterns in the incident wave field generated these morphologic features. Sediment response, and so the changes in the morphology, were considered to be only a reflection of the hydrodynamic forcing conditions. Such approach will be here indicated using the term *forced behaviour*. However, in open contradiction with the *forced behaviour* approach, it has been recently suggested that periodic features can be the result of the coupled interaction between sediment and flow. As result of such interaction, a preferred wavelength may emerge and characterise the shape of the shoreline or, more generally, of the nearshore region. This new approach, will be here indicated as *free behaviour* or *self-organisation*.

The possibility that nearshore patterns appear because of the interaction between sediment and flow has already successfully been investigated by different authors through different modelling techniques, such as *stability analysis* and *cellular automata*. The use of *stability analysis* has initially been applied to river morphodynamics (see for example Fredsøe, 1974; Parker, 1976; Richards, 1980) and has already achieved significant results for explaining the formation of bedforms appearing at various time and length scales (Blondeaux, 1990; Hulscher, 1993; Falqués et al., 1996). Numerical algorithms based on *cellular automata* have been successfully implemented in more recent years (see for example Werner and Fink, 1993; Murray and Paola, 1994; Landry and Werner, 1994) and provide a strong indication of the importance of self-organisation in morphodynamics.

The object of this thesis is to investigate the role of self-organisation in coastal morphodynamics. Two different approaches, stability analysis and cellular automata, will be applied in order to model the formation of periodic patterns in the nearshore region and to give evidence of the fundamental importance of the flow-sediment interaction for the appearance of such features. Emphasis will be given to the parameterisation of the two approaches, to the agreement with field observations and, for the self-organisation model developed throughout this study, to the complex behaviour observed in the simulations. The implication of considering coastal morphodynamics as *complex* systems will be further extended to the use of non-linear techniques for the analysis and comparison of field measurements and model results.

The structure of the thesis is organised as follows: in Chapter 2 two different approaches for analysing the formation of rhythmic features will be described and a review of the existing applications in morphodynamics will be made. This chapter will identify the potential benefit resulting from the application of such approaches in developing our knowledge in morphodynamics. Chapter 3 will describe the application of a linear stability analysis to the surf zone in order to describe the formation of patterns such as crescentic bars and giant cusps. The influence that sediment transport parameterisation might play in the formation of such features will also be examined. Chapter 4 contains an introduction to the “mystery” of beach cusp formation. The existing theories and data will be compared in order to prove whether such features are the result of standing edge wave “forcing” or if they appear because of “free” self-organisation processes. The last approach will be then investigated in detail by developing a numerical code whose sensitivity and behaviour will be documented in Chapter 5. Chapter 6 will then investigate the possibility of comparing model results and field measurements through a non-linear technique for the analysis of

time series. Conclusions will be presented in Chapter 7 together with some suggestions for improving the numerical models herein presented and the field measurements necessary for a better understanding of nearshore processes.

Chapter 2: Morphodynamic modelling

2.1 Introduction

The nearshore zone often shows regular morphological patterns at length scales well above the length scale of incident wind or swell waves. Beach cusps (Russell and McIntire, 1966), giant cusps (Komar, 1971), shore-attached oblique/transverse bar systems (Niederoda and Tanner, 1970; Hunter et al., 1979; Lippmann and Holman, 1990), crescentic bars (Bowen and Inman, 1971) and ridge and runnel systems (Mulrennan, 1992) are well known examples of such features. These patterns are certainly intriguing and are of scientific interest in themselves. But more importantly, their regularity gives an indication that the large scale complex dynamics of the nearshore zone as a whole may be understood in terms of simple physical mechanisms. At present, the understanding of coastal morphodynamics is a difficult task and idealised situations have to be hypothesised in order to predict the effects of wave motion on shore evolution. Equilibrium solutions are found for the governing equations but they are not able to explain certain phenomena, indicated in the literature as “free behaviour”, such as longshore regular patterns in shoreline morphology. More generally the term “free behaviour” indicates the possibility of periodic features appearing without a similar pattern being present in the external forcing of the system. Conversely, the term “forced behaviour” describes those cases in which variations in the system reflect the driving external forcing. An example of free and forced behaviour can be given by considering a river “free” to meander (meanders are not the result of an external forcing or of a structure inside the flow) with the opposite case being a river “forced” by human, external, intervention to flow inside river banks. As an extension, the term “forced” will be here used for situations in nearshore morphodynamics where the flow field governs shoreline processes with the sediment simply responding to it, but not interacting with it.

Through stability analysis, free behaviour in hydrodynamic wave motion has been initially considered (Bowen, 1969; Guza and Davis, 1974; Guza and Bowen, 1975) whilst, probably because of the uncertainties in the sediment transport parameterisation, only more recent studies have been focused on topographic changes. In fact, the problem of alongshore rhythmic patterns in coastal morphology may be explained by temporal or spatial modulations in the external forcing, but rhythmic patterns are observed also in the absence of such variations. Thus, mechanisms related to free instabilities of the basic steady equilibrium in the coupled system sediment-flow have also been considered.

Generally, free behaviour may be purely hydrodynamic, but it may also involve a combination, or better an interaction, between, flow and bottom perturbations (usually indicated as morphodynamics). It is also conceivable that the generation of a rhythmic topography is a phenomenon due to coupled morphodynamic and hydrodynamic instabilities (Vittori et al., 1999).

In order to investigate the possibility of free behaviour in nature, and for the present study in coastal morphodynamics, two different approaches have been considered. The first refers to the stability analysis theory, the second to the implementation of cellular automata algorithms capable of simulating chaotic behaviour and the possibility of patterns' appearance (such technique will be herein indicated also with the more general term "self-organisation").

This chapter will introduce the concepts of coastal evolution and complex dynamics. The stability (instability) approach and the conditions that may give rise to equilibrium solutions that are periodic in time and/or space will be then described. A concise review of results obtained through the stability theory in order to describe the appearance of patterns in coastal morphology will also be included. Modelling through cellular automata will also be described as well as its already existing applications in morphodynamics. A comparison between the two techniques will be finally considered.

2.2 Complex dynamics

In recent years a growing interest has been shown towards the hypothesis of coastal evolution as a strongly non-linear system so that concepts and techniques deriving from complex dynamics have been applied to coastal modelling. The word "complex" here indicates a system characterised by multiple non-linear interactions between multiple components. The evolution of a complex system will obviously be dependent on the number of interactions and components but also on the initial state and on the eventual perturbations occurring during the evolution. It is then obvious that feedback processes will play a major role in the evolution of such non-linear dynamical systems. As a result, the system can evolve through different paths and not necessarily reach a steady equilibrium (Cowell and Thom, 1995). If the word equilibrium is used to indicate a stable state, the possibility of periodic, in both time and/or space domain, and even chaotic forms of equilibrium have to be considered. The presence of non-linearities also implies that under certain steady forcing conditions the response cannot be related to the single inputs

individually. Phillips (1992) points out the interesting difference between stochastic and deterministic complexity and the possibility of applying such concepts to geomorphology. The term stochastic indicates the possibility that complexity arises from the cumulative effect of individual process-response mechanisms. Such mechanisms could be too numerous to be accounted for individually and could operate over a range of time and space scales such that they still affect each other. On the other hand, there is also the possibility that complexity arises from the non-linear dynamics of relatively simple systems of equations. This last concept, deterministic complexity, will be the underlying hypothesis when, in later chapters, a model for simulating the swash dynamics and the appearance of patterns will be presented.

2.3 Complexity in coastal processes

More than twenty years ago Wright and Thom (1977), while reviewing different approaches for morphological studies, indicated the changes from a “descriptive” approach into an “empirical” one characterised by the use of statistical analysis for explaining morphologic variations. The authors also pointed out the contributions due to sedimentological studies and the developments in hydrodynamics which allowed a better understanding of the coastal processes. The authors finally stated that the new frontier was “morphodynamics”. This approach differs from the previous ones because coastal processes are considered in relation to the interaction flow-topography and because of the importance of non-linearities in landforms’ formation. In the last twenty years the role of feedback mechanisms has been firmly established and the importance of studying coastal evolution as a non-linear dynamical system is widely accepted (Werner, 1999). That coastal morphodynamics display features that are typical of a non-linear dissipative system has already been shown by different authors (Wright and Thom, 1977; De Vriend, 1991; Cowell and Thom, 1994; Southgate and Beltran, 1996) and such features will be here only briefly recalled. The presence and significance of non-linearities needs to be investigated under two different approaches. The first relates to the non-linear relationship between hydrodynamics and sediment response usually resulting in the parameterisation of sediment transport fluxes with some power of the flow velocity (Fredsoe and Deigaard, 1992; Van Rijn, 1993). The second relates to the fact that even subsystems can have a non-linear nature. For example, hydrodynamics of shallow waters have a non-linear nature, can also interact at different frequencies, and lead to the growth of resonant motions (Guza and Davies, 1974; Bowen and Guza, 1978; Bowen and Holman, 1989). It is obvious that the effect of both kinds of non-linear processes can have a subsequent relevant effect on

sediment transport and coastal evolution. Besides, the dissipative nature of coastal morphodynamics is probably the most obvious of the features and can be easily detected by considering the continuous input of energy in the system (waves, tides) and the following dissipation (bed friction, wave breaking, work done on sediment transport). The final point leading to the conclusion that coastal morphodynamics can be studied as a complex system is related to feedback effects. Such an effect can be relevant at all the time-scales involved in the process. For example, a flow over a mobile bottom will cause fluxes of sediment and changes in the bed level that will then affect the flow. The same process can happen at different time-scales and for example, a swash or a tidal cycle will cause changes in the topography and such changes will affect the successive swash or tidal cycle. Summarising, the feedback loop, characteristic of coastal evolution, involves a continuous (in time) interaction between hydro and morphodynamics in such a way that the fluid dynamics is constantly affected and altered by topographic changes and vice-versa. The factor coupling the two systems is obviously the sediment transport which, as a confirmation of the non-linearity of the process, is modelled and usually measured to be proportional to a high-power of the fluid velocity. It is also possible to distinguish between positive and negative feedback. The first mechanism is the one responsible for enhancing and amplifying the eventually present instability and it starts and confers the properties of the self-organisation process. Negative feedback is instead the mechanism that prevents the system from moving away from an equilibrium state by damping the growth of what could be considered as “minor” perturbations (Cowell and Thom, 1995; Werner and Fink, 1993).

2.4 Stability theory

2.4.1 Linear stability analysis

The first experiments as well as the formulation of the stability problem were proposed in the nineteenth century and were dealing with the hydrodynamic stability of a flow in a container (Rayleigh, 1892; Reynolds, 1883). Hydrodynamic stability has been recognised as one of the central problems of fluid mechanics and already in 1959, Landau and Lifshitz argued that:

“The flows that occur in Nature must not only obey the equations of fluid dynamics, but also be stable”

In order to give a brief account of the fundamental concepts of stability a very simple idealised case concerning only hydrodynamics will be now considered. The analysis will

be then extended to morphodynamics by considering the typical momentum and continuity depth averaged equations and by including sediment transport (Chapter 3).

In order to analyse the stability of a laminar flow, it is important to specify the flow at each point x (x indicates a generic 3D vector) and time t . This basically means defining the velocity $U(x, t)$, pressure $P(x, t)$ and temperature $T(x, t)$. These fields define the so-called basic flow or basic state. The fields may be steady or unsteady, and should satisfy the appropriate equations of motion and boundary conditions. We obviously suppose that both the equations and the solutions are completely known.

If the basic flow is disturbed slightly, the disturbance may either die away, persist as a disturbance of similar magnitude or grow so much that the basic flow becomes a different laminar or a turbulent flow. Such disturbances can be called respectively stable, neutrally stable and unstable. These definitions can be formalised mathematically so that a basic flow is stable if, for any $\epsilon > 0$, there is some positive number δ (depending upon ϵ) such that if the norm:

$$\|u(x,0) - U(x,0)\|, \|p(x,0) - P(x,0)\|, \text{etc.} < \delta$$

then

$$\|u(x,t) - U(x,t)\|, \|p(x,t) - P(x,t)\|, \text{etc.} < \epsilon \quad \text{for all } t \geq 0$$

where u is the velocity field and p is the pressure field which satisfy the equations of motion and the boundary conditions. This definition means that the flow is stable if the perturbation is small for all time provided it is small initially. It also possible to define an asymptotically stable basic flow if moreover:

$$\|u(x,t) - U(x,t)\|, \|p(x,t) - P(x,t)\|, \text{etc.} \rightarrow 0 \quad \text{as } t \rightarrow +\infty$$

It is now assumed that the basic flow is steady and that the equations of motion and the boundary conditions may be linearised for sufficiently small perturbations. Thereby a linear homogeneous system of partial differential equations and boundary conditions is obtained. These have coefficients that may vary in space but not time because the basic flow is steady. The solution of such system can be expressed as the real parts of integrals of components, each component varying with time like $e^{\sigma t}$ for some complex number $\sigma = \sigma_R + i \sigma_I$. The linear system will determine the values of σ and the spatial variation of corresponding components as eigenvalues and eigenfunctions. Such eigenvalue problem can be solved by using the classical approach given by the method of the normal modes. Through a Fourier analysis, the small perturbations are represented as superimposition of linear modes that can be treated separately because each satisfies the linear system. This

allows for the transformation of the eigenvalue problem into a system of ordinary differential equations and boundary conditions. Such a system can then be solved analytically or numerically. The success of the technique depends on finding a complete set of normal modes to represent the development of an arbitrary initial disturbance.

If $\sigma_R > 0$ for a mode, then the corresponding disturbance will be amplified, growing exponentially with time until it is so large that non-linearity becomes significant. If $\sigma_R = 0$ the mode is neutrally stable, and linearly stable if $\sigma_R < 0$. Another definition, marginal stability, is also given for modes which are characterised by $\sigma_R = 0$ for critical values of the parameters on which σ_R depends but $\sigma_R > 0$ for some neighbouring values of the parameters. The values of the parameters resulting in marginal stability are usually considered as a criterion of stability (although marginal and neutral stabilities are different) and provide the curve of stability or curve of growth rate. The presence of a maximum in such a curve will be an indication of the fast growing mode and the associated wavelength is usually comparable with the observations. More generally, the linear analysis provides information related to the possibility of an instability of the basic equilibrium and to the physical mechanism responsible for its growth. Spacing, shape, orientation and time growth of the features refer only to the initial growth of the single mode analysed and so provide just an indication of the possible behaviour.

2.4.2 Non-linear stability and bifurcation theory

Conclusions obtained through linear theory are obviously restricted to the case of infinitesimal (zero amplitude) perturbations. A question arises in terms of how an infinitesimal perturbation, linearly unstable, evolves in a non-linear regime. For this reason results obtained through the linear stability theory need to be extended to the non-linear case usually resulting in the formulation of a finite amplitude equation that allows for more realistic comparisons with field measurements. Such an approach needs particular attention from a mathematical point of view and the analysis is further complicated by processes like the non-linear self-interaction of the dominant mode as well as the exchange of energy between different modes. On the other hand, results are of great interest and could be of great help in order to identify final stable configurations and eventual de-tuning of the instability (Guza and Bowen, 1976; Vittori and Blondeaux, 1990; Calvete, 1999).

Closely related to the problem of non-linear stability is bifurcation theory. Such theory studies the qualitative changes of the equilibrium solutions of non-linear systems as a

parameter varies. In practice this means that solutions are sought in the neighbourhood of critical conditions of linear theory. In fact, non-linear dynamical systems often exhibit discontinuities in their evolution and such discontinuities may represent the transition from one equilibrium to another or even from equilibrium to chaos. A non-linear analysis is usually performed in order to understand whether the discontinuity tends towards equilibrium or not.

In order to summarise the differences with the linear analysis, it has to be underlined that the non-linear approach is capable of providing information on the amplitude of the features arising from the instability, their shape and spacing and, in the case of bedforms, the flow pattern over the features. All these results can be compared with field measurements. Indications on the long-term evolution and the possibility of bifurcations are also explored.

2.4.3 On stability techniques in morphodynamics

By analogy with the historical experiments of flow in a container, in the morphodynamic case the perturbations we are interested in will be those related to the “container” (the beach slope) rather than the flow. The time scale at which the flow perturbations evolve is usually much smaller than the “container” perturbations, which are associated with erosion-deposition processes, so that the two systems can be decoupled. Flow perturbations will affect the mean flow field and are essentially secondary flows associated with the perturbations of the “container” shape. It is also important to underline that a complete description of the dynamics of sediment transport is still unknown to the point of limiting our understanding of the morphodynamic processes. A schematic summary of the concept of stability as applied to morphodynamics is given in Figure 2.1 where a small random perturbation is superimposed over a flat bed. Such a perturbation can be considered as the superimposition of a series of normal modes and, through linear analysis, each mode can be analysed. As a result, secondary flows will be generated and sediment moved in such a way that the mode considered could be damped (stability) or grow (instability). The patterns with the largest growth rate are then compared with field observations.

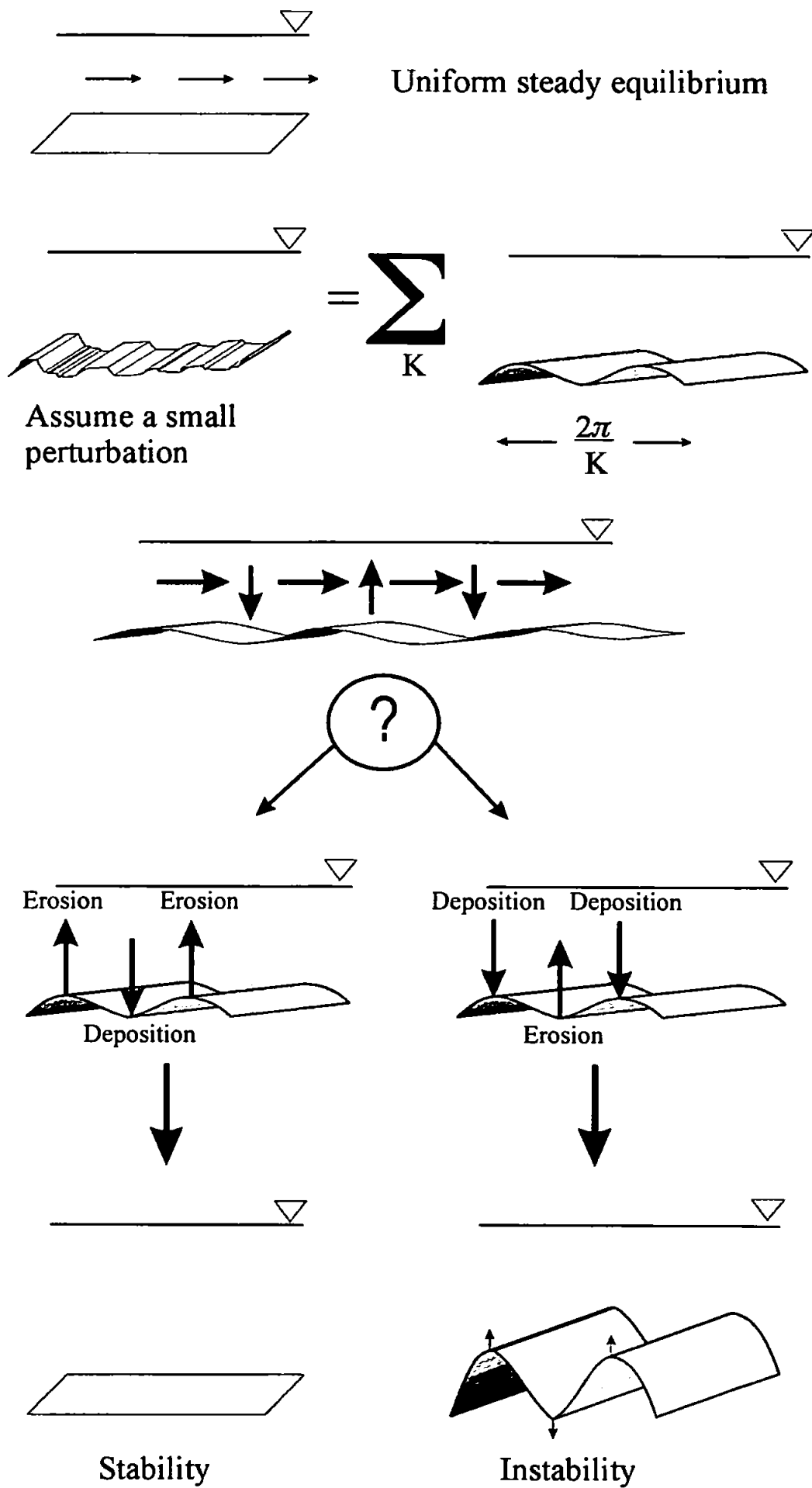


Figure 2.1 Sketch of morphodynamic instability

2.4.4 Application of stability theory to coastal morphodynamics: a review

The understanding of rhythmic features' presence in the nearshore region is obviously related to the debate on free and forced behaviour. In fact their presence has been sometimes related to the presence of low frequency waves, in particular infragravity edge waves. This is an example of a forced response. However, another possibility is that these patterns can be the result of morphodynamic instabilities of the alongshore uniform equilibrium, an example of free or self-organised behaviour of the nearshore dynamical system (Southgate and Beltran, 1998). Of course, it is plausible that in many circumstances both kinds of behaviour will interact on natural beaches.

Since the earlier suggestions by Sonu (1969) and the work of Barcelon and Lau (1973) and Hino (1975) little attention has been paid to nearshore morphodynamic instabilities. In the nineties, an increasing interest in this approach has developed, and those early investigations have been now revisited and extended by Christensen et al. (1995), Deigaard et al. (1999), Falqués (1991), Falqués et al. (1996) and (1997).

This section will deal with a review of applications of the instability theory to coastal morphodynamics with a focus on those features appearing in the nearshore region. As the main interest is directed towards the nearshore region, features like sand ridges, tidal sand banks and sand waves, typical of a further off-shore region, will not be here discussed although many authors (Trowbridge, 1995; Calvete, 1999; Huthnance, 1982a; Huthnance, 1982b; Hulscher, et al., 1993; Hulscher, 1996) have successfully proposed an instability approach for their formation.

2.4.4.1 Ripples

These features are probably the most commonly observed in nature (Plate 2.1). Because of their implication and influence on bed roughness and sediment transport (see for example Sleath, 1984; Fredsøe and Deigaard, 1992) they have been the object of several detailed studies. Different cases have to be considered depending on whether this kind of "bed waves" are current-generated or whether they are the result of an oscillatory flow (wave-generated). In the first case, the formation mechanism was initially proposed by Richards (1980) through a two-dimensional stability analysis for a unidirectional flow of low Froude number over an erodible bed. Richards' (1980) results suggest that ripples are formed by an unstable mode of the bed responding to some disturbance of the initially planar slope.



Plate 2.1 Ripple field at Teignmouth, U.K. (courtesy of Dr. Andy Saulter, University of Plymouth, U.K.)

The suggestion that the mechanism triggering the instability could be given by “bursts” of high shear stress is also made. Results depend on bed roughness (which basically means sediment size) and on the effect of the local bed slope on sediment transport. It is worth noticing that the sediment transport formulation proposed by Richard (1980) neglects suspended load and still results in features in close agreement with the observations. In agreement with field observations is also the result that, if the flow velocity exceeds some limit value, ripples are “washed out”.

The case of wave-generated ripples has been fully investigated by Blondeaux (1990) for the linear case and by Vittori and Blondeaux (1990) for the non-linear, finite amplitude, development. The theory developed by Blondeaux (1990) requires a knowledge of the difference between rolling-grain ripples and vortex ripples. The former, the first to appear on an initially plane bed, are characterised by the absence of flow separation behind the crests while vortex ripples develop as a consequence of an increase in the amplitude of velocity oscillations and of the subsequent flow separation. Results indicate the instability process as the cause of ripple formation and, in agreement with field observations, suggest again that larger grain sizes produce ripples with a wider spacing. An understanding of the physical mechanism is also provided by the destabilising effect given by secondary flows carrying sediment from the incipient troughs to the crests. The effect of gravity on the sediment particles provides the stabilising effect. The further development of the bedforms

and the transition from rolling-grain ripples to vortex ripples is given by the non-linear analysis. Vittori and Blondeaux (1990) consider the results obtained by Blondeaux (1990) and investigate the development of the most unstable bottom perturbation for parameters close to the critical ones. As a result, the geometrical shape of finite amplitude ripples can be determined although results are confined to the rolling-grain ripples as in the vortex case non-linearities are too strong. The evolution from the rolling-grain into the vortex type of ripple or the decay of the perturbation is again considered to be dependent on the value of the Froude number.

2.4.4.2 Cuspate features

As indicated by Inman and Guza (1982), according to the processes, it is possible to distinguish between two types of cusps: swash cusps and surf cusps. Swash cusps, usually known as beach cusps, are the ones formed by direct action of runup and rundown on the beach face (Plate 2.2). For this kind of feature, at the moment, the only stability approach capable of explaining their formation is purely hydrodynamic and refers to standing edge wave forcing (Guza and Davies, 1974; Guza and Inman, 1975). A detailed analysis of beach cusps (including existing theories and available measurements) will be presented in chapter 4 and 5. For the so-called surf cusps or giant cusps (Plate 2.3), the mechanism involved with their formation is related to the development of circulation cells inside the surf zone and usually associated with the presence of rip currents. As a result, these features would extend well inside the surf zone and be characterised by a wavelength of the order of several times the width of the surf zone (Komar, 1971).

The first attempt to simulate the formation of giant cusps and the related rip currents has been provided by Hino (1975). His work considers the shallow water equations, combined with a simplistic sediment transport formula (linearly proportional to the velocity) and predicts the formation of patterns periodic in the longshore direction (defined by the author as a "cuspidal coast"). The approach is linear and the hydrodynamic instability is caused by perturbations in the radiation stress that modify the circulation pattern. Simulations, run for both normal incident waves and in the presence of a longshore current, show that the fastest growing mode is characterised by a wavelength around 4 times the width of the surf zone. Such a value, indicating a spacing increasing with the incident wave energy, compares well with field observations of rip currents under moderately dissipative conditions (McKenzie, 1958; Sasaki et al. 1976).



Plate 2.2 Beach cusps (courtesy of Tony Bowen, Dalhousie University, Canada)



Plate 2.3 Giant cusps at Cape Hatteras, North Carolina, U.S.A. (taken from Dolan, 1971)

An instability mechanism resulting in the formation of giant cusps will be presented in detail in chapter 3.

2.4.4.3 Transverse and welded bars

The presence of nearshore features that run obliquely to the shoreline is quite common especially on sandy beaches in low-to-moderate wave energy conditions. Transverse bars (Plate 2.4) are usually associated with the presence of a longshore current, tend to be parallel one to the other, can be stable or migrate and their inclination can be either dowcurrent or upcurrent. Similar properties characterise welded bars (Plate 2.5) although these features have a slightly different shape with a nearly normal attachment to the shoreline.

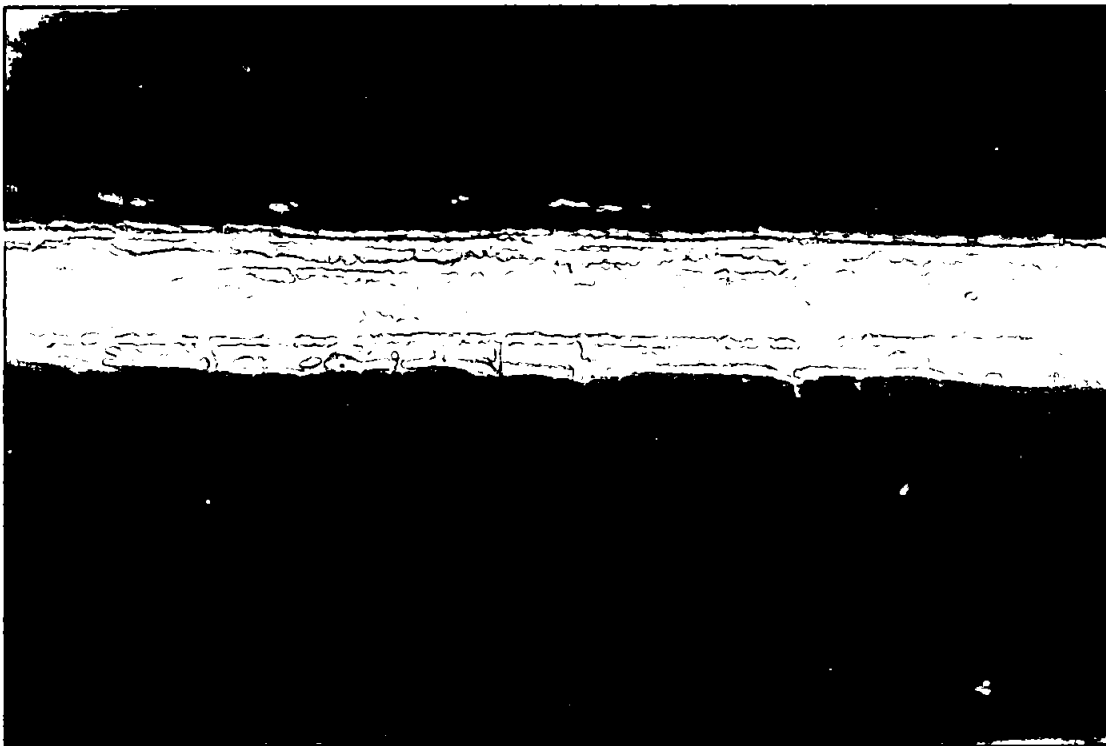


Plate 2.4 Transverse bars on Trabucador Beach on the Ebro Delta, Spain (courtesy of the 'Laboratorio de Investigacion Maritima', Barcelona, Spain)

Several authors have investigated the formation of transverse/welded bars using an instability approach. The first suggestion that they could be the result of a perturbation in the longshore current was made by Sonu (1969). Hino's results (1975) in the case of a longshore current were considerably improved by Christensen et al. (1995) by considering a sediment transport formulation which included suspended sediment transport as well as the presence of irregular waves. As a result the wavelength of the features is predicted to be around 6 times the width of the surf zone with the bar orientation being upcurrent with



Plate 2.5 Welded bars on Cape Cod, Massachusetts, U.S.A. (taken from Komar, 1998)

respect to the longshore current profile. Results showed a strong sensitivity to sediment transport parameterisation and for example instability arises only if the sediment transport rate is proportional to the depth averaged velocity with a power higher than 1.

A model for the formation of transverse bars based on a stability analysis has also been proposed by Barcilon and Lau (1973) for the case of low energy beaches although Falqués (1991) found that parameters used in the simulation of the basic flow were unrealistic.

The above mentioned research was extended by Falqués et al. (1996) by introducing a longshore current with a cross-shore gradient, bottom friction and a parameterisation of the sediment transport which also included a threshold value. The model considers a dominant influence of the longshore current. In fact it deals only with an instability of the longshore

current and does not include the effect that a perturbation of the bottom might have on the wave field through the radiation stress. The parameter controlling the growth of the perturbation seems to be the bed friction and several modes, sometimes resulting in very complicated patterns, are found. The predicted wavelength of the bedforms is in agreement with the observations although the downcurrent orientation obtained for realistic values of the parameters is not able to explain all the variation observed in the field. It is important to underline that all the previously described models are linear and so capable of describing only the very initial stage of the features' formation. On the other hand, field observations mainly report final equilibrium situations where a flow pattern providing positive feedback, and so increasing the instability, is counteracted by an opposite mechanism (negative feedback) which prevents a further growth of the feature and ensures equilibrium. Further developments of the model, especially concerning the parameterisation of sediment transport, have been considered and resulted in favourable comparisons with field observations (Falqués et al., 1999).

Just before concluding this section, it is important to notice that a distinctly different explanation has been provided for the formation of transverse bars (Holman and Bowen, 1982). The mechanism suggested by Holman and Bowen (1982) refers to a purely hydrodynamic forcing due to the interaction between two edge waves of different mode and to the resulting drift velocity pattern. Such resulting steady flow, coupled with a sediment transport model can modify the topography. Equilibrium configurations between steady flow and sediment transport have been evaluated and result in patterns very similar to the welded bars one. The study is then extended to the interaction between three edge waves and a much more irregular pattern is obtained. It is evident that only additional field observations can provide an understanding on which of the two approaches here presented is responsible for transverse bar formation.

2.4.4.4 Crescentic bars

Moving further off-shore it is frequently possible to encounter other features positioned around the breaking area and characterised by a periodic spacing in the alongshore direction and a shoreward concavity (see Plate 2.6). This submerged feature is very common and sometimes even multiple crescentic bar systems have been observed (see Plate 2.7). The origin of these features was first investigated by Bowen and Inman (1971) and, until recent years, their explanation was widely accepted. Their approach falls into the category of hydrodynamic "forced" behaviour and the features are the result of the velocity



Plate 2.6 Crescentic bars system at Duck, North Carolina, U.S.A. (taken from Lippmann and Holman, 1990)

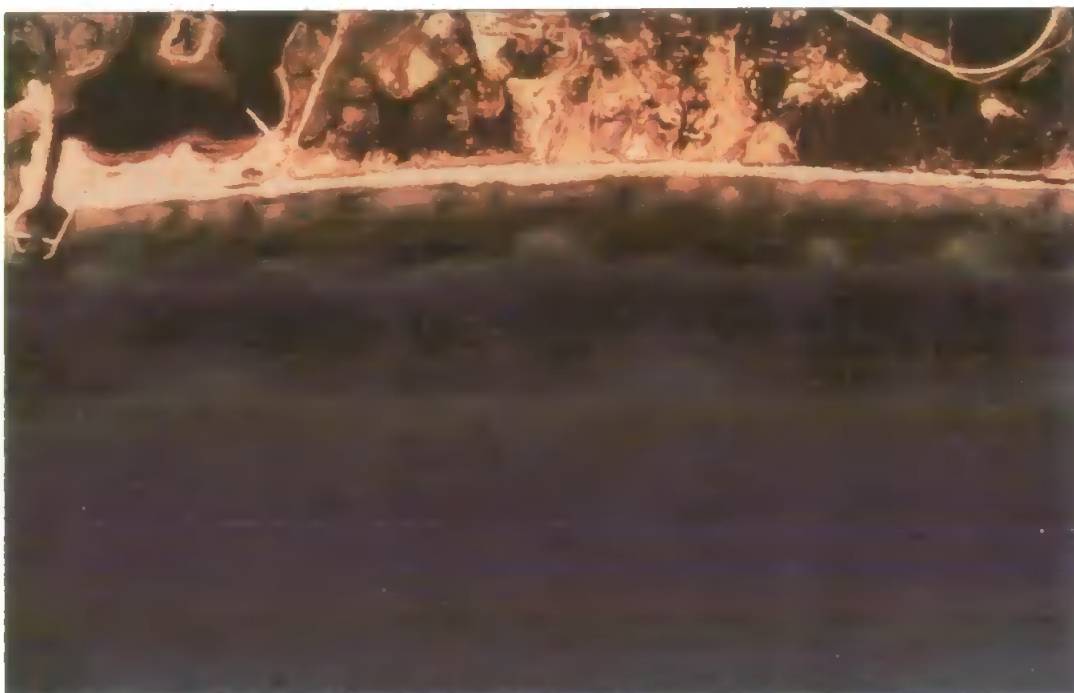


Plate 2.7 Multiple crescentic bar system (courtesy of Tony Bowen, Dalhousie University, Canada)

field associated with standing edge waves. Improvements of such a model (Holman and Bowen, 1982), laboratory experiments (Bowen and Inman, 1971) and comparisons with field observations (Huntley, 1980) provide support for this approach. On the other hand, the formation of crescentic bars on open beaches where the presence of standing edge waves is unlikely to happen, the strong dependence of standing edge waves on incident wave frequency, wave angle of approach and pre-existing topography (edge waves could also simply be the response to the developed topography, see Huntley, 1980) are all arguments against the proposed mechanism.

More recently, approaches based on stability theory have been proposed. Deigaard et al. (1999) suggested that crescentic features could be the development of instabilities of a long straight barred coast. Their instability analysis deals with a perturbation superimposed on the bar crest and is carried out for both normally and obliquely incident wave field although most of the simulations deal with an oblique approach and the resulting longshore current. The linear stability problem is solved through a numerical model that allows for wave refraction and irregular wave heights (following a Rayleigh distribution). The mechanism for the growth of the instability is related to the wave-driven circulation current with an onshore (offshore) flow where the perturbation is positive (negative). Sediment transport in the surf zone is simulated in such a way that deposition (erosion) occurs for onshore (offshore) flow leading to the amplification of the initial perturbation. The effect of the longshore current is to change the current circulation and to propagate the instability in the alongshore direction providing an additional effect to the growth/decay previously described.

Another stability analysis has been recently proposed (Vittori et al., 1999) and is again related to the formation of crescentic patterns in the nearshore zone. This approach is rather different from all the previous ones as it deals with the formation of rhythmic patterns outside the surf zone so that the effect of breaking is neglected throughout the analysis. The instability process involves the excitation of synchronous edge waves and their interaction with the incoming waves causes steady currents and results in the growth of the bottom perturbation. The reference beach cross-shore profile is also different from the previous cases analysed with an offshore region of constant slope and a very rapid increase of the slope in the proximity of the shoreline. Results indicate the possibility, and coexistence, of two maxima in the growth rate curve. The two maxima are characterised by different longshore wavelengths (one of the order of tens meters, the other of hundreds of

meters) with shape and spacing of the patterns well comparing with field observations (Allen, 1984) reporting crescentic bar systems similar to those shown in Plate 2.7.

In chapter 3, a stability analysis resulting in the formation of patterns resembling crescentic forms will be described.

2.5 Self-organisation and cellular automata models

The term “self-organisation” is used in order to indicate the mechanism driving systems where non-linear dynamics and feedback processes are dominant. The basic idea of self-organisation relates to the possibility that a perturbation of the equilibrium in the system can be amplified (positive feedback) and that the system could evolve towards a new form of equilibrium (controlled by negative feedback processes). Such an equilibrium, as previously stated, does not need to be necessarily steady but could also be periodic or chaotic. Cowell and Thom (1995) show how self-organisation can occur at different time scales (instantaneous, event and geological) but always be the product of feedback processes. Forbes et al. (1995) consider the self-organisation approach in order to describe large-scale (in time and space) morphological evolution of a system where similar and close (and so subject to the same forcing conditions) subsystems experience different behaviours. Catastrophic events are detected in the single subsystems and usually follow periods of slow evolution. Such events seem to depend more on the previous subsystem states rather than on the forcing conditions. The importance of thresholds, as related to various natural processes and their implications for the analysis of field data, will be discussed in later chapters within the wider framework of self-organised criticality.

As previously underlined, the term “self-organisation” is also considered, in a wider sense, as synonymous with free behaviour and it does not indicate a mechanism theoretically different from the one described through the stability analysis (differences will be outlined in the next paragraph). On the other hand, the term self-organisation has been widely associated with a particular technique, cellular automata, commonly used for describing complex systems and also with such meaning it will be here considered.

2.5.1 Basic theory of cellular automata

In order to simulate complexity, numerous models based on the cellular automata technique have been developed. Cellular automata are simple mathematical systems

constructed from identical components and capable of resulting in complex behaviour. Usually, cellular automata are discrete systems but, potentially, they can also be used for the simulation of continuum systems. Recent works (Wolfram, 1986; Frisch et al., 1986) have in fact showed that through this approach even the Navier-Stokes equations could be simulated successfully.

The more general rule for building a cellular automata model sees a variable at a specified location, say z_i , being updated at discrete time steps according to a deterministic rule which also involves the value of z at neighbour sites. In one dimension this would mean:

$$z_i^{(t+1)} = f(z_{i-r}^{(t)}, z_{i-r+1}^{(t)}, \dots, z_i^{(t)}, \dots, z_{i+r-1}^{(t)}, z_{i+r}^{(t)})$$

with r indicating the neighbour location. In the case of small r , the system could result in complex behaviour and exhibit self-similar patterns. Although the evolution of such systems is highly dependent on the initial state, if the set of rules is unchanged, results should be similar in the overall statistical properties and pattern shape. If the basic rules are changed, the system can produce very different patterns.

One of the most typical features of cellular automata is that, although starting from different configurations, the overall evolution of the system can result in a special "organised" configuration. As a final summary of cellular automata models, it is possible to indicate the following basic characteristics:

- a) discrete in space: the model domain consists of a discrete grid of cells or sites
- b) discrete in time: time is updated as a sequence of discrete values
- c) synchronous: all the sites are simultaneously updated
- d) deterministic: each site behaviour is governed by the same set of rules (which depends on the values of the neighbour sites at the previous time step)

2.5.2 Self-organisation models applied to morphodynamics: a review

The self-organisation approach has already been applied to analyse numerous patterns in chemistry, physics, environmental and social sciences in general (for a review see for example Hastings and Sugihara, 1993; Bak, 1997; Science, 1999) but only recently started to appear a useful tool to explain the appearance of morphological features (for an early review see, for example, Hallet, 1990). The most successful applications of self-organisation in geomorphology are given by models capable of describing, through simple and well-accepted physics, phenomena like braided or meandering rivers (Murray and Paola, 1994; Stølum, 1996), eolian ripples (Anderson, 1990; Nishimori and Ouchi, 1993;

Landry and Werner, 1994), eolian dunes (Werner, 1995), beach cusps (Werner and Fink, 1993), stone stripes (Werner and Hallet, 1995). All of these models are basically trying to reduce the many processes operating over the system to those essential dynamics able to explain the pattern formation. In most of the cases the algorithm, instead of integrating the Eulerian equations of motion and continuity, approximates the system and considers the behaviour of single grains or single water particles. The motion of such particles is generally described through very simple physics. The modelling of such small scale system(s) results in a larger system exhibiting a self-organised pattern on a much bigger scale. Because of the simplifications, such models are not capable of reproducing detailed field observations but they are able to indicate which kind of pattern can emerge and its variability.

The use of this technique for the simulation of coastal morphodynamics is at its very beginning and, at the moment, the only model available concerns beach cusp formation (Werner and Fink, 1993). Such a model will be described in detail in later chapters when dealing with the formation of beach cusps and when a similar model will be presented. In the next sections the potential of this technique will be considered by briefly reviewing two interesting different systems showing natural patterns and complex behaviour.

2.5.2.1 River dynamics

The two most typical features possibly characterising the path of a river are undoubtedly the continuous sequence of smooth curves defined as meandering (Plate 2.8) or the breaking of the flow into a series of interconnected channels, usually defined as “braiding” (Plate 2.9). Both features have been investigated through the use of cellular automata models. Stølum (1996) studied the possibility that river meandering can be described in terms of chaotic behaviour and self-organisation criticality. Feedback seems in fact to be the controlling factor with lateral migration increasing the sinuosity (positive feedback) and cutoffs stabilising the system (negative feedback). The interesting feature of the system is that the effect of cutoffs is “context-dependent”. This means that in a highly “disorganised” state, cutoffs help to stabilise the system but, if the system is in a “quasi-ordered” state, cutoffs cause a perturbation in the system bigger than the stabilising effect. As a result, the system tends towards a dynamical state of self-organised criticality (Bak, 1997). Fluctuations from such state are possible and likely to happen in the form of events clustered in time and space (in the literature defined as “avalanches”).



Plate 2.8 Meandering river

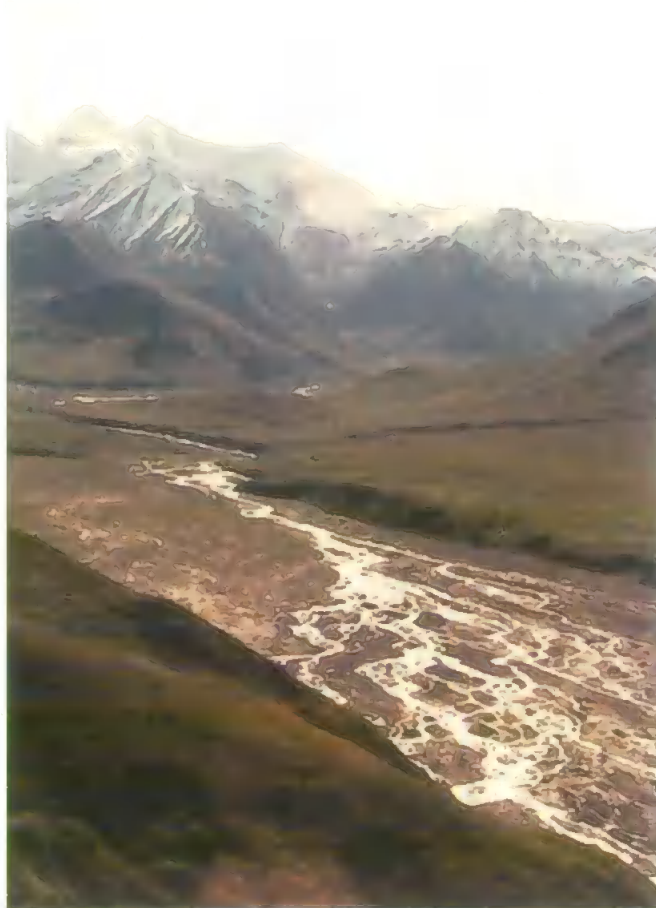


Plate 2.9 Braided river in Alaska (courtesy of Jim Apriletti, University of California, U.S.A.)

Murray and Paola (1994) studied the development of braided rivers through a very simplistic abstraction of the physics governing the system. Flow is characterised by a carrying capacity proportional to a power of the water discharge and affects the shape of the bed. The presence of random perturbations in the bed and the use of a non-linear relationship between flow velocity and sediment flux allow the development of braided patterns resembling natural features. This model, although applied to simulate completely different features, is in many aspects very similar to the one herein developed for the formation of patterns in the swash zone (see chapter 5).

2.5.2.2 Eolian ripples

These kind of features, caused by wind motion and easily observed in different environments, look very similar (Plate 2.10) to the ones previously described through the stability theory and due to their regularity they have intrigued many authors.

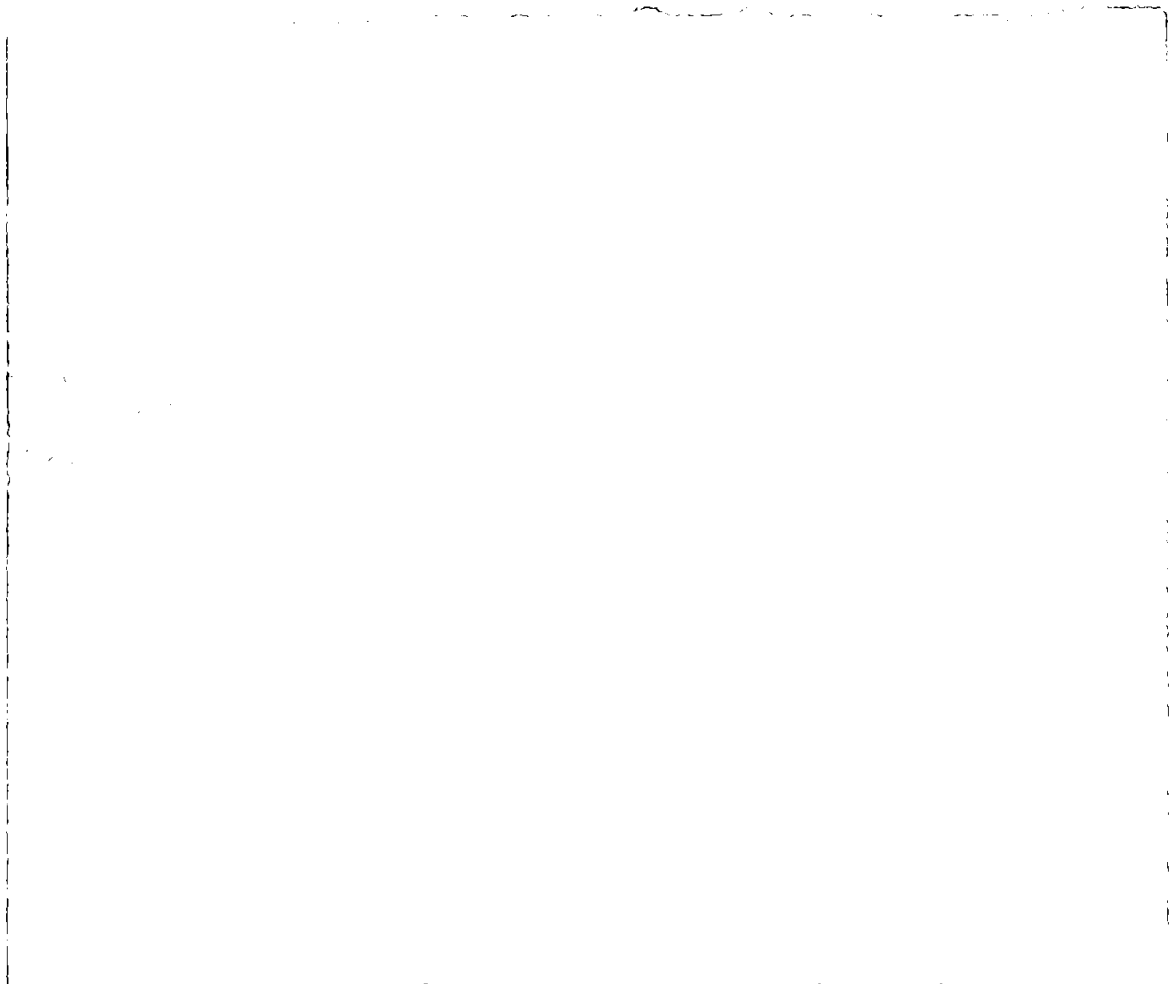


Plate 2.10 Eolian ripple field

Also in this case, the emergent pattern is characterised by a length scale that cannot be directly associated with a forcing template. In other words, the transition from a non-patterned into a patterned state happens under no direct external influence. The usually observed patterns indicate wavelengths around 10 cm and the sorting of sediment (coarsest grains accumulate in the crests, the finest in the troughs). The 2D model by Anderson (1990) was based on the cellular automata approach and considered a grain randomly entering the domain, impacting the surface and rebounding at a slower velocity. Besides the numerous simplifications (one-size sediment, steady wind, simplification in the grain trajectory), this model was already able to show the emergence of a favourite ripple wavelength.

Improvements to the simple model by Anderson (1990) have been proposed by different authors (Nishimori and Ouchi, 1994; Landry and Werner, 1994) that considered 3D simulations which, together with the addition of other features (different interactions when grains collide, the presence of an angle of repose), lead to interesting results comparing positively with the observations (ripple geometry related to the grain size). The simulations by Laundry and Werner (1994) also showed ripples' merging during the formation process and gave evidence for the initiation of bedforms (positive feedback) and their stabilisation (negative feedback) as a result of the relationship between sediment transport and ripple geometry. The model by Nishimori and Ouchi (1993) was also able to simulate the formation of features of much larger scale like dunes through only minor changes in the grain trajectory simulation. This result confirms the suggestion that cellular automata are, in certain cases, very sensitive to the set of deterministic rules set at the beginning of the simulations (the model by Laundry and Werner (1994) seems to be much more stable). Other developments have also been proposed so that sediment sorting (Anderson and Brunas, 1993) and the formation of a vertical stratigraphy (Forrest and Haff, 1992) could be simulated during ripple formation.

2.6 Comparison between stability theory and self-organisation models

As previously stated, the two approaches are both useful techniques to study and have a better understanding of free behaviour and complex systems in general. The main advantage of the stability theory is that, by following a more traditional approach, it allows for an easier understanding of the physical process(es) triggering the instability and driving the development of the bedforms. On the contrary, the so-called self-organisation, with its simplified rules, sometimes acts as a "black box" and the internal physics resulting in the

growth of a favoured wavelength are not always clear. It should also be considered that the use of simplified rules could be successful in identifying the minimum physics required to produce and develop the instability. The stability theory, in its linear application, can also lead to misleading interpretation of the results because of the lack of interaction between different modes. The patterns obtained are also not related to equilibrium states but only to the initial development of the bedform growth. Finally, bedform growth rates obtained for the linear case, are always the result of a “deterministic” analysis involving the superimposition of a given perturbation over the basic state and the evaluation of its growth. These disadvantages are obviously overcome by implementing a non-linear analysis which is unfortunately much more complicated. Self-organisation/cellular automata models allow for completely stochastic inputs (so that growth rates are not uniquely determined), they are implicitly non-linear and allow for the growth of the instability to equilibrium. On the other hand, the major drawback of self-organisation models is related to the strong assumptions on which they rely (for example, continuous systems are approximated by “discrete” arrays of particles) so that the validity of a model can only be assessed by comparison with field observations.

It is clear that the techniques herein presented constitute a very powerful tool in order to model morphodynamics and it is possible to predict that further developments will allow for an even better insight of the processes governing the nearshore region. For this reason in the next chapter a linear stability model for the formation of periodic patterns in the surf zone will be presented in an attempt to clarify whether the presence of such features is the result of a hydrodynamic forcing or the result of the interaction between flow and sediment. In the same way, a self-organisation model will be developed in chapter 5 for the formation of beach cusps in the swash zone. These features, whose origin cannot be clearly deduced from the existing field and laboratory measurements, are at the centre of a strong debate concerning their origin. In fact, a previously accepted model based on the hydrodynamic forcing due to the presence of standing edge waves has been recently called into question by a recently developed self-organisation model (Werner and Fink, 1993). A similar self-organisation model will be presented here and its behaviour discussed in order to establish the origin of such features.

Chapter 3: A stability model for the formation of rhythmic patterns in the surf zone

This chapter is based on "A mechanism for the generation of wave driven patterns in the surf zone" by Falqués, A., Coco, G., and Huntley, D.A. submitted for publication by the Journal of Geophysical Research. Throughout this work a model (MORFO13) developed by Prof. Falqués has been used. Section 3.3 has been developed by Prof. Falqués and is here included for the sake of the argument. The personal contribution to this work is the development of a different sediment transport parameterisation in the model, the introduction of a sediment stirring function varying in the cross-shore direction, as well as the numerical simulations shown herein and the interpretation of the modelled features in terms of observed features.

3.1 Introduction

Morphodynamic instabilities arise from the coupling that sediment transport induces between the small perturbations on a reference uniform bottom topography and the disturbances thereby produced on water motions. In the case of normal wave incidence, where there is no longshore current, this coupling can occur through the perturbation that the bedform causes on the incident wave field. Basically, the shoals and the troughs cause wave energy redistribution, variations in the breaking point, wave refraction, reflection and diffraction that produce in turn a radiation stress distribution which is no longer in equilibrium with the setup/setdown and a steady circulation is created. This interaction will be indicated as bed-surf interaction.

When there is a significant longshore current the deflection that the bedforms produce on the current is another source of morphodynamic interaction. This mechanism is responsible for the formation of free bars in rivers and can also be important in the nearshore environment in case of currents generated by tides, by wind stress or by river discharge. This interaction will be indicated as bed-flow interaction. From a conceptual point of view, bed-flow interaction is worth investigating in isolation (Falqués et al., 1996) and it is suggested (Falqués et al., 1997) that it can eventually lead to the formation of morphological patterns in the nearshore region like, for example, transverse or oblique bars.

Thus, normal wave incidence is assumed in the present work to avoid a mean longshore current. This occurs relatively often on natural beaches. But in addition, it seems that a

satisfactory understanding of each of the individual processes –bed-flow and bed-surf – in isolation is very convenient before dealing properly with the general situation of oblique wave incidence. As far as it has been found in the literature, instability in case of normal wave incidence is essentially unexplored. For example, the model of Christensen et al. (1995) could not deal with the case of $\theta_b = 0$. Apparently, Hino (1975) did some numerical experiments with normal incidence. However, even though his results were promising, there appears to be a lack of a systematic investigation by both numerical and analytical tools.

The purpose of the present chapter is to present a first detailed investigation of bed-surf interaction as a source of morphodynamic instability. Interest will be here concentrated on a single bed-surf effect: wave energy redistribution in the surf zone that is believed to be the major source of bed-surf interaction at an initial stage. This analysis shows that even with this rather simplified modelling morphodynamic, instability indeed develops and produces bedforms that compare well with features that can occur on natural beaches. Furthermore, this study suggests some interesting links between morphological patterns and sediment transport modes. The present study is restricted to the case of non-barred beaches and other effects like the variation of the breaking point due to the bedforms or wave refraction are left for further research.

In section 3.2 the theoretical setting of morphodynamic stability will be presented. Some general properties of the instability are given in section 3.3 and the physical mechanisms are investigated. This is done by means of analytical tools and by considering an idealised situation. Numerical experiments in case of more realistic conditions are presented in section 3.4. A brief summary, some discussion and a comparison with natural morphological patterns are given in section 3.5.

3. 2 Governing equations and stability analysis

3.2.1 Governing equations

A planar beach will be considered with a shoreline given by the y axis and with a topography given by $z=z_b(x,y,t)$ where x is the cross-shore coordinate and z the vertical one (positive upwards, see Figure 3.1). The 2DH nearshore hydrodynamics on time scales larger than the incident waves proceed from depth averaged momentum and mass conservation and read:

$$\frac{\partial v_i}{\partial t} + v_j v_{i,j} = -gz_{s,i} - \frac{1}{\rho D} (\tau_i + S_{ij,j}) + \frac{1}{D} [vD(v_{i,j} + v_{j,i})]_{,j} \quad i=1,2 \quad (3.1)$$

$$\frac{\partial D}{\partial t} + (Dv_j)_{,j} = 0 \quad (3.2)$$

Here, $\bar{v} = (v_1, v_2)$ is the depth-averaged horizontal velocity, the derivative with respect to x_i has been indicated by the subindex “,i” with $x_1=x$, $x_2=y$ and repeated indexes assumed to be summed. The total depth is $D=z_s-z_b$, where $z_s(x,y,t)$ stands for the free surface elevation. The bottom shear stress is $\bar{\tau}$, and the water density is ρ . The lateral mixing from wave breaking turbulence is parameterised by means of the eddy viscosity coefficient, $\nu(x)$. The forcing from incident waves is given by the radiation stresses that read:

$$S_{i,j} = \left(\frac{k_i k_j}{k^2} + \frac{1}{2} \delta_{ij} \right) E \quad i, j = 1, 2 \quad (3.3)$$

where \bar{k} and E are the wave number and the energy of incident waves (Horikawa 1988). Since shallow water waves are considered, it is assumed that the phase and the group celerities approximately coincide so that $c_p=c_g=c$.

The morphological evolution is given by the sediment conservation equation:

$$\frac{\partial z_b}{\partial t} + \nabla \cdot \bar{q} = 0 \quad (3.4)$$

where $\bar{q}(\bar{v}, z_b)$ is the horizontal sediment flux vector.

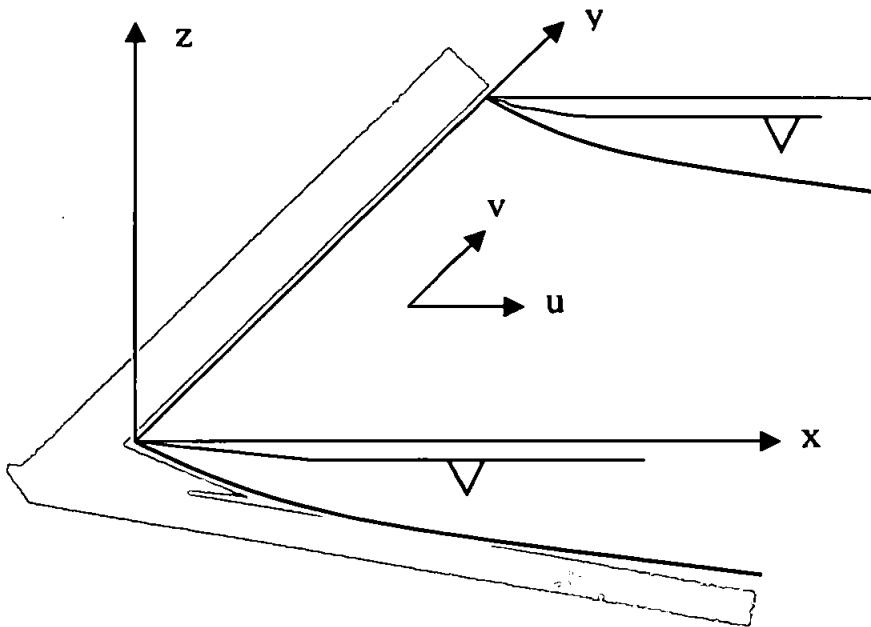


Figure 3.1 Sketch of the geometry and coordinate system

3.2.2 Basic state

By considering a regular incident wind or swell waves approaching the beach normally with energy distribution $E=E_0(x)$, it is possible to look for a basic undisturbed state which is a steady and motionless solution of (3.1), (3.2), (3.4), that is:

$$v_1=v_2=0, \quad z_s=\zeta_0(x), \quad z_b=-d_0(x) \quad (3.5)$$

The radiation stress will take the form:

$$S_{xx} = \frac{3}{2}E_0(x), \quad S_{yy} = \frac{1}{2}E_0(x), \quad S_{xy} = 0 \quad (3.6)$$

Furthermore, it will be assumed that both the bottom shear stress and the sediment flux are proportional to some power of the mean flow velocity. Therefore, since $\bar{v} = 0$, the bottom friction and the sediment flux will vanish, $\bar{\tau} = 0$, $\bar{q} = 0$. As a result, the cross-shore component of (3.1) reads:

$$g \frac{d\zeta_0}{dx} = -\frac{3}{2\rho} \frac{1}{d_0 + \zeta_0} \frac{dE_0}{dx} \quad (3.7)$$

while the rest of the governing equations are automatically verified. Thus, the basic undisturbed state is defined as a steady setup/setdown of the mean water level given by $z_s=\zeta_0(x)$, over a fixed topography without mean motion.

3.2.3 Linear stability equation

Any departure from the basic planar topography will produce a modification of the incident wave field. The wave energy distribution will change and waves will be refracted. As a result, the setup and setdown of the basic state, $\zeta_0(x)$, will not be in equilibrium any longer and a mean flow will thus be generated. This flow will carry sediments so that the initial topographic disturbance will evolve. A morphodynamic loop will thus be formed and if a positive feedback occurs, a new topography coupled to an horizontal circulation will develop in time. To look at this possibility, a small perturbation will be assumed on the topography and on the mean free surface:

$$z_b(x,y,t)=-d_0(x)+\chi(x,y,t), \quad z_s(x,y,t)=\zeta_0(x)+\eta(x,y,t) \quad (3.8)$$

and a small horizontal mean flow:

$$\bar{v}=(u(x,y,t),v(x,y,t)) \quad (3.9)$$

will be assumed as well. The dynamics of these small perturbations will be considered by linearising the governing equations (3.1), (3.2) and (3.4).

A difficult and crucial point is how the disturbance will affect the incident wave field. In a saturated surf zone, this will basically happen through three effects: wave energy redistributions, wave refraction by depth variations and currents and the modification of the breaking point by growing shoals and pools at the breaking line. Wave refraction and the modification of the breaking point are both first order effects (with respect to the perturbations). However, they will be assumed to be comparatively small with respect to wave energy redistribution and will be neglected throughout this study. As a result, waves approaching normally to the shore will be considered with their energy suffering small modifications due to depth variations. For this purpose, it will be assumed that wave energy in the nearshore is a known function of the total depth:

$$E=E(D) \quad (3.10)$$

This allows to describe one source of coupling between morphology and waves in a simple manner. How wave refraction and the variation of the breaking point affect this mechanism is left for future research. Note that equation (3.10) is not valid in case of barred beaches. As previously indicated, a monotonic beach profile will be here considered.

Equation (3.10) can easily be determined for a saturated surf zone, where:

$$E = \frac{1}{8} \rho g \gamma_b^2 D^2 \quad (3.11)$$

is usually assumed with $\gamma_b \approx 1$ being a breaker index. The Green law for wave amplitude in the shoaling zone is also in accordance with the form of (3.10) (Mei, 1989).

Sediment transport parameterisation is another important point. The sediment flux is usually parameterised as being proportional to some power, m , of the mean flow. Since there is no flow in the basic state, the sediment transport in the perturbed state will be proportional to the power m of \bar{v} which is first order. Then if $m > 1$, there would be no sediment transport in the linearised problem. Therefore, it will be assumed $m=1$ in the linear analysis and the non-linear problem will be left for future research, checking the robustness of the instability mechanism to the choice of m . Thus, it will be assumed

$$\bar{q} = \alpha(x)\bar{v} - \hat{\gamma}(x)\nabla\chi \quad (3.12)$$

This linear parameterisation of sediment transport can be interpreted as the sediment being stirred by wave motion and then advected by the mean current. Thus, $\alpha(x)$ is a wave stirring coefficient which is expected to have a cross-shore gradient (see section 3.2.4). Furthermore, due to both wave oscillations and to wave-breaking turbulence, any bump superimposed on the nearshore sea bottom will be potentially smoothed out if no positive

feedback occurs into the water motion. This is parameterised through a morphodynamic diffusion coefficient $\hat{\gamma}(x)$ in (3.12).

Bottom shear stress will also be parameterised as being proportional to the mean flow through a coefficient that depends on the wave orbital velocity, U_0 ,

$$\frac{\tau_{bx}}{\rho D} = \hat{\mu}_x u, \quad \frac{\tau_{by}}{\rho D} = \hat{\mu}_y v \quad (3.13)$$

where $\mu_x = 2\mu_y = 4c_f U_0 / (\pi D_0)$ and where, in the surf zone, $U_0 = (\gamma_b / 2) \sqrt{g D_0}$ (Horikawa 1988). Here, c_f is the drag coefficient that relates the instantaneous bottom shear stress to the squared instantaneous velocity, $\tau = \rho c_f v^2$.

The momentum diffusion will be parameterised as:

$$v(x) = N x \sqrt{g D} \quad (3.14)$$

in the surf zone (N is a constant), and as an exponential decay beyond the breaking line.

It is now possible to introduce a scaling. The width of the surf zone, X_b , is chosen as horizontal length scale and a vertical length scale βX_b will be introduced where β is some mean slope of the basic topography, $O(dd_0/dx) = \beta$. An arbitrary velocity scale, U , is also considered. The natural time scale for hydrodynamics is then X_b/U . However, morphological evolution is much slower, with a time scale T that will be defined later ($\epsilon = (X_b/U)/T \ll 1$). Then, the non-dimensional variables will be defined as:

$$(x, y) = X_b (x', y'), \quad \chi = \beta X_b \chi', \quad D_0 = \beta X_b D_0'$$

$$(u, v) = U (u', v'), \quad \eta = \frac{U^2}{g} \eta', \quad t = T t'$$

Hereinafter, primes will be dropped for simplicity. Then, the linearised non-dimensional form of the governing equations (3.1), (3.2) in the surf zone will read:

$$\epsilon \frac{\partial u}{\partial t} + \mu_x u + \left(1 + \frac{3}{8} \gamma_b^2\right) \frac{\partial \eta}{\partial x} - v_x = \frac{3}{8} \frac{\gamma_b^2}{F^2} \frac{\partial \chi}{\partial x} \quad (3.15)$$

$$\epsilon \frac{\partial v}{\partial t} + \mu_y v + \left(1 + \frac{1}{8} \gamma_b^2\right) \frac{\partial \eta}{\partial y} - v_y = \frac{1}{8} \frac{\gamma_b^2}{F^2} \frac{\partial \chi}{\partial y} \quad (3.16)$$

$$\epsilon \frac{\partial}{\partial t} (F^2 \eta - \chi) + \frac{\partial}{\partial x} (D_0 u) + \frac{\partial}{\partial y} (D_0 v) = 0 \quad (3.17)$$

where a Froude number $F = U / \sqrt{g \beta X_b}$ has been introduced and $\mu_x = \hat{\mu}_x X_b / U$, $\mu_y = \hat{\mu}_y X_b / U$ have been defined. The non-dimensional coefficients, μ_x , μ_y depend on the

drag coefficient, c_f , through $r=c_f/\beta$, that will be adopted as frictional parameter for our simulations (see also Falqués et al., 1996). Notice that the same equations will be valid out of the surf zone, but, since there are no perturbations on the radiation stress, γ_b must be substituted by 0. The momentum diffusion terms read:

$$v_x = \frac{2}{D_0} \frac{\partial}{\partial x} \left(v D_0 \frac{\partial u}{\partial x} \right) + v \frac{\partial}{\partial y} \left(\frac{\partial u}{\partial y} + \frac{\partial v}{\partial x} \right)$$

$$v_y = \frac{1}{D_0} \frac{\partial}{\partial x} \left[v D_0 \left(\frac{\partial u}{\partial y} + \frac{\partial v}{\partial x} \right) \right] + 2v \frac{\partial^2 v}{\partial y^2}$$

To scale the sediment conservation equation (4), a non-dimensional wave-stirring coefficient will be first defined:

$$\hat{\alpha}(x) = \bar{\alpha} \alpha(x)$$

where $\alpha(x)$ is order one. By carrying out the scaling equation (3.4), the coefficient $UT\bar{\alpha}/\beta X_b$ appears in front of $\alpha(x)$ in the divergence of the sediment flux. Therefore, if significant morphological changes are required during one time unit a morphological time scale must be chosen:

$$T = \beta \frac{X_b^2}{U\alpha} \quad (3.18)$$

Then, from (3.4) the bottom evolution becomes:

$$\frac{\partial \chi}{\partial t} + \frac{\partial}{\partial x} (\alpha u) + \frac{\partial}{\partial y} (\alpha v) = \frac{\partial}{\partial x} \left(\gamma \frac{\partial \chi}{\partial x} \right) + \frac{\partial}{\partial y} \left(\gamma \frac{\partial \chi}{\partial y} \right) \quad (3.19)$$

where $\gamma = \hat{\gamma}T/X_b^2$.

Now the linear stability analysis proceeds in its standard way by assuming alongshore periodic perturbations of the form:

$$[u(x, y, t), v(x, y, t), \eta(x, y, t), \chi(x, y, t)] = \Re e \left\{ e^{\sigma t + ik y} [\hat{u}(x), \hat{v}(x), \hat{\eta}(x), \hat{\chi}(x)] \right\} \quad (3.20)$$

where $2\pi/k$ is the alongshore wavelength and σ the growth rate. By inserting this form of the solution into the system of the governing equations (3.15)-(3.16)-(3.17)-(3.19) an eigenproblem is obtained, where σ is the eigenvalue and $[\hat{u}(x), \hat{v}(x), \hat{\eta}(x), \hat{\chi}(x)]$ is the eigenfunction. Its structure is the same as that (3.15)-(3.16)-(3.17)-(3.19) but with substitution of $\partial/\partial t$ by σ and $\partial/\partial y$ by ik .

A spectral numerical technique based on the use of rational Chebyshev functions has been applied in order to solve the eigenvalue problem. This method has already been successfully applied to other morphodynamic models (see, for instance, Falqués et al., 1996 and 1997, where a description of the technique can also be found) and allows for the determination, for a given wavenumber, of as many eigenvalues as the number of

discretization points. The numerical model that solves the present eigenproblem is called MORFO13. The relevant morphodynamic instability modes have real σ in this case. This means a growth (if $\sigma > 0$) in place without migration. The model is also able, however, to describe purely hydrodynamic models like edge waves. In this case the imaginary part of σ is the frequency and it gives the alongshore phase speed.

3.2.4 Sediment transport parameterisation

In this section the link between the sediment transport parameterisation described through equation (3.12) and other already accepted models will be shown on the basis of an energetics approach. Bowen (1980) applied the Bagnold (1963) energetics equation to the case of a sinusoidal wave velocity and a much smaller mean flow, and showed that the net sediment transport rate for both suspended and bedload transport rate takes the form:

$$i_r = \frac{16\varepsilon_{ss}c_f\rho}{3\pi w} \left[U_1 U_0^3 + \frac{\beta}{5w} U_0^5 \right] \quad (3.21)$$

where: ε_{ss} = suspended sediment transport efficiency, c_f = drag coefficient, ρ = water density, w = settling velocity, U_0 = maximum wave orbital velocity, U_1 = steady current. A comparison between such a formulation and the one given in equation (3.12) implies that:

$$\alpha(x) = C_1 U_0^3, \quad \gamma(x) = -C_1 \frac{U_0^5}{5w} \quad (3.22)$$

where $C_1 = 16\varepsilon_{ss}c_f\rho/3\pi w$.

A simple model of wave velocities under normally incident shallow water waves provides a form for the cross-shore dependence of these functions $\alpha(x)$ and $\gamma(x)$. By assuming shoaling waves out of the surf zone and depth limited waves inside the surf zone with $H=\gamma_b D$, one obtains:

$$U_0^2 = C_2 x^{-3/2} \text{ for } D > D_b \text{ and } U_0^2 = C_2 x \text{ for } D < D_b$$

where: $x = D/D_b$ and $C_2 = g\gamma_b^2 D_b / 4$.

Thus it is possible to obtain the expression for the variation of the maximum orbital velocity (U_0), and so of $\alpha(x)$ and $\gamma(x)$ with the offshore distance. In fact, outside the surf zone:

$$\alpha(x) = C_1 C_2^{3/2} x^{-9/4}, \quad \gamma(x) = -\frac{C_1}{5w} C_2^{5/2} x^{-15/4} \quad (3.23)$$

while inside the surf zone:

$$\alpha(x) = C_1 C_2^{3/2} x^{3/2}, \quad \gamma(x) = -\frac{C_1}{5w} C_2^{5/2} x^{5/2} \quad (3.24)$$

These are the functions of x that have been modelled in this chapter.

The case of $\alpha(x)$ and $\gamma(x)$ increasing towards the shoreline is related to a wave field dominated by the presence of edge wave motions. The edge wave theory is already well-established (Eckart, 1951; Ursell, 1952) and for the present purposes it is only important to note that a standing edge wave in shallow water has a velocity potential given by:

$$\Phi = \frac{g a_n}{\sigma_w} L_n(2\lambda x) e^{-\lambda x} \cos \lambda y \cos \sigma_w t \quad (3.25)$$

where: a_n is the amplitude of order n , σ_w is the frequency, $L_n(2\lambda x)$ is the Laguerre polynomial of order n , x and y are the horizontal coordinates in the offshore and alongshore direction, t is time and λ is the longshore wavenumber of the edge wave.

The cross-shore orbital velocity field is given by the gradient of the velocity potential and it results in a cross-shore profile of the form:

$$u_x(x) = -\frac{\partial}{\partial(\lambda x)} [L_n(2\lambda x) e^{-\lambda x}] \quad (3.26)$$

In nature one would expect to find the co-existence of edge waves characterised by different modes and wavelengths. For example Figure 3.2 shows the effect of superimposing the velocity squared of the first seven modes of an edge wave of arbitrary wavelength and under the hypothesis of non-correlation between the different modes. The rapid increase towards the shoreline is at least qualitatively modelled by the exponential forms used in the simulations in this chapter.

3.3 Analysis of the instability mechanism

In section 3.4, by using the numerical model MORFO13, it will be shown that morphodynamic instability indeed develops, and the properties of such a process will be explored for realistic conditions. However, the use of analytical tools, when possible and perhaps in very idealised situations, gives a better understanding of the outputs of the numerical models and a higher confidence in them. This section is devoted to some analytical developments on the bed-surf interaction.

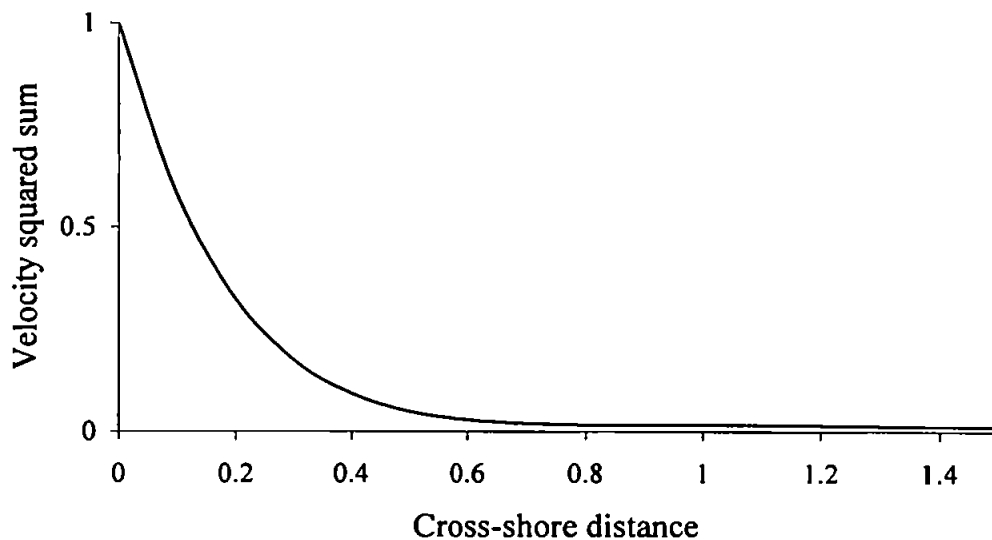


Figure 3.2 The sum of the squares of the cross-shore velocities for the first seven edge wave modes on a linear slope (arbitrary units)

3.3.1 Bottom evolution equation

A very useful tool for analysing the morphodynamic instabilities is a bottom evolution equation where only the cross-shore flow component is involved (Falqués et al., 1996). This form of equation can easily be obtained by substituting $\partial v/\partial y$ from the mass conservation equation (3.17) into the sediment conservation equation (3.19). Since the morphologic evolution is much slower than the fluid motions, it is safe to consider $\epsilon=0$ in this section. Then, the bottom evolution equation will read:

$$\frac{\partial \chi}{\partial t} - \frac{\partial}{\partial x} \left(\gamma \frac{\partial \chi}{\partial x} \right) - \frac{\partial}{\partial y} \left(\gamma \frac{\partial \chi}{\partial y} \right) = -u\alpha \frac{d}{dx} \ln \left(\frac{\alpha}{D_0} \right) \quad (3.27)$$

The conditions leading to the instability are immediately found from this equation. The growth of any bedform requires $\partial \chi/\partial t > 0$ where $\chi > 0$ and $\partial \chi/\partial t < 0$ where $\chi < 0$. In the linear theory each of these conditions implies the other. So it is possible to examine when the first condition occurs. The second and the third terms on the left side are diffusive so that they play just a damping role and any instability will be related to the right hand term. Thus, since $\alpha > 0$, instability requires that

$$u \frac{d}{dx} \ln \left(\frac{\alpha}{D_0} \right) < 0 \quad (3.28)$$

where $\chi > 0$, that is over the shoals. Then, if $\alpha(x)/D_0(x)$ is a growing (decreasing) function, instability requires $u < 0$ ($u > 0$) where $\chi > 0$. In other words, if the stirring coefficient

increases seaward faster (slower) than the water depth, the growth of bedforms needs a shoreward (seaward) flow over the shoals.

This can be understood as follows. Assume first a constant α . A seaward flow over a sloping beach has to converge in order to preserve mass, as the depth is increasing following the water motion. Since α is constant, this implies a convergence of sediments, and therefore sedimentation. Assume now a constant depth but an increasing wave stirring, α , and assume again a seaward flow. Its divergence will now vanish. However, given a control volume, the sediment concentration will be smaller at its shoreward side than at its seaward side. Therefore, more sediment will go out than the sediment entering the control volume so that erosion will occur. Thus, one gets two counteracting effects, one related to the gradients in depth, $D_0(x)$, the other related to the gradients in the stirring function, $\alpha(x)$. To conclude this stability analysis it is now needed to know, for any given topographic pattern, whether the cross-shore flow will be seaward or shoreward over the shoals. This requires solving the flow equations (3.15)-(3.16)-(3.17) for a given bottom perturbation χ , that is, the “flow over topography problem” that will be hereafter referred to as the FOT problem.

3.3.2 Flow over topography (FOT) problem

It will be now assumed that the bottom perturbation and the flow related to it are periodic in the alongshore direction, that is the form given by equation (3.20). Lateral momentum mixing will be here neglected since it is not essential for the instability mechanism. Its effect will be investigated numerically in section 3.4. Also, the quasi-steady approximation, $\epsilon=0$, will be adopted as in the previous section. For simplicity the hats on u , v , η , χ are dropped. With all these assumptions, and defining the parameters:

$$m = \frac{1}{8} \gamma_b^2, \quad s = \frac{\gamma_b^2}{8F^2}$$

the flow equations (3.15)-(3.16)-(3.17) can be written as:

$$\mu_x u + (1 + 3m) \frac{\partial \eta}{\partial x} = 3s \frac{\partial \chi}{\partial x} \quad (3.29)$$

$$\mu_y v + ik(1 + m)\eta = iks\chi \quad (3.30)$$

$$\frac{\partial}{\partial x} (D_0 u) + ikD_0 v = 0 \quad (3.31)$$

Substitution of v and η from (3.30) and (3.31) into (3.29) leads to a single equation in u :

$$\frac{\partial}{\partial x} \left[\frac{\mu_y}{D_0} \frac{\partial}{\partial x} (D_0 u) \right] - \frac{1+m}{1+3m} \mu_x k^2 u = - \frac{2sk^2}{(1+3m)} \frac{\partial \chi}{\partial x} \quad (3.32)$$

As for the flow equations (3.15)-(3.16)-(3.17), this equation is only valid within the surf zone. However, the same equation works outside the surf zone if one substitutes γ_b with 0, i.e., if $s=m=0$ is considered. Appropriate boundary conditions are a vanishing mean cross-shore flow at the shoreline and far offshore, $u(0)=u(\infty)=0$.

An interesting property of the solutions of the FOT equation (3.32) is that they satisfy the inequality:

$$\int_{x_1}^{x_2} D_0 u \frac{\partial \chi}{\partial x} dx > 0 \quad (3.33)$$

where x_1, x_2 are any cross-shore positions within the surf zone with $u(x_1)=0$ and either $u(x_2)=0$ or $x_2=1$. This can be obtained by multiplying equation (3.32) by $D_0 u$ and choosing two arbitrary cross-shore locations in the surf zone $0 \leq x_1 < x_2 \leq 1$ where the cross-shore velocity vanishes:

$$u(x_1) = u(x_2) = 0 \quad (3.34)$$

Then, integrating by parts leads to:

$$\int_{x_1}^{x_2} \frac{\mu_y}{D_0} \left[\frac{\partial}{\partial x} (D_0 u) \right]^2 dx + k^2 \frac{1+m}{1+3m} \int_{x_1}^{x_2} \mu_x D_0 u^2 dx = \frac{2sk^2}{(1+3m)} \int_{x_1}^{x_2} D_0 u \frac{\partial \chi}{\partial x} dx \quad (3.35)$$

If both cross-shore positions were outside the surf zone, $1 \leq x_1 < x_2$, one would then obtain:

$$\int_{x_1}^{x_2} \frac{\mu_y}{D_0} \left[\frac{\partial}{\partial x} (D_0 u) \right]^2 dx + k^2 \int_{x_1}^{x_2} \mu_x D_0 u^2 dx = 0 \quad (3.36)$$

Since $\mu_x, \mu_y, D_0 > 0$, it then follows $u(x) = 0$ for $x_1 \leq x \leq x_2$. By taking $u(\infty) = 0$ and by choosing $x_2 \rightarrow \infty$, one then has $u(x) = 0$ for $x \geq x_2$. Finally, by continuity, x_1 can be lowered up to the breaker line, $x = 1$. Therefore, either $u(x) = 0$ for all $x \geq 1$ or $u(x) \neq 0$ for all $x \geq 1$.

Another possibility would be $0 \leq x_1 \leq 1 < x_2 \rightarrow \infty$. In this case one obtains:

$$\int_{x_1}^{\infty} \frac{\mu_y}{D_0} \left[\frac{\partial}{\partial x} (D_0 u) \right]^2 dx + k^2 \frac{1+m}{1+3m} \int_{x_1}^1 \mu_x D_0 u^2 dx + k^2 \int_1^{\infty} \mu_x D_0 u^2 dx = \frac{2sk^2}{(1+3m)} \int_{x_1}^1 D_0 u \frac{\partial \chi}{\partial x} dx \quad (3.37)$$

Therefore, it is possible to conclude that equation 3.33 is satisfied whenever $u(x_1) = 0$ and either $u(x_2) = 0$ or $x_2 = 1$.

Essentially, this inequality means that a decrease of the bottom slope with respect to the equilibrium ($\partial \chi / \partial x > 0$ makes $-\partial z_b / \partial x$ smaller) produces an offshore flow, $u > 0$ (on average). This can be understood because a smaller bottom slope induces smaller cross-shore

gradient in radiation stress so that the equilibrium setup becomes too large and induces a seaward current. A priori, however, this is not so straightforward since there is also a contribution from free surface variations which are implicitly taken into account.

3.3.3 The instability mechanism in a simple case

A simple idealised situation will be now considered. In such a case, morphodynamic instability can be predicted by the analytical tools developed in the last two sections. The basic assumption is that α/D_0 is a monotonically increasing function. This may be realistic in the surf zone but not beyond the breaking line. However, this case provides an example of how bed-surf interaction can lead to morphodynamic instability. More realistic situations will be dealt with in the next section by means of numerical experiments. The example described here provides some confidence in the numerical model set up to solve the instability equations in realistic conditions.

Assume a shoal with a monotonically decreasing amplitude seaward $\partial\chi/\partial x < 0$. Then, according to inequality (3.33), the cross-shore velocity is shoreward ($u < 0$) everywhere on the shoal. Indeed, assume that there was a cross-shore location, $x = x_3$, where $u(x_3) > 0$. Then, by continuity, there would exist x'_1, x'_2 such that $0 \leq x'_1 < x_3 < x'_2 \leq \infty$ such that $u(x'_1) = u(x'_2) = 0$ and $u(x) > 0$ for all $x'_1 < x < x'_2$. In this case, inequality (3.33) would not be satisfied.

Therefore, such a shoal would produce a shoreward current on it (and of course, due to the alongshore periodicity, a seaward current in the troughs between shoals). But then, according to the bottom evolution equation (3.27), since α/D_0 is an increasing function, an inshore flow over the shoals will produce a growth of such shoals (see Figure 3.3). Thus, the motionless equilibrium on a plane sloping beach would be unstable with respect to this kind of topographic perturbations. Of course, this depends on the basic assumption of an ever increasing α/D_0 function, which is not realistic. By numerical simulation, it will be shown that the topographic and flow patterns emerging from the instability are very sensitive to this function.

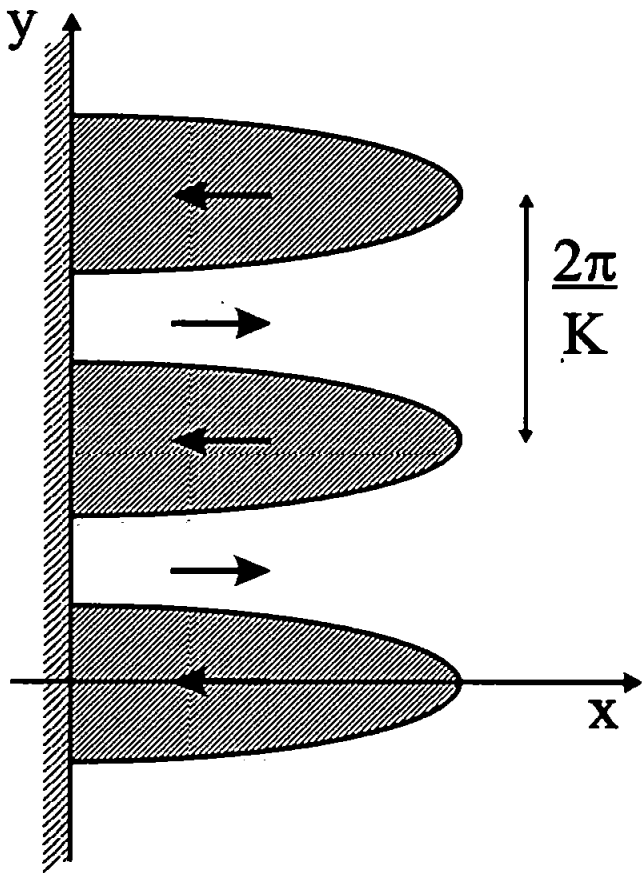
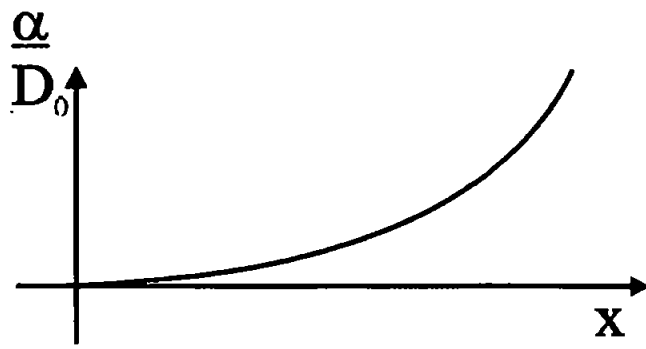


Figure 3.3 Sketch of the bed-surf instability mechanism in the idealised case on a monotonically increasing α/D_0 function

3.4 Numerical simulation

The previously described eigenvalue problem has been here solved numerically in order to assess the sensitivity of the morphodynamic instabilities and their along-shore spacing to parameters such as the bottom friction, the eddy viscosity and the morphodynamic diffusion. The numerical model has also been used to evaluate the sensitivity of the results to the quasi-steady hypothesis and the convergence of the numerical solution for different number of discretization points. Finally, the dependence of the results on the way the stirring function is parameterised in the sediment transport formulation has been carefully analysed. A plane sloping beach has been assumed through all the numerical simulations. Physically realistic ranges of parameter values have been used. The parameter related to the bottom friction, r , has been varied between 0.1 and 1 and that representing the eddy viscosity, N , between 0.001 and 0.02. For the morphodynamic diffusion parameter, γ (eq. 3.12), a profile changing with the cross-shore velocity gradients has been considered with a maximum value, ranging between 0.01 and 0.1, chosen at the beginning of the simulation. Some of these parameters have sometimes been used out of the defined range in order to understand their effect and importance for the growth of the instability. The simulations show robustness towards all the parameters concerning hydro- and morpho-dynamic behaviour but a very strong dependence on the form of the stirring function α (eq. 3.12) used in the sediment transport formulation. For this reason, results will be analysed separately for a series of qualitatively distinct forms of the stirring function $\alpha(x)$.

For simplicity the first case analysed is a stirring function $\alpha(x)$ quadratically increasing from a small shoreline value to the breaking line. Seaward of the surf zone, the stirring function is kept constant and equal to the value at the breaking line (simulations have also been run with an exponential decrease beyond the breaking line but results are not significantly affected by such change). Figure 3.4 shows the influence of the bed friction parameter on the growth rate. It shows a consistent decrease of the growth rate with increasing the bed friction parameter but also the consistent presence of a definite maximum, always around the same wavelength. Figures 3.5 and 3.6 show the sensitivity of the instability towards the morphodynamic diffusion and the eddy viscosity parameters respectively, and show a similar decrease of the growth rate with increasing parameter value, though in this case there is also a rapid decrease in the peak wavenumber. In general, results indicate an along-shore spacing of the resulting features around three times the width of the surf zone. Significantly different values are obtained only when the input parameters are extended towards non-realistic values. A feature that all these simulations

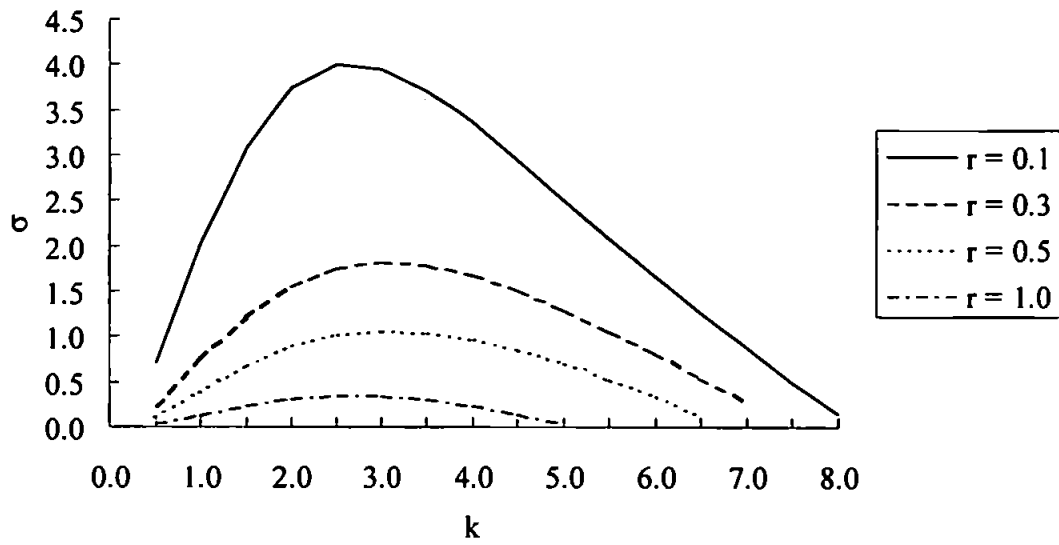


Figure 3.4 Instability curves for different values of r , $N=0.01$, $\gamma=0.02$, $\alpha(0)=0.1$

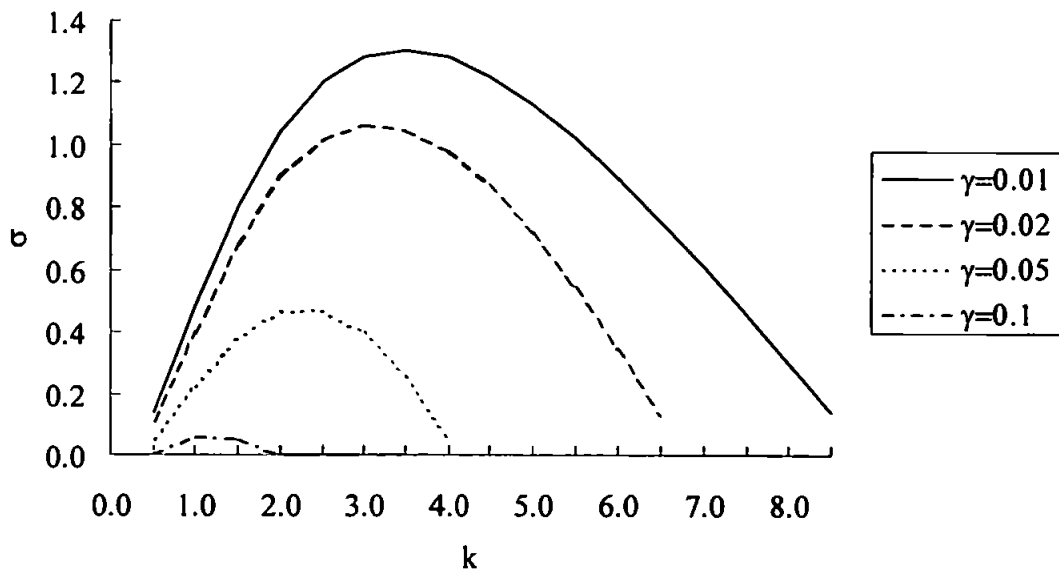


Figure 3.5 Instability curves for different values of γ , $r=0.5$, $N=0.01$, $\alpha(0)=0.1$

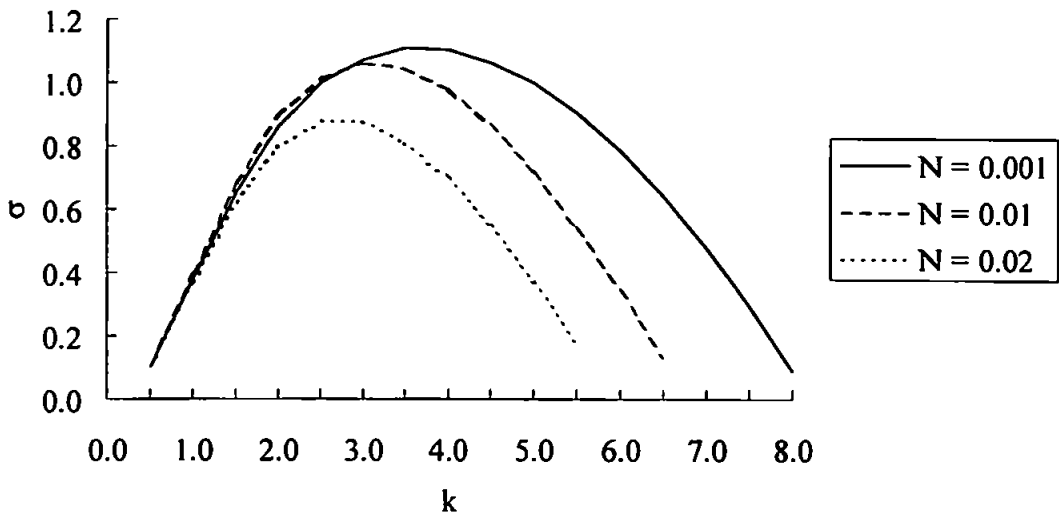


Figure 3.6 Instability curves for different values of N , $r=0.5$, $\gamma=0.02$, $\alpha(0)=0.1$

have in common, as well as most of the ones that will be shown in the following sections, is the lack of other modes displaying unstable wavenumbers ($\sigma > 0$). Other modes are obviously present but they are all characterised by negative growth rates unless unrealistically low values for the parameters related to the damping of the topography (bed friction and diffusivity) are chosen.

The typical perturbation contour pattern obtained is shown in Figure 3.7 while Figure 3.8 is a contour plot of the basic slope and the topographic disturbance and also shows the flow pattern. It has to be underlined that, because of the linear analysis, the amplitude of the topographic disturbance is arbitrary. A 3d view is also given in Figure 3.9, and clearly shows the presence of periodic features around the breaking line, resembling what in the literature have been defined as crescentic bars (Bowen and Inman, 1971; Lippmann and Holman, 1990). A form of 'mirroring effect' offshore of the breaking line is also present such that opposite to deposition an area of erosion is present and vice-versa. In agreement with the theoretical analysis of section 3.3, the flow pattern is such that inshore flow is present over the shoals and offshore flow over the troughs within the surf zone, where α/D increases. Beyond the breaking line, the opposite occurs, since α/D decreases.

For the cases just analysed a shoreline value of the stirring function equal to 0.1 has been used but an interesting result is obtained when such value is set to zero. In this case the instability curve (Figure 3.10) shows the presence of a second mode, though its growth rate is much smaller than that related to the dominant mode, and it is positive only for a restricted number of wavelengths. However it presents an interesting pattern which is very similar to the one observed in nature when beach cusps are present (Figure 3.11). These bedforms, characterised by a very large spacing (around 6 times the width of the surf zone), are characterised by a horn divergent flow pattern (Figure 3.12) and are much closer to the shoreline than to the breaking line (see Figure 3.13). In reality, rhythmic features like beach cusps are usually associated with reflective conditions and so with a situation where sediment close to the shoreline is likely to be moved. This condition is then contrary to the hypothesis of a stirring coefficient equal to zero at the shoreline. A non-linear analysis is required in order to understand whether the importance of this second mode is negligible or not and if such forms could grow and be compared to features commonly observed in nature.

Another interesting result which has revealed its consistency throughout all the simulations concerns the quasi-steady hypothesis. The model, in fact, allows one to verify the influence

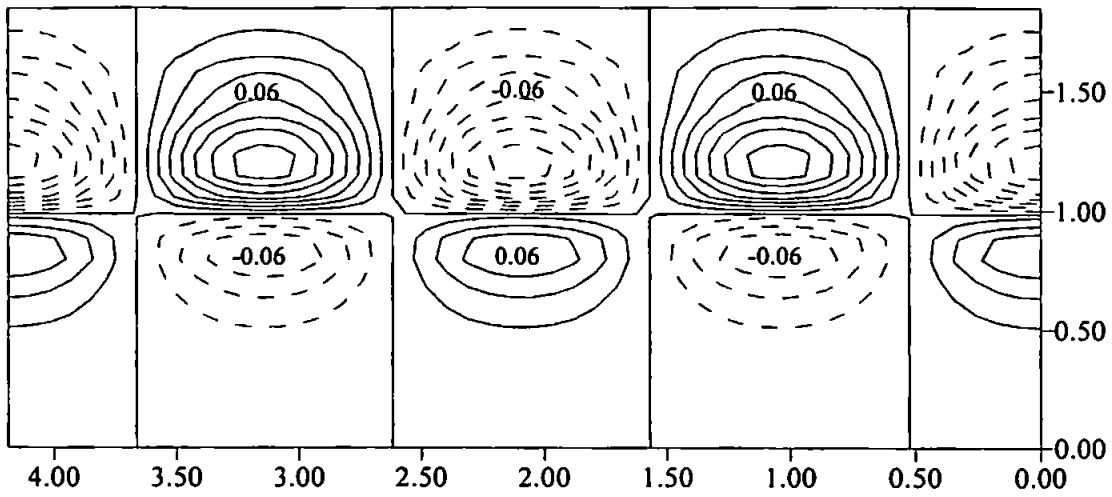


Figure 3.7 Contour lines of the topographic perturbation for $k=3.0$, $r=0.5$, $N=0.01$, $\gamma=0.02$, $\alpha(0)=0.1$. For these plots the alongshore direction is on the horizontal axis while the vertical axis indicates the cross-shore direction; darker areas correspond to greater depths

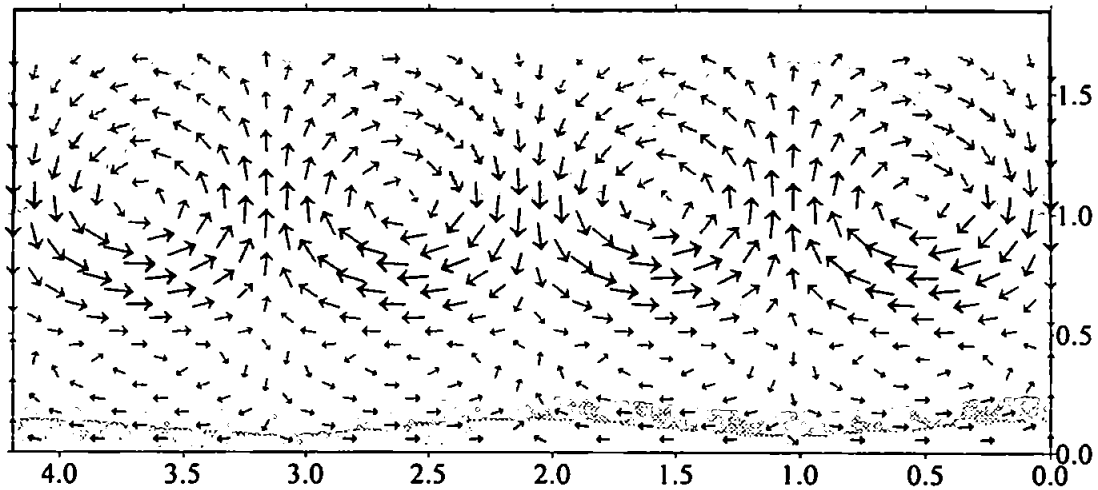


Figure 3.8 Topographic perturbation and relative flow pattern for $k=3.0$, $r=0.5$, $N=0.01$, $\gamma=0.02$, $\alpha(0)=0.1$

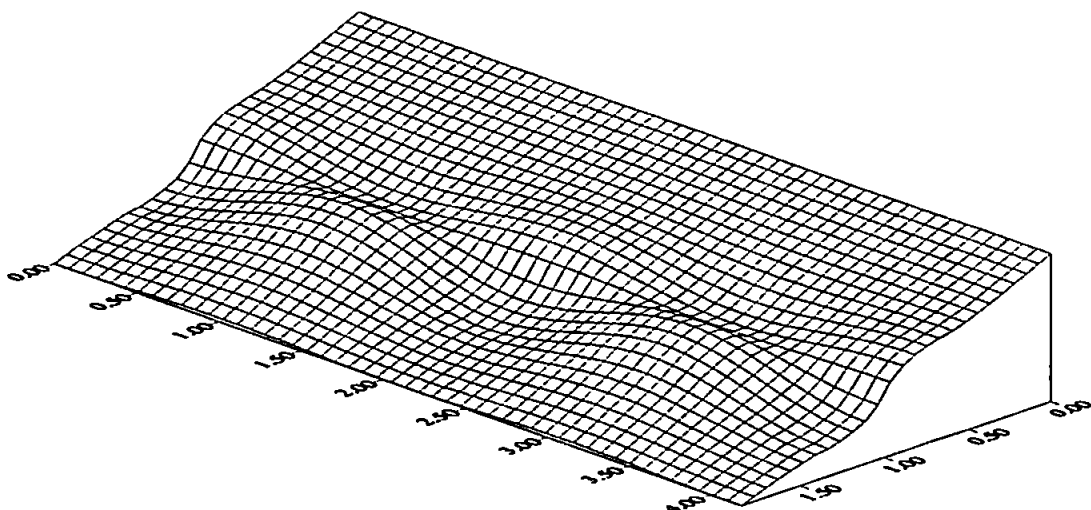


Figure 3.9 3d-view of the topographic perturbation (basic slope and perturbation amplitude have been chosen arbitrarily) for $k=3.0$, $r=0.5$, $N=0.01$, $\gamma=0.02$, $\alpha(0)=0.1$

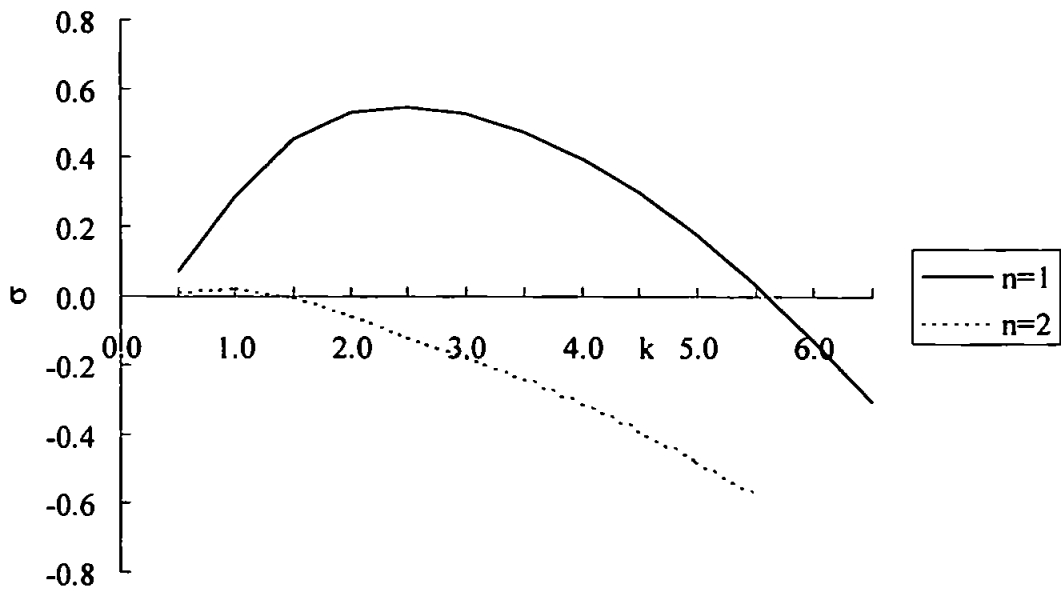


Figure 3.10 Instability curves for different values of $N=0.01$, $r=0.5$, $\gamma=0.02$, $\alpha(0)=0.0$

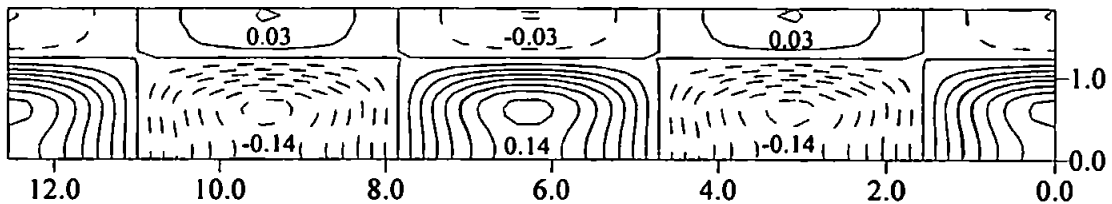


Figure 3.11 Contour lines of the topographic perturbation for mode $n=2$ and $k=1$ ($r=0.5$, $N=0.01$, $\gamma=0.02$, $\alpha(0)=0.0$)

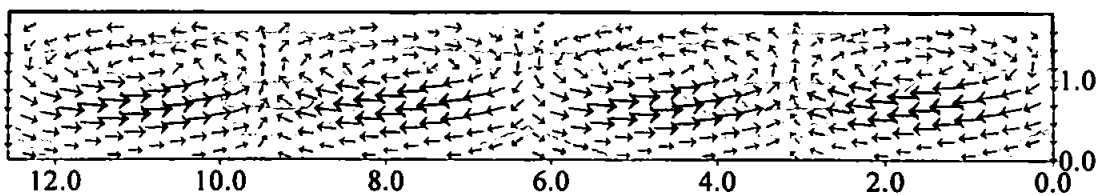


Figure 3.12 Topographic perturbation and relative flow pattern for mode $n=2$ and $k=1$ ($r=0.5$, $N=0.01$, $\gamma=0.02$, $\alpha(0)=0.0$)

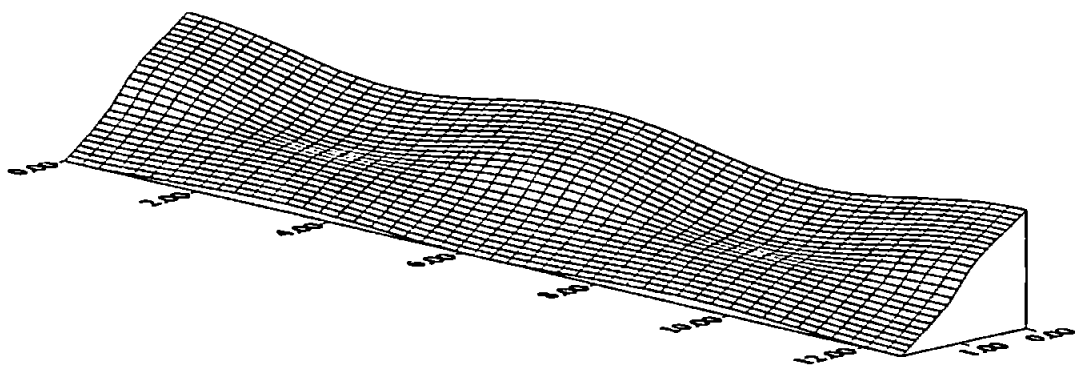


Figure 3.13 3d-view of the topographic perturbation (basic slope and perturbation amplitude chosen arbitrarily) for mode $n=2$ and $k=1$ ($r=0.5$, $N=0.01$, $\gamma=0.02$, $\alpha(0)=0.0$)

of this hypothesis by changing the value of the previously defined coefficient ϵ . Figure 3.14 shows that the adoption of relatively small values ($\epsilon = 0.01$) results in an instability curve which does not differ much (less than 2%) from considering $\epsilon = 0$. This is probably because the instability is on a morphological scale much larger than the hydrodynamical one so that the fluid adjusts instantaneously to the topographic changes. However differences appear, though primarily more in the magnitude of the growth rate rather than in the wavelength, when comparable values are used for the time and hydrodynamical scale (i.e. $\epsilon = 0.1$).

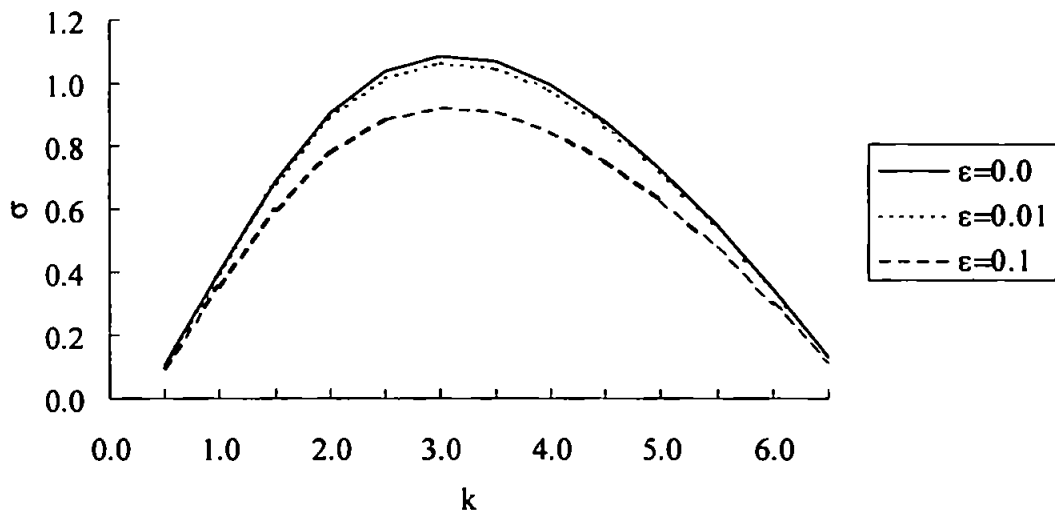


Figure 3.14 Instability curves for different values of ϵ , $r=0.5$, $N=0.01$, $\gamma=0.02$, $\alpha(0)=0.1$

Simulations have also been performed in such a way that the sediment transport parameterisation is very similar to the approach given by Bowen (1980) and Bailard (1981). As shown in section 3.2.4, this approach results in a stirring coefficient and in a morphodynamic diffusion increasing inside the surf zone as off-shore distance to a power of $3/2$ and $5/2$ respectively; and decreasing out of the surf zone to a power of $-9/4$ and $-15/4$ respectively. The pattern obtained through this simulation is qualitatively similar to that for the quadratic function of offshore distance. The only difference is that the perturbation is smaller than that showed in Figures 3.7 and 3.8. The use of such exponents should not be considered as an attempt to obtain more realistic results (in the next sections it will be shown that field conditions exhibits much more complex behaviours) but to indicate the robustness of the results and the possible link with already accepted approaches.

So far only a sediment transport stirring function, $\alpha(x)$, which increases through the surf zone has been considered. The use of a constant value of α throughout the whole cross-shore section does not affect the process generating the instability and all the results of the sensitivity analysis previously shown are confirmed, although growth rates are much larger (Figure 3.15, 3.16, 3.17). It is again possible to see that the influence of the friction coefficient r is primarily on the strength of the growth rate and only in a negligible way the wavenumber. An increase in the maximum value of the morphodynamic diffusion profile γ and of the eddy viscosity coefficient N again results in a decrease in the growth rate but also in a decrease in the peak wavenumber. For the other cases a decrease of the wavenumber is observed with increasing the parameter. Compared to the previously analysed cases, results seem to indicate a higher variability of the wavelength such that the spacing of the bedforms may vary between 2 and 6 times the width of the surf zone.

The difference between an increasing $\alpha(x)$ and a constant $\alpha(x)$ is much more evident when the bottom perturbation and the flow pattern are analysed. For constant α the shape of the bottom perturbation (Figure 3.18) now extends to the shoreline and is not restricted to around the breaking line. The flow (Figure 3.19) is off-shore over the shoals so that the final pattern, for both flow and topography, is very similar to that related to rip currents and giant cusps as reported by different authors (Shepard, 1963; Komar, 1971). The mirroring effect is not present anymore, as can be clearly seen from the 3d view given in Figure 3.20. The flow pattern obtained is again in accordance with the theoretical analysis in section 3.3 since α/D is now decreasing through the surf zone. The case of constant α does not present any other mode with a positive growth.

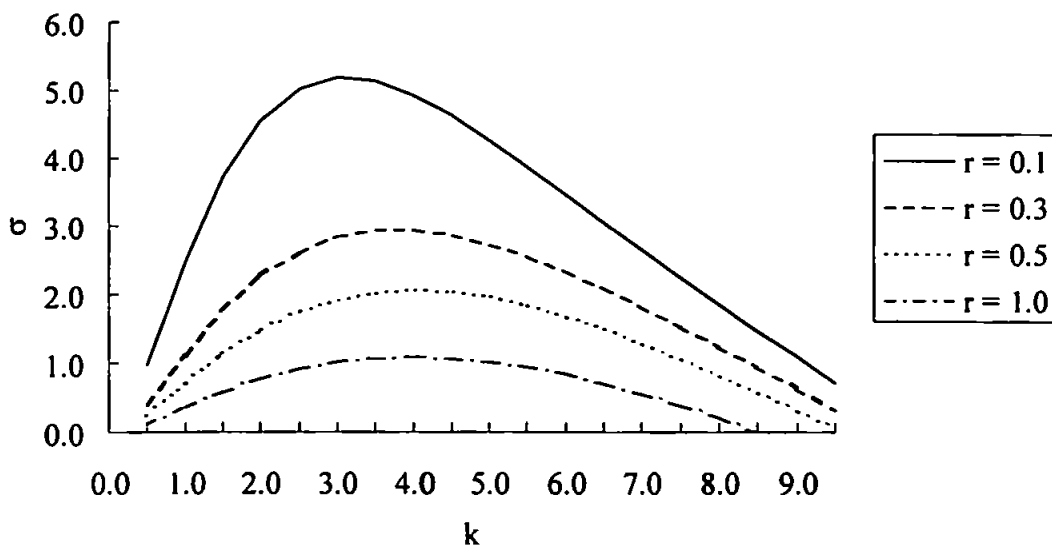


Figure 3.15 Instability curves for different values of r , $N=0.01$, $\gamma=0.02$, $\alpha(x)=\text{constant}$

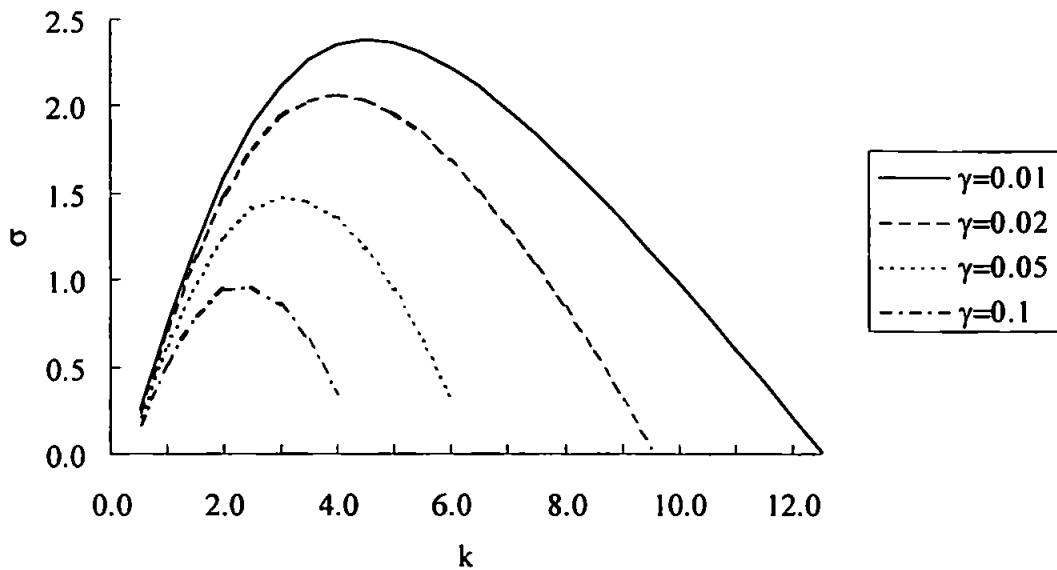


Figure 3.16 Instability curves for different values of γ , $r=0.5$, $N=0.01$, $\alpha(x)=\text{constant}$

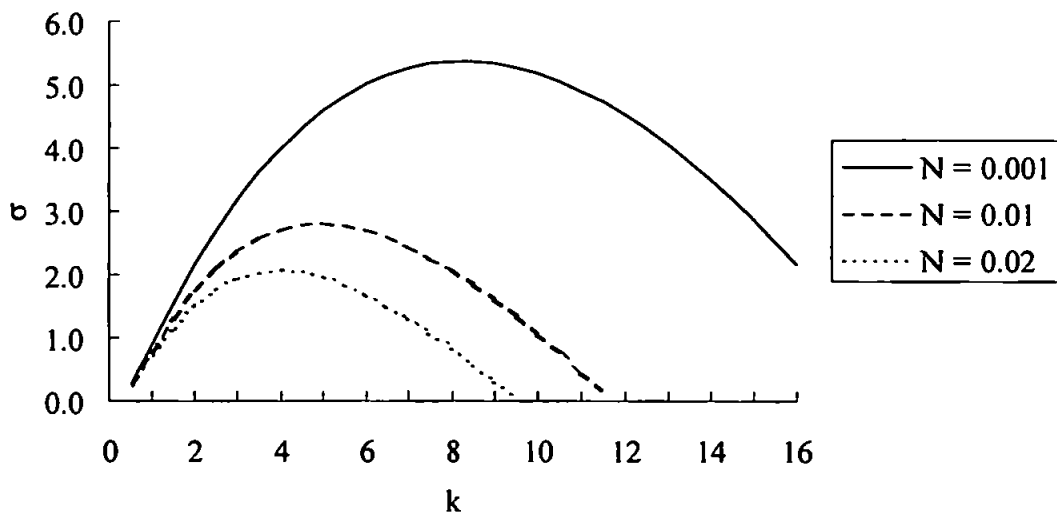


Figure 3.17 Instability curves for different values of N , $r=0.5$, $\gamma=0.02$, $\alpha(x)=\text{constant}$

Because of the different patterns obtained only by changing the stirring function from a quadratic law to a constant value, the conditions responsible for the change from one behaviour to the other have been investigated. As previously indicated, the quadratic law considered depends on an initial value, arbitrarily assigned, at the shoreline. By increasing this value it is possible to analyse the transition from one behaviour to the other. Note that, because of the non-dimensional variables used throughout this study, a value of 1 at the shoreline would mean a constant stirring coefficient in the surf zone. For example, a value of the stirring function at the shoreline equal to 0.3 results in the perturbation pattern shown in Figure 3.21. Here the perturbation is already different from that observed in Figure 3.7, with the patterns only present outside the surf zone, although still resembling

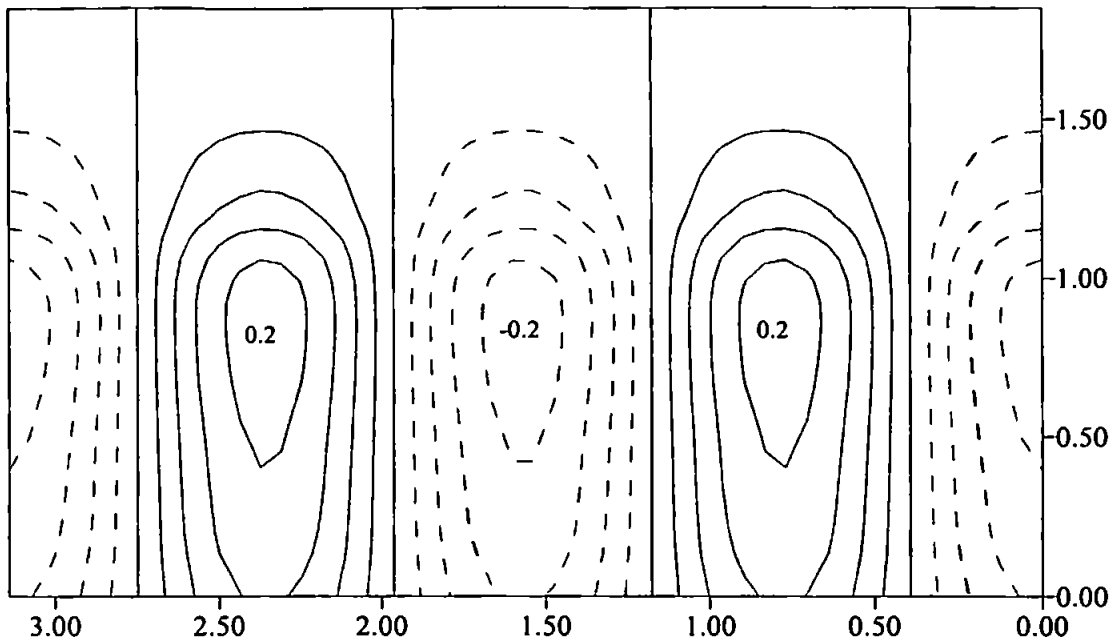


Figure 3.18 Contour lines of the topographic perturbation for $k=4.0$ ($r=0.5$, $N=0.01$, $\gamma=0.02$, $\alpha(x)=\text{constant}$)

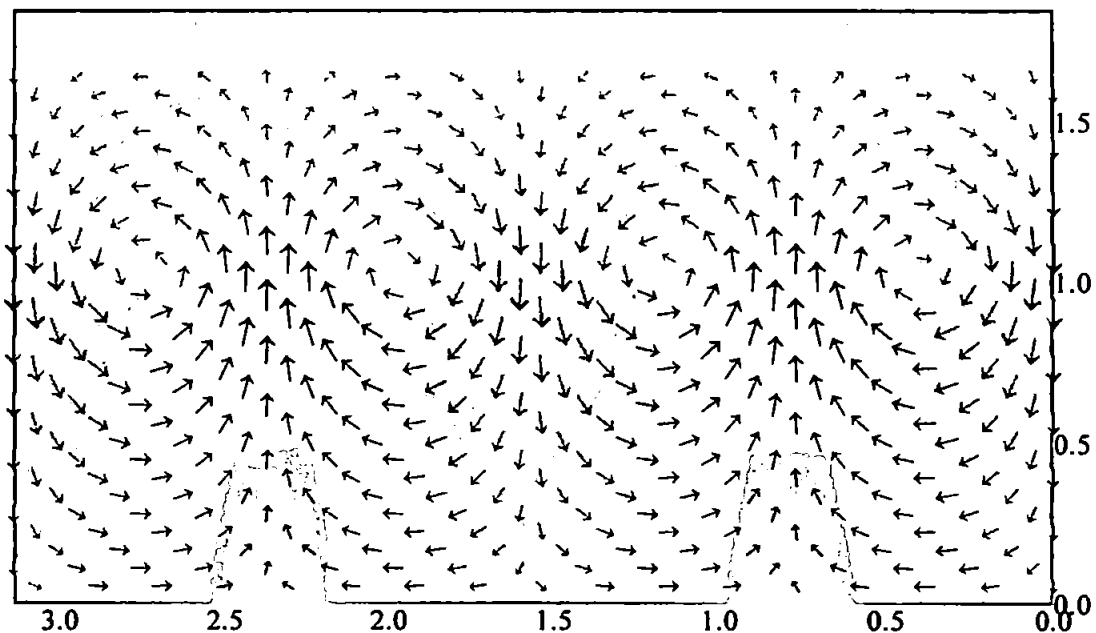


Figure 3.19 Topographic perturbation and relative flow pattern for mode for $k=4.0$ ($r=0.5$, $N=0.01$, $\gamma=0.02$, $\alpha(x)=\text{constant}$)

crescentic forms. Further increase of the stirring coefficient at the shoreline results in the patterns shown in Figure 3.22 and Figure 3.23 respectively for $\alpha(0)=0.5$ and $\alpha(0)=0.7$. It is evident that the perturbation is extending its effect towards the shoreline and that, rather than crescentic forms, patterns more similar to those shown in Figure 3.18 are present.

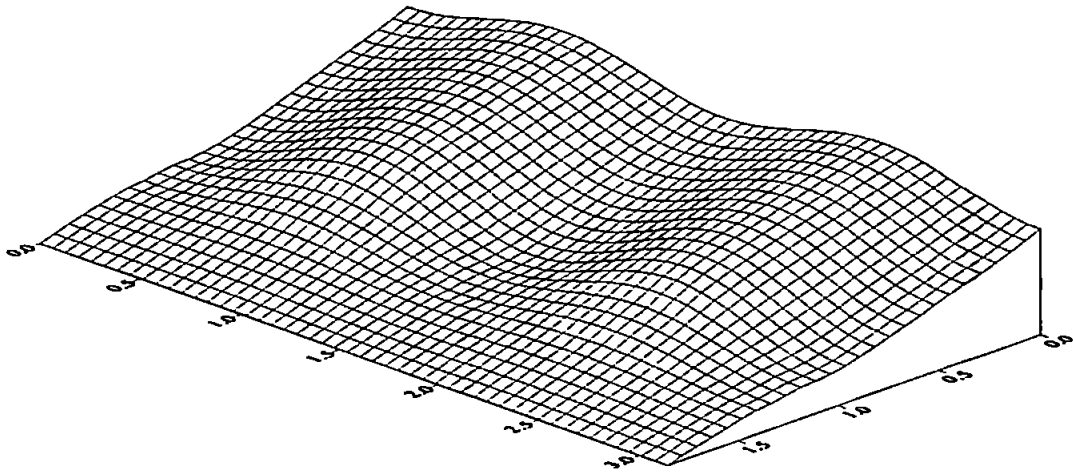


Figure 3.20 3d-view of the topographic perturbation (basic slope and perturbation amplitude have been chosen arbitrarily) for $k=4.0$ ($r=0.5$, $N=0.01$, $\gamma=0.02$, $\alpha(x)=\text{constant}$)

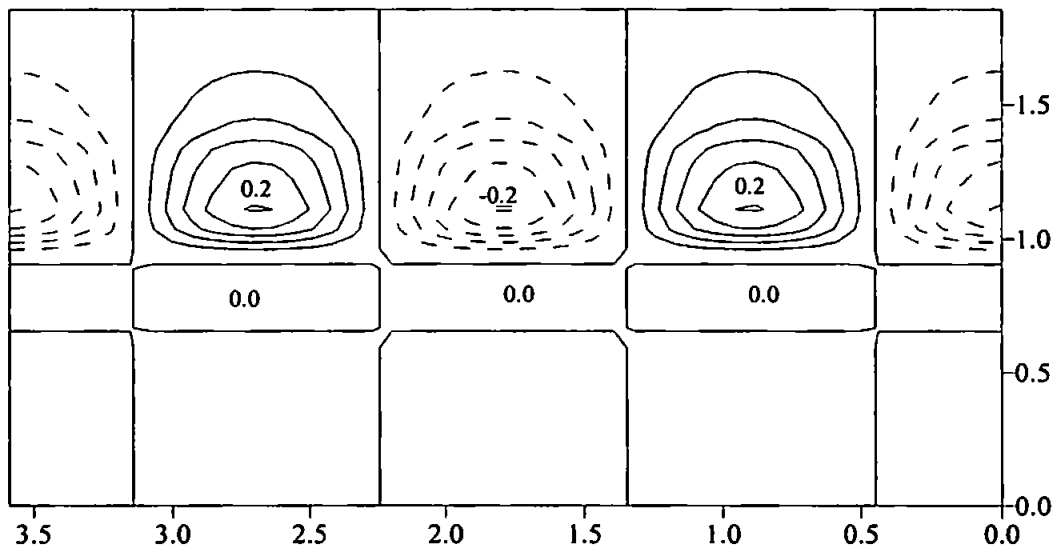


Figure 3.21 Contour lines of the topographic perturbation for $k=4.0$ ($r=0.5$, $N=0.01$, $\gamma=0.02$, $\alpha(0)=0.3$)

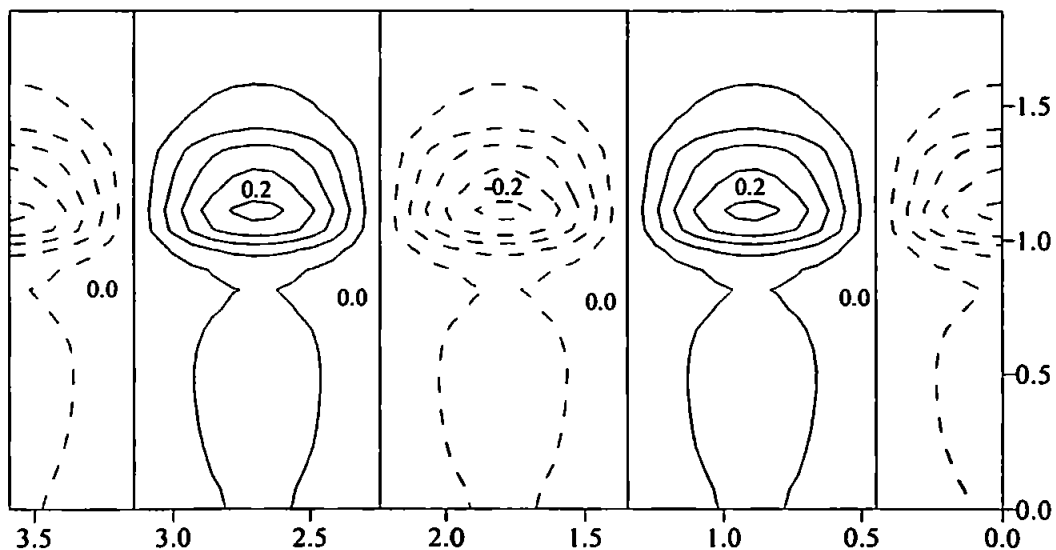


Figure 3.22 Contour lines of the topographic perturbation for $k=4.0$ ($r=0.5$, $N=0.01$, $\gamma=0.02$, $\alpha(0)=0.5$)

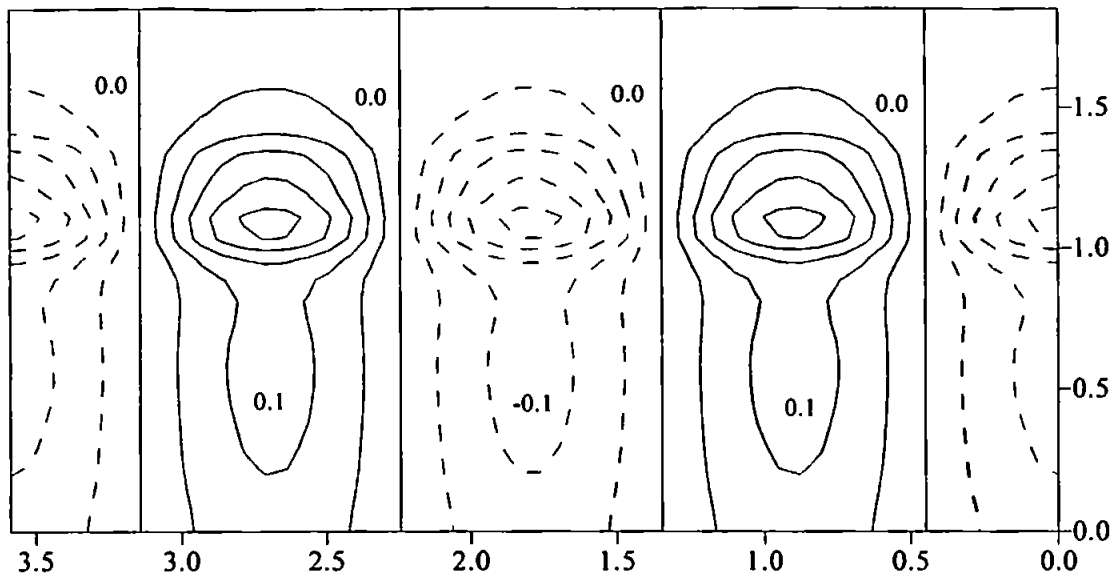


Figure 3.23 Contour lines of the topographic perturbation for $k=4.0$ ($r=0.5$, $N=0.01$, $\gamma=0.02$, $\alpha(0)=0.7$)

As an example of a stirring coefficient $\alpha(x)$ which is decreasing from the shoreline, an exponentially decaying form has also been studied. As discussed in section 3.2.4, such runs might simulate conditions where reflection at the shoreline or infragravity motions are predominant. The morphology resulting from such simulations is always that previously associated with the "giant cusps" patterns, and the only effect of increasing the power of the exponential decay is a shift of the maximum of the perturbation towards the shoreline.

3.5 Discussion

It has been shown that the perturbations of the incident wave radiation stress induced by the topographic irregularities in a saturated surf zone can drive a cellular flow with a sediment transport pattern which is able to reinforce the bottom perturbations. In this way a positive feedback that leads to the coupled growth of nearshore large scale bedforms and horizontal circulation with rip currents may occur. Basically, two instability modes may appear depending upon the form of the sediment stirring function, $\alpha(x)$.

For an α function with an increase seaward across the surf zone a "crescentic pattern" is generated. This consists of alternating shoals and pools on both sides of the breaking line, showing a "mirroring effect". The associated flow pattern extends through the whole surf zone but has its maximum strength around the breaking line. The alongshore wavelength of such features ranges between 2 and 4 times the surf zone width, X_b , and depends on the bottom friction, lateral momentum diffusion and morphological diffusion.

Alternatively, for an α function more or less constant or even decreasing seaward across the surf zone, a “giant cusp pattern” occurs. This consists of transverse bars attached to the shoreline and extending across the whole surf zone. The associated flow has rips over the crests and a return flow in between. For simplicity, the present linearised model keeps the shoreline fixed. However, it seems conceivable that a model capable of describing shoreline changes would generate cusps at the shoreline attachments of these bars. The alongshore spacing between the bars is between 2 and 6 times X_b , typically somewhat longer than the wavelength of the crescentic pattern. Bottom friction, lateral momentum diffusion and morphological diffusion are the damping factors on both instability modes. However, for values of the damping parameters in accordance with the literature (see, for example, Horikawa 1988), growth rates are usually positive.

An indication of the order of magnitude of the growth time of these features can be obtained from the morphological time scaling defined in eq. 3.18. According to the data reported in Antsyferov and Kos'yan (1990) or by Russell (1993), 5 Kg/m^3 seems to be an appropriate order of magnitude of the suspended sediment concentration. Assuming a reference depth of 0.5 m one obtains $\bar{\alpha} \approx 10^{-3} \text{ m}^3/\text{m}^2$. The velocity scale can be calculated from the Froude number used in the computations, $F=0.12$, so that $U = 0.12\sqrt{g\beta X_b}$. Thus, one can estimate:

$$T_{\text{gro}} \approx 2.6 \cdot 10^3 \beta^{1/2} X_b^{3/2} \sigma^{-1}$$

By assuming a growth rate of $\sigma \approx 1$, a beach slope $\beta \approx 0.05$ and a surf zone width of $X_b \approx 10\text{m}$, the features, whose wavelength would be about 30m, would grow significantly within some 5 hours. According to this, bedforms for $X_b \approx 5\text{m}$, would grow within 1.8 hours, while very large bedforms for $X_b \approx 20\text{m}$ would not grow significantly until some 14 hours. These figures seem very sensible and suggest that the larger scale bedforms are not observed very often perhaps due to the fact that their growth time is longer than the typical time scale of wave conditions' variability.

For suspended sediment transport, the function α in equation (3.12) models the cross-shore profile of the depth-integrated mean suspended sediment concentration. The relatively small number of published observations of mean concentration in the nearshore zone confirm that this cross-shore profile can take any of the qualitatively different forms which have been used here. Antsyferov and Kos'yan (1990) show measurements from a natural beach under ‘relatively constant small swell’ (estimated breaker height ca. 1m), where mean concentrations increase seawards from near-zero at the shoreline, reach a maximum

at the breakpoint and then decay further seawards. This profile shape is qualitatively similar to the form resulting in the crescentic topography (Figures 3.7 and 3.8). On the other hand, observations described by Hwang et al. (1997) from a beach of mild slope and offshore wave heights of between 1.6 and 2.2m, show almost constant concentration through the surf zone, a form found to create giant cusp topography (Figures 3.18 and 3.19). The observations of Russell (1993), for a breaker height in excess of 3m, suggest that during storm conditions the concentration can even increase towards the shoreline, a form of which also creates giant cusp topography.

Breaking incident waves alone would be expected to result in concentrations which decrease towards the shore; the simple model of the stirring effect of breaking wave currents described in section 3.2.4 is in fair agreement with the observations of Antsyferov and Kos'yan (1990). However, waves reflected at the beach would have significant amplitude at the shoreline (see also section 3.2.4). There is strong evidence that long-period reflected wave height and velocity increase approximately linearly with breakpoint wave height (Guza, 1982; Huntley et al., 1993). Thus the cross-shore concentration profiles observed by Hwang et al.(1997) and Russell(1993) for larger incident waves heights may be the result of the addition of significant long wave stirring, with a profile which would generally increase towards the shoreline. In fact Russell (1993) shows that long wave motion was dominant for his observations from the inner surf zone.

These considerations suggest that crescentic patterns are likely to occur under relatively low wave conditions, but that giant cusp patterns are more likely under high wave conditions, when reflected long-period motion becomes significant. There is also the intriguing possibility that very low amplitude incident waves, with a high reflection coefficient, will also result in giant cusp patterns. These patterns may be related to beach cusps which are often observed under these conditions.

These speculations clearly need further investigation. In particular the assumption that long period motion is simply a stirring mechanism, affecting the results only through α , neglects its direct contribution to the hydrodynamics. Direct influence through the bottom shear stress (equation 3.13) is not expected to be qualitatively significant (see figure 3.4). Other limitations of the present study are that only regular incident waves have been considered and that the effect of incident wave refraction by the growing bedforms and the currents on the instability mechanism has been neglected. Also, the variation of the breaking point as soon as the instability reaches a significant amplitude can be very important, in particular

for the crescentic pattern, and deserves future research. The robustness of the instability mechanism with respect to using non-linear (in the mean flow) sediment transport is worth investigating too.

Having investigated the possibility of “free behaviour” in the surf zone, attention in the next chapters will be turned towards the swash zone and the formation of beach cusps. Such features have been investigated for more than 50 years, several formation theories have been proposed and a considerable number of field and laboratory measurements exists. Still, it is not clear whether beach cusps are the result of an hydrodynamic “forcing” characterised by an alongshore structure (“forced behaviour”) or the result of self-organisation processes (“free behaviour”).

Chapter 4: Beach cusps: a comparison of data and theories for their formation

A shortened version of this chapter has been published in the Journal of Coastal Research (vol. 15, no. 3, pp. 741-749) by Coco, G., O'Hare, T.J., and Huntley, D.A. with the title: "Beach cusps: a comparison of data and theories for their formation".

4.1 Introduction

Shorelines are rarely straight for long distances. More often, they look like an extremely irregular series of forms in which no system can be detected. At times the pattern is regular, there being a series of cusped forms uniformly spaced in the alongshore distance. These ridges of sediment, built by wave action, trending at right angles to the shoreline, and separated by bays are commonly known as "beach cusps" (Figure 4.1, Plate 4.1, Plate 4.2). These kinds of rhythmical longshore patterns are concave seaward and have been observed both in field and laboratory studies. Because of their regularity, as well as their common occurrence, beach cusps have attracted many observers and much speculation has been made concerning their origin. A full comprehension of the mechanism for beach cusp formation and development would substantially contribute to the understanding of swash processes in terms of both hydrodynamics and onshore-offshore sediment transport.

A classification of cusped forms according to their longshore spacing (horn to horn), but not related to the physical processes, has been proposed (Dolan and Ferm, 1967) and is widely accepted as a method for better identification of this natural phenomenon. The smallest of these forms are called "beach cusplets" ($\cong 1.5$ m), but more typical are the larger "beach cusps" which range from about 8 to 25 m and whose life could last even days. Still larger crescentic forms include "storm cusps" (70 ~ 120 m) and "giant cusps" (700 ~ 1500 m). Such features are characteristic of periods of relatively heavy seas and might be even associated with the presence of strong littoral currents.

More useful, in relation to the physical processes, is the classification proposed by Inman and Guza (1982) indicating only two types of beach cusps: surf-zone cusps and swash cusps. The first, herein modelled in chapter 3, are formed by the currents of the nearshore circulation cell and shape the beach on a scale that is of the order of the surf zone width. The second term refers to cusps formed by the swash and backwash acting directly on the beach face and berm.

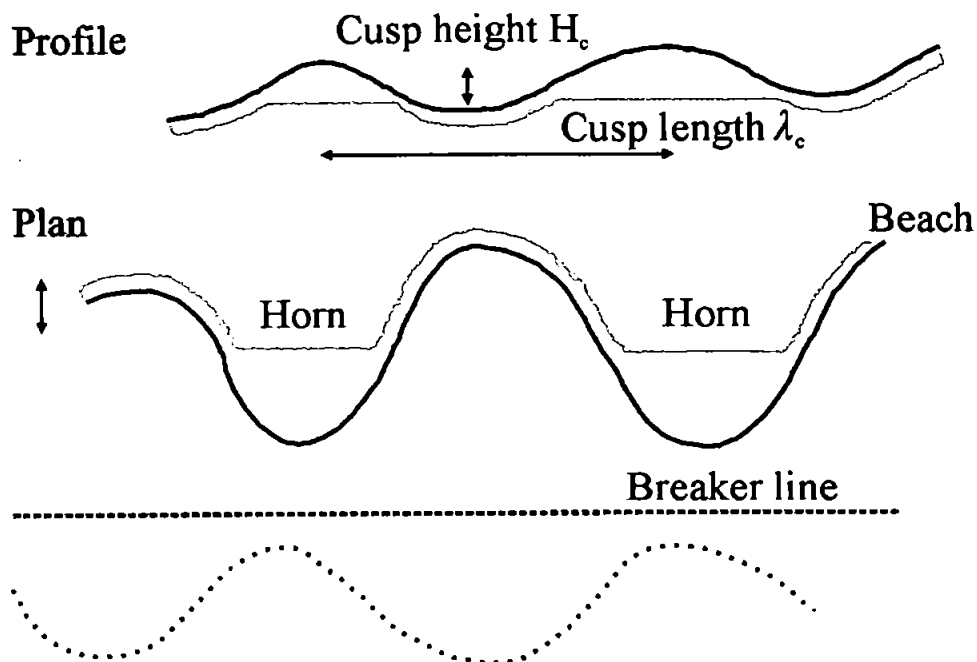


Figure 4.1 Planar and profile view of a cusped system

In this chapter all the available observations and measurements concerning field and laboratory investigations will be reviewed underlining beach and wave conditions corresponding to beach cusp formation and development. The principal features of theories concerning beach cusp formation and development will then be reviewed. The available measurements will be finally used to test the possible correlation with specific parameters and with the existing theories.

4.2 Field and laboratory observations

A large amount of observations and measurements of beach cusps are reported in the scientific literature. All these data have been collected in order to summarise the distinctive beach cusp features observed by different authors in field (Table I) and laboratory (Table II) investigations. Sources of error are present as, for example, some authors do not specify if the wave height they provide refers to the offshore or to the breaking value. On the other hand, the evaluation of the beach slope for a cusped beach is a difficult task and another possible source of error. Nevertheless, this data set will be used throughout this chapter in order to test the existing theories for cusp formation and development and will be denoted as the “Cusp Data Set”.



Plate 4.1 Beach cusps (courtesy of Tony Bowen, Dalhousie University, Canada)



Plate 4.2 Beach cusps (courtesy of Tony Bowen, Dalhousie University, Canada)

Table I Summary of parameters for field data (for notes see bottom of Table)

Author	$\tan \beta$	d (mm)	λ_c (m)	H (m)	T (sec)	S (m)	H_c (m)	
Krumbein (1947) ^(a)	0.179 ^(b)	0.83 ^(b)	66.6	1.84	9.3			
	0.188 ^(b)	0.60 ^(b)	54.6	1.85	9.8			
	0.099 ^(b)	0.51 ^(b)	52.5	1.71	8.8			
	0.124 ^(b)	0.34 ^(b)	52.2	1.58	9.9			
	0.179 ^(b)	0.23 ^(b)	52.5	1.37	8.7			
	0.198 ^(b)	0.90 ^(b)	44.7	1.88	12.5			
	0.146 ^(b)	0.51 ^(b)	44.1	1.88	10.7			
	0.204 ^(b)	0.27 ^(b)	45.9	1.40	11.1			
Longuet-Higgins & Parkin (1962) 12-4-56	0.134	2.54	4.9		3.7			
23-4-56	0.157		2.8		2.85			
24-4-56	0.114		2.8		3.55			
9-6-56	0.2	0.254 -2.54	4.3	0.46	6.2	1.82		
16-6-56	0.16		5.5	0.76	6.1	5.79		
21-6-56	0.14		4.3	0.30	5.4	3.66		
22-6-56	0.14		3.7	0.23	6.2	1.98		
23-6-56	0.14		4.0	0.08	6.85	1.37		
6-7-56	0.1		10.0	1.07	5.0	13.72		
8-7-56	0.09		6.4	0.46	6.3	6.10		
9-7-56	0.09		6.4	0.38	6.3	5.18		
10-6-56	0.1		8.8	0.76	6.2	10.67		
King (1965)	0.045	Horn 0.346	Bay 0.277	14.8	9.5		0.198	
Williams (1973) 2-10-69	0.105	0.1 - 2		5.6	0.15	3.5	3.5	0.089
13-1-70	0.094			4.4	0.15	5	4.5	0.096
19-1-70	0.096			7.0	0.10	6	4	0.075
21-1-70	0.096			7.3	0.15	6	4	0.098
22-1-70	0.144			6.0	0.15	4	5	0.095
2-2-70	0.135			14.2	0.20	5	6	0.121
3-2-70	0.156			10.0	0.10	5.5	4	0.103
14-4-70	0.1			11.8	0.10	3.5	5.5	0.082
25-6-70	0.137			3.8	0.25	4	2	0.145
25-7-70	0.144			4.5	0.15	6	2	0.129
7-9-70	0.094			6.0	0.15	9	4	0.09
2-12-70	0.149			5.6	0.15	7.5	4	0.129
19-1-71	0.138			6.4	0.10	10	5.5	0.009
1-6-71	0.124			4.8	0.25	4	2	0.118
Komar (1973) May-1971	Horn	Bay	Horn	Bay	0.304	1.0		
21-6-71	0.123	0.087	2.19		0.322	1.0	0.13	
22-6-71	0.154	0.07	1.15	0.76	0.591	1.4	0.20	
29-6-71		0.07	2.30	0.52	0.292	2.0		
8-7-71	0.092	0.087			0.229	1.0	0.18	
15-6-72	0.128	0.07	0.49	0.23	0.11	1.3	0.21	
17-6-72	0.056	0.056	1.60	1.21	0.21	0.9	0.22	
15-5-73	0.105	0.105	1.41	0.91	0.275	1.0	0.15	
17-5-73	0.114	0.114	1.20	0.87	0.207	0.77	0.15	
Darbyshire (1977) ^(a)								
18-7-75	0.062 ^(b)			20.0	1.3	8.5		
20-8-75	0.088 ^(b)			22.85	1.5	12.5		
				11.42	0.5	8.3		
6-2-76	0.053 ^(b)			29.0	1.5	19.5		
5-9-75	0.034 ^(b)			6.0	0.4	11.75		
26-2-76-3-3-76	0.049 ^(b)			12.0	1.5	13.33		
21-5-76	0.059 ^(b)			13.7	5	8.0		
Dubois (1978) 10-8-76	Horn	Bay						
	0.146	0.1	0.31	35.0	0.6	10		
Dubois (1981) 5-28-6-79	0.096	0.078	0.33	32.5	1.3	7-11	0.34	
Huntley & Bowen (1978)	0.081		sand	12.7	0.12	6.9	7.8	
Sallenger (1979)	0.07			12.3	0.17	6.5		
	0.07			10.9	same	6.5		

Table I Summary of parameters for field data (continued)

Author	$\tan \beta$	d (mm)	λ_c (m)	H (m)	T (sec)	S (m)	H_c (m)
Sallenger (1979)	0.06		8.6	same	6.5		
	0.111		5.4	0.07	3.9		
	0.091		5.4	0.07	3.9		
	0.099		3.6	0.07	3.9		
	0.16		0.7	few cms	2.3		
	0.099		0.7	few cms	2.3		
Dean & Maurmeyer (1980)	0.04	0.2	23.2	0.335	15.4	12.5	
Guza & Bowen (1981)	0.075		12.6		7.14		
	0.07		8				0.045
	0.07		20				0.035
	0.17		67.5				1.0
	0.10		21.4				0.1
	0.10		43				0.41
	0.086		66				0.49
	0.097		76				0.61
	0.104		71				0.61
	0.085		51				0.27
	0.130		61				0.86
	0.08		7.3				0.09
	0.08		11.5				0.13
0.07		13.5				0.17	
Inman & Guza (1982)	0.083		46				0.77
	0.2		38				1.3
	0.2		44				1.8
	0.335		18.3				1.0
Takeda & Sunamura (1983) ^(a)	0.120 ^(b)	0.34	35	1.30	8.0	15	
	0.097 ^(b)	0.34	20	0.66	6.3	14	
	0.083 ^(b)	0.30	28	0.98	9.2	12.5	
	0.106 ^(b)	0.30	22	0.74	6.5	8.5	
	0.097 ^(b)	0.30	16	0.66	6.3	8	
	0.053 ^(b)	0.28	21	0.98	9.2	11	
	0.109 ^(b)	0.28	15	0.76	8.4	15	
	0.126 ^(b)	0.28	25	0.86	7.8	15	
	0.060 ^(b)	0.28	22	1.48	9.8	18	
	0.091 ^(b)	0.28	17	0.74	6.5	12	
0.162 ^(b)	0.28	15	0.66	6.3	11		
0.092 ^(b)	0.28	19	0.48	5.6	12.5		
Orford & Carter (1984)	0.1-0.13	0.176-1.0	42.5	<10	9-11.5		0.9
			61.3				0.9
Seymour & Aubrey (1985)	0.05	0.23	40	0.60	16		0.75
Miller et al. (1989)	0.07-0.105	Sand	36.0	5 (max)	10-12		0.5
Rasch et al. (1993)	0.14		7.4		2.6		
Sherman et al. (1993)	0.169	0.15-0.25 20-250	20-25	0.41	6.5		
Allen et al. (1996)	0.119	0.47	27.5	0.48	16.7	17	
Holland & Holman (1996)							
15-10-94	0.083	0.35	36	3.1	10.9		
16-10-94			29	3.5	11.2		
17-10-94			32	2.1	10.6		
18-10-94			36	1.5	11.5		
19-10-94			40	1.3	14.2		
20-10-94			37	1.2	13.5		
21-10-94			20	0.9	11.3		
Masselink & Pattiarat. (1998)							
7-3-95	0.11	0.4	30	0.3	13	15	
10-2-96	0.14	0.5	40	0.55	17	18	
14-2-96	0.18	0.5	20	0.4	11	10	
Nolan et al. (1999) 25-2-93	0.087		29.77				0.30
21-5-93	0.087		30.55				0.60
2-3-93	0.052		26.60				0.20

Table I Summary of parameters for field data (continued)

Author	$\tan \beta$	d (mm)		λ_c (m)	H (m)	T (sec)	S (m)	H_c (m)
Nolan et al. (1999) 18-4-93	0.061	Horn	Bay	26.46				0.40
18-2-93	0.105			25.50				0.30
4-5-93	0.445	51.27	30.06	15.90				0.30
17-2-93	0.101	0.16	0.14	11.40				0.20
12-1-93	0.141			12.20				0.35
26-3-93	0.087			18.18				0.70
2-4-93	0.123			26.36				0.80
31-5-93	0.087	28.84	1.80	20.45				0.70
16-12-92	0.087	3.68	0.47	18.49				0.40
12-1-93	0.096			14.95				0.45
3-2-93	0.105			23.32				0.75
26-3-93	0.087			9.44				0.30
18-2-93	0.123	9.85	1.45	4.58				0.30
16-4-93	0.268			13.10				0.50
5-7-92	0.123			46.36				0.30
8-5-93	0.141			25.74				0.85
25-9-92	0.079			32.54				0.20
30-5-95	0.052	7.83	1.15	2.95				0.05
15-5-93	0.052	0.13	0.16	33.71				0.10

Notes:

^(a) edge wave wavelength taken from graph or table;

^(b) values estimated with formulae;

$\tan \beta$ = beach slope;

d = mean diameter;

λ_c = cusp spacing;

H = wave height;

H_c = cusp height;

T = wave period;

S = swash excursion.

Table II Summary of parameters for laboratory data (for notes see bottom of Table I)

Author	$\tan \beta$	d (mm)	λ_c (m)	H (cm)	T (sec)	S (m)	H_c (m)
Longuet-Higgins & Parkin (1962)	0.185	fine sand	0.533	1.7	1.5	0.254	
Guza & Inman (1975)	0.105	fine sand	1.8		2.4		
	0.105	fine sand	1.0		2.7		
			0.025				
Dalrymple & Lanan (1976)	0.163	sand	1.14	1.25	1.04		
	0.146	sand	1.32	1.25	0.96		
			1.05		0.92		
			1.05		0.90		
Sunamura et al. (1977) ^(a)	0.102 ^(b)	0.20	0.13	1.3	0.56		
	0.102 ^(b)	0.20	0.12	1.5	0.56		
	0.102 ^(b)	0.20	0.16	2.0	0.56		
	0.102 ^(b)	0.20	0.15	2.2	0.56		
	0.102 ^(b)	0.20	0.16	2.8	0.56		
Ann (1979) ^(a)	0.106 ^(b)	0.2	0.20	3.0	0.85		
	0.100 ^(b)	0.2	0.17	2.8	0.78		
	0.106 ^(b)	0.2	0.24	4.1	0.86		
	0.100 ^(b)	0.2	0.24	4.1	0.78		
Tamai (1980) ^(a)	0.106 ^(b)	0.28	2.21	7.5	2.20		
	0.106 ^(b)	0.28	1.73	12.6	2.19		
	0.101 ^(b)	0.28	1.28	11.3	1.78		
	0.109 ^(b)	0.28	1.40	12.8	1.80		
Guza & Bowen (1981)	0.105	sand	1.3		2.7		0.014
Takeda & Sunamura (1983)	0.1	0.69	0.34	4.2	1.0	0.20	
	0.1	0.69	0.20	2.0	1.0	0.10	
Kaneko (1985)	0.081	0.0028	1.5	3.4	2.38		
	0.081	glass beads	0.75	3.1	1.72		
	0.081	of $\rho=2.43$	0.50	2.7	1.71		
	0.081		0.75	3.3	1.58		
	0.081		0.50	4.0	1.27		
	0.081		0.38	3.5	1.15		
	0.081		0.30	3.5	0.85		
	0.107		0.30	3.5	1.11		
	0.107		0.38	3.2	1.06		
	0.107		0.25	3.3	1.01		
	0.107		0.30	3.4	0.98		
	0.107		0.30	3.0	0.94		
	0.107		0.25	3.0	0.88		
	0.107		0.21	3.5	0.76		
	0.118		0.75	3.6	1.38		
	0.141		0.75	2.6	1.38		
	0.141		0.38	4.2	0.98		
Takeda et al. (1986)	0.30	0.69	0.10	0.6	0.8	0.076	
	0.30	0.69	0.13	0.7	0.9	0.092	
	0.32	0.69	0.125	1.0	0.9	0.126	
	0.32	0.69	0.129	1.0	0.9	0.129	
	0.30	0.69	0.13	1.1	0.9	0.125	
	0.31	0.69	0.16	1.3	1.0	0.133	
	0.25	0.69	0.17	1.4	1.0	0.130	
	0.23	0.69	0.23	0.8	1.2	0.149	
	0.23	0.69	0.20	0.9	1.2	0.167	
	0.24	0.69	0.23	1.8	1.2	0.190	
	0.36	1.30	0.10	1.3	0.8	0.085	
	0.36	1.30	0.125	1.8	0.9	0.08	
	0.33	1.30	0.125	1.0	0.9	0.108	
	0.30	1.30	0.125	1.3	0.9	0.136	
	0.26	1.30	0.20	1.4	1.2	0.201	
	0.24	1.30	0.20	1.5	1.2	0.20	
	0.24	1.30	0.20	1.8	1.2	0.239	
0.26	1.30	0.20	2.1	1.2	0.240		

Particular attention has been also been paid to the nature of cusp occurrence, sedimentology and current patterns. It will be subsequently shown that different observations disagree so strongly that a unifying explanation for their formation can not be given and that a better assumption is given by considering cusps as a final equilibrium configuration for different mechanisms.

4.2.1 Beach cusp occurrence and nature

A very interesting set of observations from sites spread throughout the world (Russell and McIntire, 1965) reveals that cusps develop in a wide variety of beach deposits ranging from boulders to fine sand and suggests that cusp spacing might increase with wave height. Later studies have confirmed that beach cusps occur more frequently on coarse-sand and gravel beaches or where the beach material contains a mixture of sand and shingle. The importance of wave conditions will be investigated in detail later in this chapter.

As beach cusps have been observed also in lakes (Komar, 1973), or during all the stages of the tide, the role of tides in cusp formation is not of fundamental importance. Nevertheless, it seems evident that the presence of tides can largely influence beach morphology, which in turn affects the process of formation and development of beach cusps (Longuet-Higgins and Parkin, 1962; Dubois, 1978). It is also clear that the importance of tides on beach cusp formation depends on the tidal range through its effect on providing a "fixed" shoreline for a time long enough to allow cusp development. This could probably be the reason why, on gentle slopes, cusps are more likely to appear if the site is characterised by diurnal tides rather than semi-diurnal or, more generally, by a small tidal range. As a result of tidal variation, it is also possible to observe, on the same beach, more than one set of cusps (Russell and McIntire 1965, Williams, 1973; Komar, 1998; Nolan et al. 1999). In all these cases, the largest cusp spacings occur at the top of the beach. Nolan et al. (1999) measured cusp dimensions over a variety of sites (around 15 different locations) and concluded that the geometrical shape of these features remains the same, with the different dimensions (cusp spacing, depth, elevation, amplitude) proportionally changing with the site and with the forming conditions.

It is generally reported (Longuet-Higgins and Parkin, 1962; Russell and McIntire, 1965, Sallenger, 1979) that cusps form more frequently when the wave field is regular and the wave crests are parallel to the shoreline. It should also be underlined that other

investigations indicate that cusps could form under an oblique wave approach or even under intersecting wave trains (Dean and Maurmeyer, 1980). A very interesting study, based on nine years of images from Duck (U.S.A.), was recently undertaken by Holland (1998). He studied the preferential conditions for beach cusp formation and development and found that in 98% of cases, cusps appeared with waves approaching the shoreline with an angle of approach smaller than 12° .

Cusp formation has also been associated with the escape of ponded water from a ridge or other barriers on the berm (Dubois, 1978; Sallenger, 1979, Dubois, 1981). But, since beach cusps have also been observed in their absence, it is possible that, rather than a mechanism of formation, the presence of ridges or berms can only enhance or diminish cusp development.

Significant attention has also been given to the dissipative-reflective nature of the system, with cusps found to preferentially form on steep reflective beaches; Holland (1998) concluded that reflective conditions are required for cusp formation. Many authors have also emphasised the importance of the wave condition at the breaking point. It has generally been observed that cusps form with plunging breakers, though on this matter an interesting debate is still going on. For example, Kaneko (1985) performed a series of laboratory experiments concluding that cusp formation has only a weak correlation with the breaker type.

Another matter of controversy is the accretional or erosional nature of beach cusps. Smith and Dolan (1960) for example stated that "*truncation of primary structures by cusp surfaces constitutes the fundamental evidence for erosive origin*" while numerous other authors suggest an opposite behaviour (Kuenen, 1948; Russell and McIntire, 1965; Komar, 1973; Huntley and Bowen, 1978; Dean and Maurmeyer, 1980; Sato et al. 1981; Takeda and Sunamura, 1983; Holland and Holman, 1996; Masselink et al. 1997). In other cases, it has been shown that both mechanisms can coexist, producing and finally maintaining the typical sinusoidal shoreline form. Miller et al. (1989) show that, though a significant erosional and depositional sequence was measured, net aggradational or degradational changes on the beach were minor. Their sedimentologic and stratigraphic analysis provides significant indications of cusp formation processes as horns were characterised by parallel planar beds representing accretion deposit while scour seemed to be mostly concentrated in the bays. Such results were obtained during and subsequent to a storm, and this may be

the reason for the differences encountered with other authors. For example, Sallenger (1979) reports the development of cusped forms as being the product of both erosion and accretion but this time resulting in net accretion of the foreshore. Also of interest are results obtained by Antia (1989) on the Atlantic coast of Nigeria stressing the possible role of the presence of cusps as indicators of beach volumetric accretion and erosion.

Less controversy seems to exist concerning beach cusp destruction or inhibition due to strong longshore currents or storm waves, although even in this case literature reports one storm as having generated cusps (Orford and Carter, 1984). The most interesting link between cusps and storms has been pointed out by Holland (1998). His findings indicate that cusps usually appear 2-4 days after a storm. Storms would then be "useful" for cusp formation as they would flatten the topography and allow for cusps to develop. Furthermore, the site where Holland's (1998) study was performed (Duck, U.S.A.), typically shows a narrowing of the forcing frequency after a storm. Other authors (Inman and Guza, 1975) consider such narrow-bandedness conditions to be an essential requirement for beach cusp formation. Similar to a minor storm is also sea breeze that, as shown by Masselink and Pattiratchi (1998a), can reduce the prominence of a cusped shoreline.

4.2.2 The sediment properties of beach cusps

As previously stated, beach cusps usually develop on beach deposits ranging from boulders to fine sand and, as shown in Figure 4.2 where the Cusp Data Set has been used, no evident relationship between cusp spacing and mean diameter can be easily found. From a sedimentological point of view, the most important and typical feature observed on beach cusps is certainly the sorting of the sediments with the coarsest material in the horns and the finest in the bays (Plate 4.3). Although there seems to be a general acceptance of this phenomenon (Bagnold, 1940; Longuet-Higgins and Parkin, 1962; Russell and McIntire, 1965; Worrall, 1969; Komar, 1973; Williams, 1973; Sallenger, 1979; Chafetz and Kocurek, 1981; Dubois, 1981; Sherman et al., 1993) in a few cases it has been shown that such a sorting is not present (Williams, 1973; Dean and Maurmeyer, 1980). This could be probably due to the beach material (size and stratification) although Russell and McIntire (1965) observed that well-developed and stable cusps tend to reduce the difference in grain size between horns and bays. Closely related to the sorting is the observed and measured (Longuet-Higgins and Parkin, 1962; Antia, 1987) difference in permeability between horns

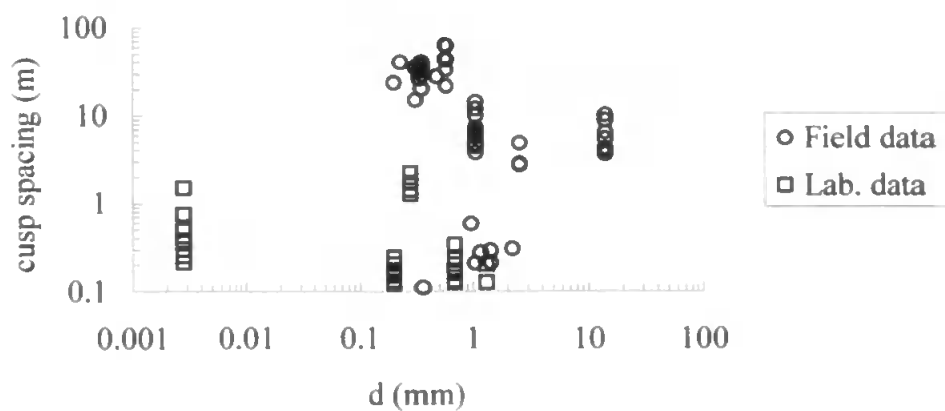


Figure 4.2 Variation of measured cusp spacing and mean diameter



Plate 4.3 Sediment sorting on a cusped beach (taken from Darbyshire, 1977).

and embayments, which could also have an influence on the motion of incoming waves encountering cusps and the following circulation.

Several times, it has also been reported that horns are steeper than bays and this kind of feature is an obvious complication when, in order to test one of the existing theories for cusp formation, the evaluation of an overall beach slope is required.

4.2.3 Current patterns

The nature of water movements in the cusp region is another matter of controversy. However, the results found by Bagnold (1940), supported by numerous authors' observations (Longuet-Higgins and Parker, 1962; Komar, 1973; Dean and Maurmeyer, 1980) using small particles of dye or equivalent, tends to be mainly accepted. In this case a wave appears to advance up the beach until it meets the seawards extremities of the cusps (Figure 4.3).

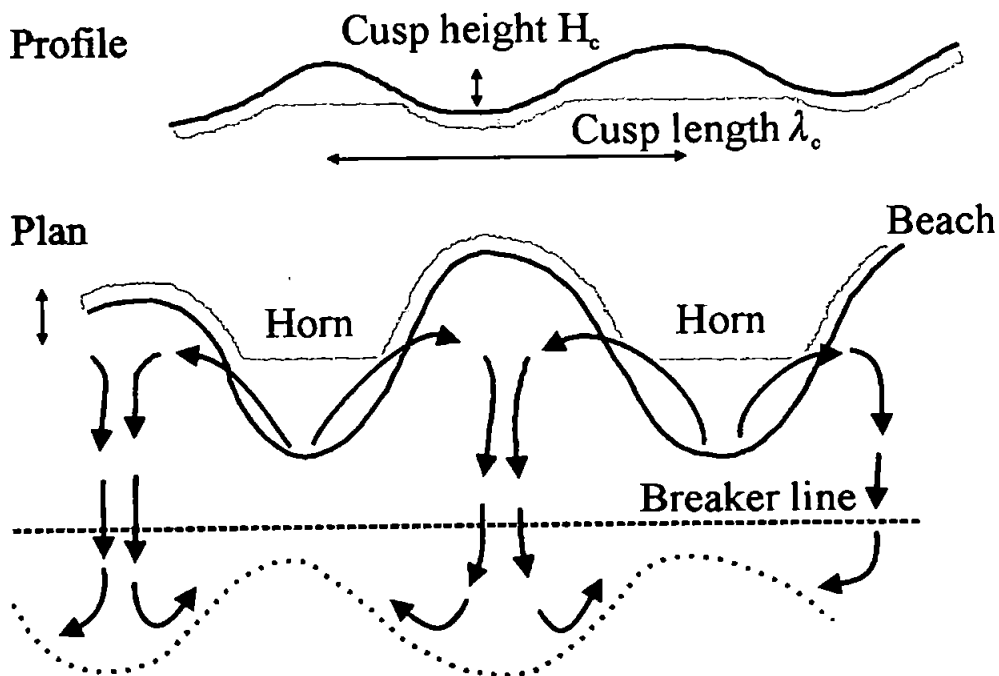


Figure 4.3 Swash circulation pattern over a cusped beach

Then the wave divides and water is added to the volume within the bay. The backwash in the bay is thus greatly enhanced reinforcing the erosion of the bay and resulting in a strong return flow. The effect of this flow out of the bay is to stop abruptly the water it meets from the next wave. Conversely, the water opposite the horn is unimpeded and, as before, it rushes up. The role that refraction might play leading water towards cusp horns and then causing the subdivision has also been suggested (Zenkovich, 1967).

Opposite to this circulation pattern is the one observed by Kuenen (1948), and confirmed by Dalrymple and Lanan (1976) and Komar (1971) suggesting that wave motion initially invades bays, where refraction causes sediment to be transported from the bays towards the cusp horns. Water then moves outward in the form of rip currents at the cusp horns. The edge wave theory, which will be shown later, is associated with a circulation pattern which is very similar to the Kuenen (1948) one as the maximum runup occurs at the antinodes of the edge wave, corresponding to the bays of the beach cusps, and then flows towards the horns.

A conceptual model for beach cusp flow circulation patterns and their relationship to beach cusp formation or disappearance has been recently proposed by Masselink and Pattiaratchi (1998). It is suggested that a horn divergent flow is associated with the maintenance of the cusp shape. On the other hand, an oscillatory flow (a two dimensional flow unaffected by the cusped morphology and so with weak horn divergence and embayment convergence) would cause filling of the embayment and cusp disappearance. A horn convergent flow, especially if associated with some overtopping of the horn, would result in horn erosion and, again, in cusp disappearance.

4.3. Beach cusp formation theories

4.3.1 Instabilities in the breaking waves or in the swash

Different theories propose a mechanism by which a rhythmic spacing is already present in the incoming waves or in the swash. This would “force” an initial rhythmic cusp spacing which could subsequently develop because of the previously described current pattern (Bagnold, 1940).

Cloud (1966) suggests that waves, breaking directly against a beach whose profile of equilibrium has been steepened by storm waves or rising tide, could be approximated to a cylindrical form. Plateau's (1864) found that a 4mm diameter cylinder of oil in a mixture of alcohol and water can become unstable and separate with a ratio length/diameter between 15.5 and 16.7. Applying Plateau's rule to a real breaking wave implies that the cusp spacing should be proportional to the height of the breakers. This theory, requiring the absence of longshore drift, suggests that cusps, once formed, can then persist until a change of regime happens.

Gorycki (1973) suggests that salients, zones of fast velocities due to breaking waves and swash, can move grains of sediment forward and/or laterally, which then tend to be deposited with the diminishing of velocity. The laterally transported grains are swept into turbulent zones of retarded flow where they drop from suspension and accumulate to form elongated, equally spaced, ridges which run parallel to the direction of water motion. The suggestion that salients' spacing might increase with distance travelled was made but not fully developed. Furthermore, there is no evidence that the "salient pattern", studied only in the case of very small spacings, would result in a regular cusp spacing also when applied into a larger scale. Also there is no evidence that a wave front running up a beach would equally divide in the longshore direction.

As the previously discussed approaches both imply a relationship between cusp spacing and the incoming wave height, the Cusp Data Set has been used in order to investigate such possibility. Figure 4.4 clearly shows poor agreement between cusp spacing and wave height ($R^2=0.4$). Because of the lack of correspondence with field observations, both theories are nowadays completely discarded.

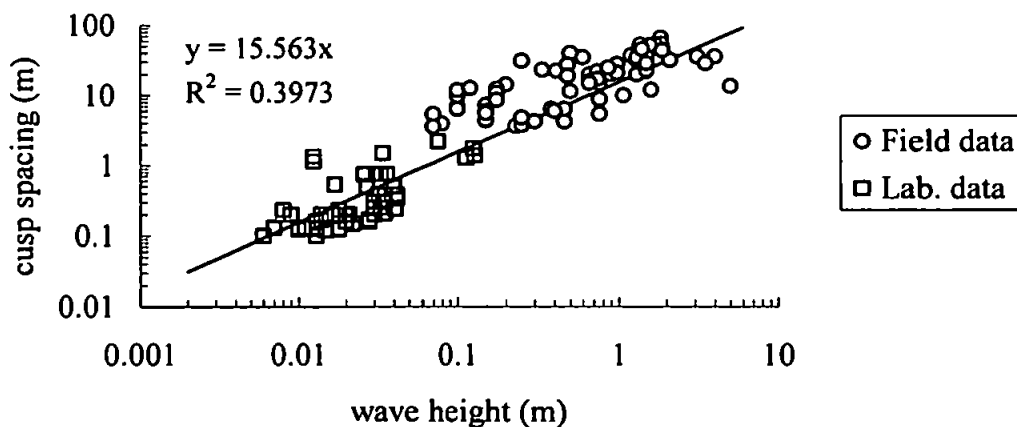


Figure 4.4 Variation of measured cusp spacing and wave height

4.3.2 Instability of the littoral drift

Schwartz (1972) hypothesises that the action of littoral shore drift and swash motion act in such a way that longshore spaced sand ripples or waves are initially formed and subsequently "crests become the horns and the troughs the bays". No field evidence of this theory has been found during this literary research while, as previously stated, there is evidence that a longshore drift wipes cusps away.

4.3.3 Rip currents

The theory concerning the formation of rip currents has been proposed by Bowen (1969) and then experimentally verified by Bowen and Inman (1969) through a series of laboratory and field investigations. The mechanism proposed for rip current formation is that of a longshore variation in the radiation stress in the surf zone. This results in a system of longshore currents increasing in magnitude from zero midway between the rip currents to a maximum where the water flow turns seaward to enter the rip currents. Water removed from the surf zone is then replenished by a slow drift of water shoreward through the breaker zone. Such a current system consisting of two rip currents, associated longshore currents, and a drift through the breaker zone, defines a nearshore circulation cell. The longshore currents will cause a general drift of sediment along the shore towards the rip currents, and because the transport rate is mainly governed by the magnitude of the longshore current, the transport will initially be greatest near the rip currents and decrease to zero at the centre of the cell. Assuming that all this transported sediment is carried out by the rip currents to deep water, it might be expected that a cusp would develop at the centre of the cells where the transport rate is zero. This mechanism, proposed by Komar (1971), does not agree with laboratory (Komar, 1971) and field (Shepard, 1962) investigations where such features, at least during the initial formation stages, appear instead in the direction of the rip current. However, no doubts exist concerning the importance of rip currents in the formation of "giant" cusps.

4.3.4 Intersecting wave trains

Dalrymple and Lanan (1976) suggested that cusp formation could be related to more than one single mechanism. They indicated intersecting wave trains of the same period as a possible mechanism for the generation of rip currents and so of beach cusps. In fact, the water surface elevation obtained combining two intersecting waves has the form:

$$\eta = a \cos[k(\sin\theta)y + k(\cos\theta)x + \sigma t] + b \cos[k(\sin\xi)y + k(\cos\xi)x + \sigma t] \quad (4.1)$$

where:

η = water surface elevation;

a, b = wave amplitude;

θ, ξ = angle of wave approach;

$k = 2\pi/L$ = wave number;

L = wavelength;

$\sigma = 2\pi/T$ = wave frequency;

T = wave period.

Rearranging eq. 4.1, one obtains:

$$\eta = 2a \cos \left[\frac{k}{2} (\sin \theta + \sin \xi) y + \frac{k}{2} (\cos \theta + \cos \xi) x + \sigma t \right] \cos \left[\frac{k}{2} (\sin \theta - \sin \xi) y + \frac{k}{2} (\cos \theta - \cos \xi) x \right] + (b - a) \cos [k(\sin \xi) y + k(\cos \xi) x + \sigma t] \quad (4.2)$$

which has a longshore periodicity varying with $\cos[k/2(\sin \theta - \sin \xi)]$ so that the length of the periodicity is equal to:

$$\lambda = \frac{L}{\sin \theta - \sin \xi} \quad (4.3)$$

By using Snell's law for refraction of shoaling waves it is also possible to rewrite eq. 4.3 in terms of the deep water values. Such longshore periodicity causes a variation in the setup and originates rip currents. This theory is in good agreement with Dalrymple and Lanan's (1976) laboratory tests but obviously contradicts most of the field observations describing cusps formation under a regular normally incident wave field.

4.3.5 Edge wave theory

Edge waves are defined as free modes of nearshore water motion trapped against the shoreline by refraction, whose amplitudes decay exponentially offshore and vary sinusoidally alongshore. Edge waves appear as a set of waves with their crests normal to the shoreline and perpendicular to the incoming waves. Eckart (1951) and Ursell (1952) investigated edge waves theoretically and provided equations to describe their motion, while Huntley and Bowen (1973) first gave evidence of their presence in the field. Edge wave theory indicates that there are several possible modes characterised by the same period and by a different number of zero-crossings in the cross-shore profiles (the mode number n). Figure 4.5 shows the cross-shore variations in the amplitude of a series of edge waves characterised by modes $n=0-3$. Figure 4.6 presents a 3D plot of an edge wave of mode $n=2$ at a fixed time so that it is possible to show the sinusoidal longshore variation and the cross-shore decay. The wavelength of the edge wave is the given as:

$$L_e = \frac{g}{2\pi} T_c^2 \sin[(2n + 1)\beta] \quad (4.4)$$

where

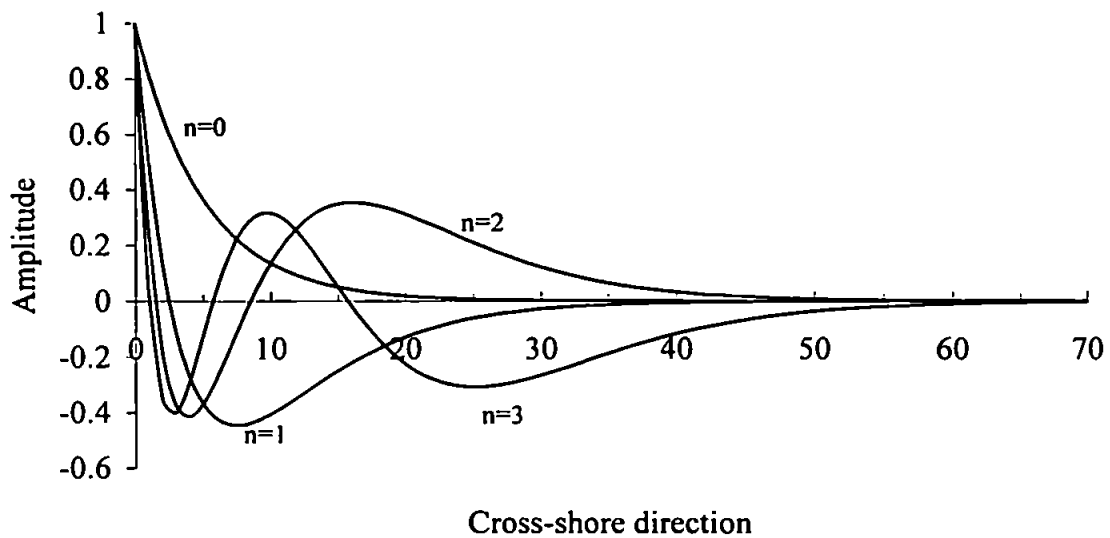


Figure 4.5 Cross-shore variations in the amplitude of edge waves ($n=0-3$)

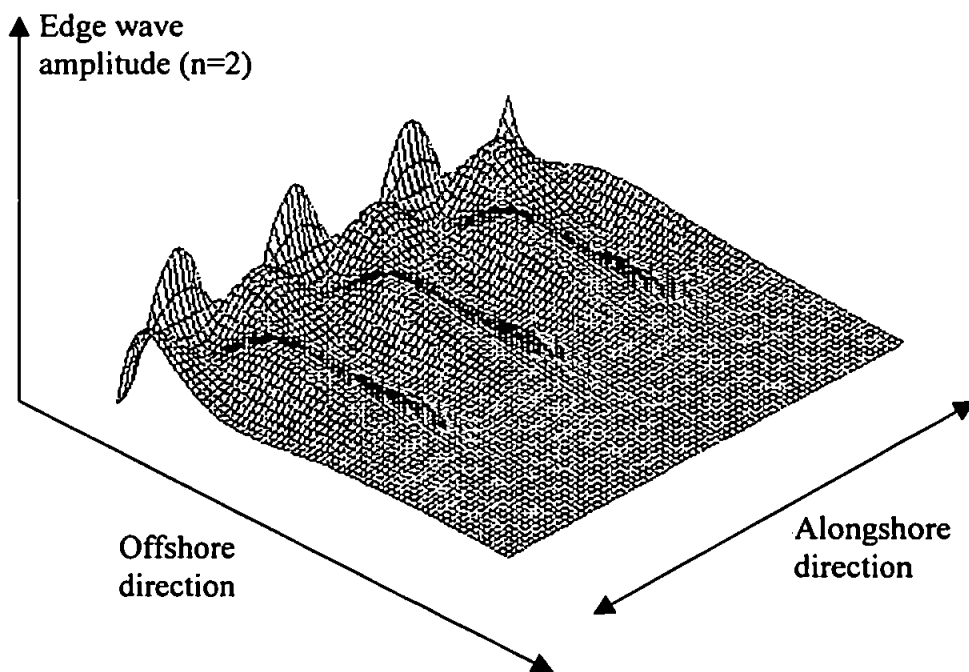


Figure 4.6 3D view of an edge wave of mode $n=2$

β = beach slope angle;

T_e = period of the edge wave.

Bowen (1972) suggested that the existence of regular features indicates that a particular edge wave mode is often dominant, the characteristics of the dominant mode depending on the geometry of the nearshore area and the width of the surf zone. It has also been shown that the most easily excited mode is $n=0$ which would therefore be predicted to correspond to the largest amplitude. The edge wave period may be equal to that of the incoming wave ($T_e = T_i$, "synchronous edge wave"), or not, this latter case being particularly interesting if $T_e = 2T_i$ ("subharmonic edge waves"). It is very important to study the superimposition of incident and standing edge waves as it results in regular longshore variations of maximum wave runup on the beach, which can then be related to the cusp spacing. As subharmonic standing edge waves and incident waves are alternatively in phase and antiphase (they differ by T_i), the cusp wavelength λ_c is equal to one-half the wavelength of a subharmonic standing edge wave ($\lambda_c = L_e/2$) (see Figure 4.7).

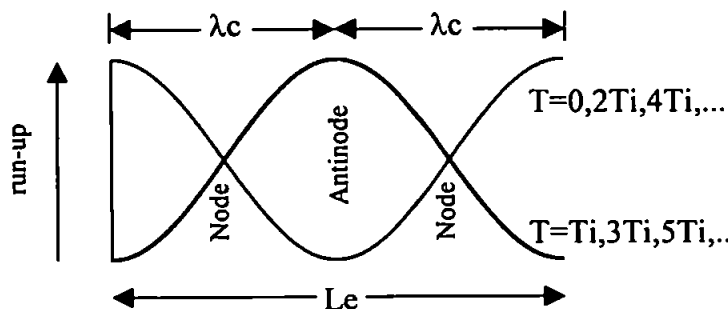


Figure 4.7 Maximum runup and cusp spacing for subharmonic standing edge waves

On the other hand, synchronous standing edge waves and incident waves are in phase for every runup and so the cusp wavelength λ_c is equal to the wavelength of a synchronous standing edge wave ($\lambda_c = L_e$) (see Figure 4.8). It follows that for $n=0$ cusp wavelength results in:

$$\lambda_c = \frac{L_e}{2} = \frac{g}{\pi} T_i^2 \sin \beta \quad \text{subharmonic} \quad (4.5)$$

$$\lambda_c = L_e = \frac{g}{2\pi} T_i^2 \sin \beta \quad \text{synchronous} \quad (4.6)$$

or, unifying the two equations:

$$\lambda_c = m \frac{g}{\pi} T_i^2 \sin \beta \quad (4.7)$$

with $m=1$ and $m=0.5$ for subharmonic and synchronous standing edge waves respectively.

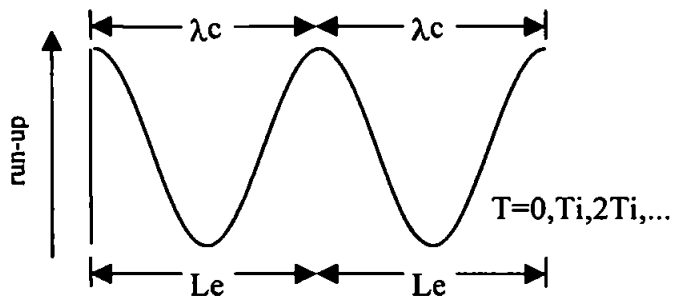


Figure 4.8 Maximum runup and cusp spacing for synchronous standing edge waves

For both the subharmonic and the synchronous case, sediment would passively be driven by the flow pattern so that cusp formation would be the reflection of a spatially (in the longshore direction) “organised” hydrodynamic forcing (“forced behaviour”).

For the standing edge wave theory to be valid, a graph of measured cusp spacing (λ_c) against the parameter given by (4.7) should be a straight line with zero intercept and gradient of 1 or 0.5 depending upon whether subharmonic or synchronous mode zero standing edge waves are associated with the cusps. This graph is shown in Figure 4.9, along with lines which show the expected relationship for cusps due to both subharmonic (solid) and synchronous (dashed) standing edge waves. The graph is plotted on log-log scales to allow easy visualisation of the more than 150 data points over three orders of magnitude and, although the use of log-log scales visually compresses much of the data variability, it reveals a relationship between cusp spacing and the edge wave parameter given by eq. 4.7 (a least square fit to quantify the behaviour of the edge wave parameter results in a regression coefficient equal to 0.72). There is a cluster of data points for which both edge wave relationships over-predict the cusp spacings, but the vast majority of the data lie close to one or other of the lines, and within a margin of error which is reasonable considering the inaccuracies inherent in estimating the various parameters (particularly beach gradient). It is less clear whether the data is better represented by the subharmonic or synchronous relationship, although the least square fit of Figure 4.9, characterised by a slope equal to 0.8, indicates that the subharmonic standing edge wave prediction provides the best description for the majority of the data.

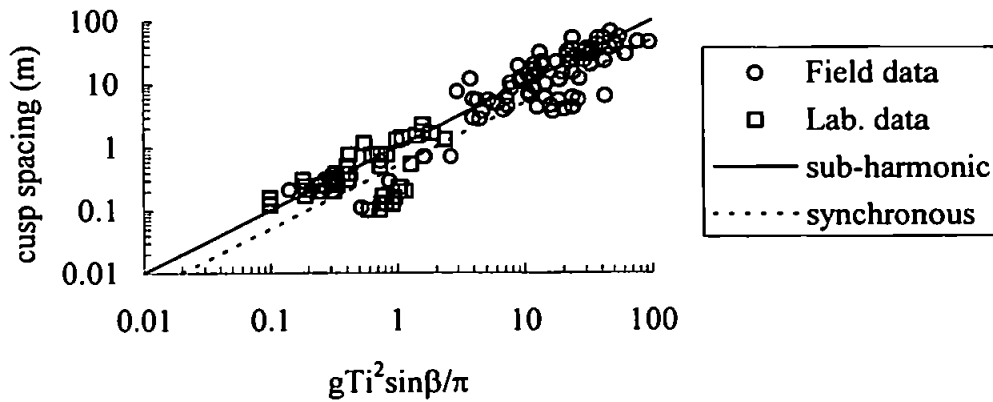


Figure 4.9 Comparison of measured cusp spacing with subharmonic and synchronous mode zero edge wavelength.

It is important to underline that, besides the previously mentioned possible error in the measurement of the beach slope for such 3D features, one of the factors that can mainly influence cusp spacing prediction is the value of the incident wave period whose exact evaluation is rather difficult and that is present in the formulas (eq. 4.5 and 4.6) with an exponent equal to two.

Taken on its own Figure 4.9 provides support for the standing edge wave theory. However, it should be noted here that standing edge waves characterised by a time period and mode number that, according to the theory, could have caused the measured cusp spacing, were not explicitly observed in any of the studies from which the data are taken. Indeed, in at least two cases (Holland and Holman, 1996; Masselink and Pattiaratchi, 1998b), the presence of synchronous or subharmonic mode zero standing edge waves was convincingly ruled out. In the absence of direct evidence for edge wave motion, it is possible to assess the likelihood of subharmonic edge wave excitation by using the following parameter (Guza and Inman, 1975):

$$\epsilon = \frac{4\pi^2 a_b}{gT_i^2 \sin^2 \beta} \quad (4.8)$$

with a_b equal to the breaking wave amplitude.

As a result of a series of laboratory experiments Guza and Inman (1975) suggested that if this parameter is bigger than 2, subharmonic edge wave excitation is weak or non-existent. This parameter has been plotted on Figure 4.10 and, although it must be considered as only a semi-quantitative criterion, it is evident that for a large number of the observed cusps,

edge waves are not, on this basis, expected to exist. In fact ϵ would have to be as large as 18 in order to encompass all of the observations.

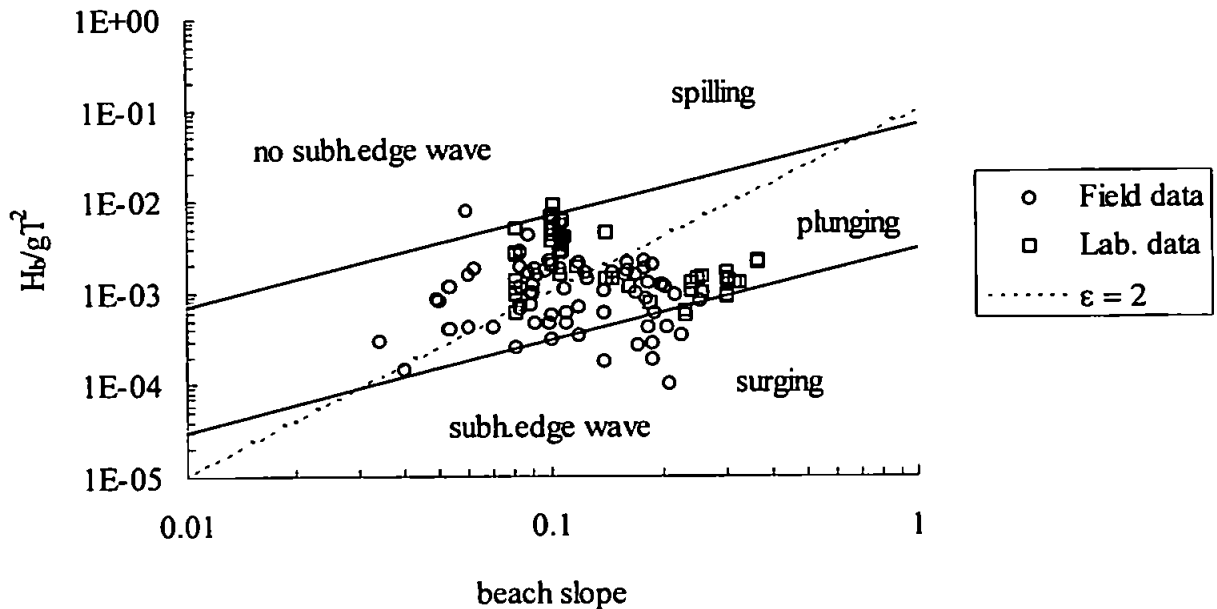


Figure 4.10 Cusp existence and breaker type

The appearance of edge waves is also usually related to surging breaking waves. It is possible to use the Cusp Data Set in order to classify and distinguish between different breaker types observed during cusps' presence. The following inshore parameter defined by Galvin (1968) has been used:

$$\frac{H_b}{gT_i^2 \sin \beta} \quad (4.9)$$

with the values of 0.003 indicating the transition from surging to plunging breaker and 0.068 the transition from plunging to spilling. The following analysis has been performed by considering the wave height measurements given by the different authors to be equal to breaking height. An estimation of the likely error has been made by considering exactly the opposite case, namely treating the measures given by the authors as referring to deep-water wave heights, and evaluating the breaker wave height through an expression given by Takeda and Sunamura (1983). Results indicate a potential error that, at worst, is around 75% (on average the error ranges between 40-60%) of the deep-water wave height. Such a variation does not substantially affect the results. Results shown in Figure 4.10 clearly identify plunging breakers as the predominant type associated with cusp presence. The values appearing well into the surging region all refer to Williams (1973).

The recent work by Masselink (1999) also investigates the importance of edge waves on beach cusp formation. The site where Masselink's measurements (1999) have been taken is characterised by an alongshore variation in the cusp spacing. Local slopes were also measured and, from the results, cusp spacing was found to diminish where slope increases. This is obviously against the prediction provided by the theory (equations (4.5) and (4.6) suggest a linear relationship between cusp spacing and beach slope). However, the lack of detailed hydrodynamic measurements and the fact that measurements were taken by Masselink (1999) when cusps were well-formed does not allow for complete evidence.

Laboratory investigations by Guza and Inman (1975) report in a very detailed way the interaction between morphology and standing edge waves and the negative feedback associated with cusp growth. More recently, it has been then suggested (Seymour and Aubrey, 1985) that standing edge waves could only cause an "initial" perturbation on the beach shoreline and that then they are not subsequently strictly required to ensure cusp existence and evolution. The development of a cusped beach has been studied in detail by Guza and Bowen (1981) and by Inman and Guza (1982) so that limiting amplitude values for beach cusp growth are proposed. Such limiting values are a function of beach slope and cusp spacing and are given in the following form:

$$H_c/(\lambda \tan \beta) \leq 0.13 \quad \text{and} \quad H_{c,\max}/(\lambda \tan \beta) \leq 0.24 \quad (4.10)$$

The first of the two equations indicates a sort of minimum value for cusp amplitude. It should be considered a minimum value because the value 0.13 results from hypothesising the presence of cusps with negligible changes in the beach slope and the persistence of standing edge waves. On the other hand, the value 0.24 is obtained assuming that standing edge waves are providing only the initial longshore perturbation and that the finite development of beach cusps does not require further edge waves. Moreover, the development of beach cusps would have a detuning effect on the subharmonic motion initially associated with cusp formation. Field measurements of cusp amplitude are available (Table I and II) and seem to be in fair agreement with the theory (Figure 4.11). That some of the measurements do not fit the upper and lower boundaries provided by (4.10) could be related to measurements taken on non-equilibrium situations (non-completely developed cusps or cusps being destroyed by wave activity).

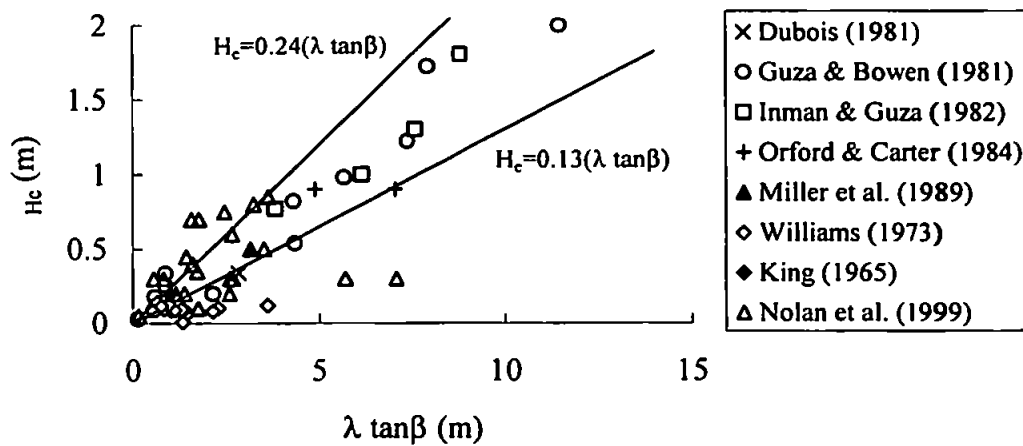


Figure 4.11 Observed cusp amplitude (H_c) versus cusp steepness ($\lambda \tan\beta$)

4.3.6 Theories related to swash dynamics

Longuet-Higgins and Parkin (1962) first suggested a relationship between swash excursion and cusp spacing. Their empirical relationship ($\lambda = 2.8 + 0.54L_{\text{max-swash}}$) contained the obvious problem of predicting cusps even in the case of swash excursion being equal to zero. Probably for this reason, this approach was initially discounted.

The first attempt to model the swash circulation over a cusped beach was developed by Dean and Maurmeyer (1980). In their model, beach cusp topography was considered and, by analysing the water particle motion on such topography, the authors expressed cusp spacing (λ) in terms of the maximum swash ($L_{\text{max-swash}}$) and of a site-dependent parameter (χ):

$$\lambda = 3.9\sqrt{\chi}L_{\text{max-swash}} \quad (4.12)$$

Using a mean value for χ , derived from sites where their field experiments were taken, the authors obtain a linear coefficient equal to 1.5 for cusp spacing prediction.

More recently, Werner and Fink (1993) proposed a “self-organisation” model coupling flow, sediment transport and morphology change to simulate cusp formation and development. Flow is described through cubical water particles moving in accordance to gravitational forces and pressure gradients. The new important step is that the initial morphology is completely arbitrary and that the model is able to predict conditions under which cusps do not form. The beach is composed of slabs of sediment deposited or eroded by water particle motion in accordance with the slope of the beach so that “simulated beach

cusps develop through a combination of positive feedback between morphology and flow that creates incipient relief and negative feedback that inhibits net deposition or erosion on well-formed cusps". Different initial water particle trajectories, or the random order in which the algorithm moves water particles, cause the initial random alongshore variation from a plane beach. Deposition then occurs preferentially on the runup over topographic highs while erosion occurs on lows during the runout so that lows can evolve into bays and highs into horns. The final circulation pattern is similar to the Bagnold (1940) one although no interaction between the runout of a cycle and the runup of the next is considered. Equilibrium of cusp spacing is then proportional to swash excursion through a non-free parameter of the model varying from 1 to 3.

Using the Cusp Data Set, a comparison between observed swash excursion and cusp spacing is made (Figure 4.12) which results in a clear linear relationship between the two variables.

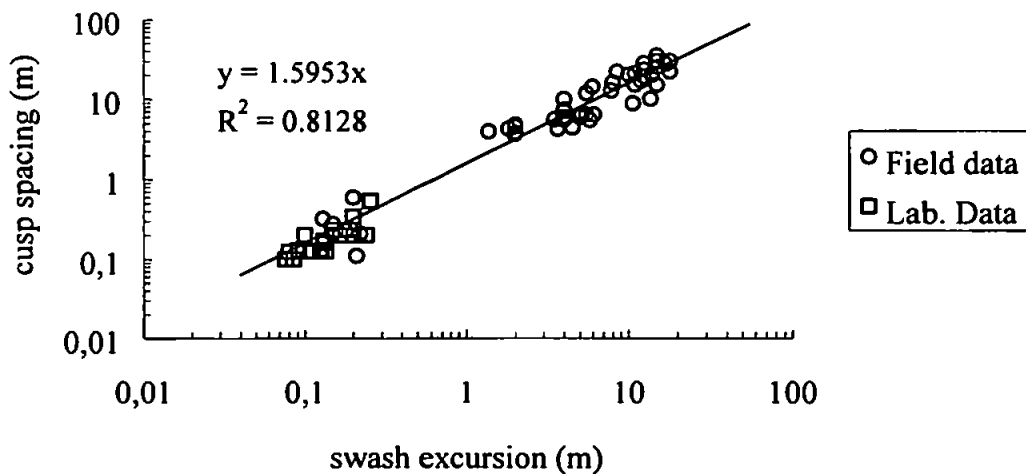


Figure 4.12 Variation of measured cusp spacing with swash excursion

4.4 Compatibility between the edge wave and the self-organisation approach

As the edge wave and the self-organisation model are both reasonably able to predict cusp spacing, a question arises in terms of their co-existence or of the possibility of distinguishing between the two mechanisms. Werner and Fink (1993) argue that the two models are incompatible. However the parameters involved in the cusp spacing prediction may actually be related in such a way that the ratio between the two predictions is a constant close to 1. The conclusion drawn by Werner and Fink (1993) is that measurements

of cusp spacing cannot discern between the models. In the next two sections it will be shown, through an analytical analysis validated by field data and through simulations with the self-organisation model respectively, that the two models could coexist. In fact, it appears that, if subharmonic motions are present, they would result in a swash excursion related to the cusp spacing the same way as predicted by the self-organisation approach.

A study conducted by Miche (1951) suggests that swash excursion saturates at a critical value of the following non-dimensional parameter (Iribarren and Nogales, 1949):

$$\epsilon_s = \frac{4\pi^2 a_s}{gT_i^2 \tan^2 \beta} \quad (4.13)$$

where “ a_s ” indicates the vertical swash excursion at the shoreline. Several authors investigated the possibility of a critical value of ϵ_s .

A widely accepted empirical formula for the evaluation of the runup height over a smooth slope has been proposed by Hunt (1959) and, for $0.1 < \xi < 2.3$, has the form:

$$R_{up} = 2a\xi \quad (4.14)$$

where a is the incident wave amplitude, and

$$\xi = \frac{\tan \beta}{\sqrt{2a/L_0}} \quad (4.15)$$

is a similarity parameter (Iribarren and Nogales, 1949) with β being the beach slope and L_0 the deep-water wavelength of wave period T :

$$L_0 = gT^2/2\pi \quad (4.16)$$

Laboratory experiments by Battjes (1975) indicate that, under certain conditions (involving the beach slope, the wave steepness and $0.3 < \xi < 1.9$) the rundown height can be approximated by:

$$R_{down} = (1 - 0.4\xi)R_{up} \quad (4.17)$$

The amplitude at the shoreline, combining eq. 4.17 with 4.14 and 4.15, would then be given by:

$$a_s = \frac{1}{2}(R_{up} - R_{down}) = \frac{1}{2}(R_{up} - R_{up} + 0.4\xi R_{up}) = \frac{1}{2}(0.4\xi R_{up}) \quad (4.18)$$

Further substitution of eq. 4.18 and 4.16 into eq. 4.13 results in $\epsilon_s \approx 1.26$. Moreover, the field experiments by Guza and Bowen (1976) suggested $\epsilon_s \approx 3 \pm 1$, while Van Dorn's (1978) laboratory measurements indicated a slightly smaller value ($\epsilon_s \approx 2 \pm 0.3$). Field measurements of swash runup spectra (Huntley et al., 1977) also indicated the possibility

of a constant ϵ_s around 2-3. In agreement with such observations (only the results by Battjes (1975) follow a slightly different trend), Baldock and Holmes (1999) derive, for a saturated swash motion, a theoretical value of ϵ_s . They hypothesise the shoreline motion moving under only the effect of gravity. The swash excursion, in the plane of the beach, S , can then be either described in terms of the vertical swash excursion or in terms of the natural swash period:

$$S = \frac{2a_s}{\beta} = \frac{1}{2}g\beta \frac{T_{sw}^2}{4} \quad (4.19)$$

which can be rearranged to give:

$$a_s = \frac{1}{16}g\beta^2 T_{sw}^2 \quad (4.20)$$

By assuming that the swash period is equal to the incident wave period, it is possible to rearrange equations (4.13) and (4.20) and obtain:

$$\epsilon_s = \frac{\pi^2}{4} \approx 2.5 \quad (4.21)$$

which, as previously shown, is very close to the values measured in the laboratory and field experiments.

On the other hand, it is possible to combine ϵ_s (eq. 4.13) with the cusp spacing prediction in case of subharmonic or synchronous standing edge waves (equation 4.7). As a result, a linear relationship is obtained between swash excursion and cusp spacing of the form:

$$\lambda_c = m \frac{2\pi}{\epsilon_s} S \quad (4.22)$$

Equation (4.22), if coupled with the previous results concerning the possibility of a constant ϵ_s in a saturated swash, leads to a proportionality coefficient between swash excursion and cusp spacing, of around 2.5 or 1.26 for subharmonic and synchronous edge waves respectively. Thus, if we hypothesise that cusps are predominantly formed under conditions of saturated swash excursion, equation (4.22) indicates that standing edge waves, either subharmonic or synchronous, would produce a pattern consistent with the one obtained through the self-organisation mechanism.

It is now clear why “simple” measurements of cusp spacing will not allow for an understanding of which of the two mechanisms is responsible for the formation of beach cusps. In order to discern between the two mechanisms there is the need of very detailed hydrodynamic measurements capable of assessing the eventual presence of standing edge waves during cusp formation. The suggestion that the two mechanisms, although

conceptually different, can co-exist also needs to be considered, as well as the possibility that beach cusps are the result of an instability mechanism that can be either simply due to the hydrodynamics, or the result of the interaction flow-sediment.

4.5 Discussion

Several theories have been discussed in order to describe the formation and development of beach cusps. Many of the proposed theories are not able to explain the variability of the observed cases, or to predict the cusp spacing in agreement with the field and laboratory measurements undertaken in the last 50 years (Cusp Data Set). The debate has therefore been restricted to only two mechanisms with the first referring to the presence of standing edge waves (“forced behaviour”) and the second to feedback processes between flow and sediment (“free behaviour”). These two theories, although usually considered to be incompatible, suggest a very similar spacing, such that the Cusp Data Set cannot establish which of the two is closer to the observations. It has also been shown that, under certain hypotheses, the two mechanisms could even co-exist. While the standing edge wave approach is well established, there is the need of a closer investigation of the more recent self-organisation approach. For this reason, a model based on self-organisation will be presented in the chapter 5, and its behaviour will be analysed in detail as well as the possibility of coexistence under the presence of standing edge waves. The problem of comparing results obtained through the self-organisation model and field measurements will be then investigated in chapter 6, through the use of a non-linear technique for the analysis of beach elevation time series.

Chapter 5: A self-organisation model for the swash zone

A shortened version of this chapter has been published in the Proceedings of Coastal Sediments '99, New York (ASCE, pp. 2190-2205) with the title: "Beach cusp formation: analysis of a self-organisation model" by Coco, G., Huntley, D.A., and O'Hare, T.J.

5.1 Introduction

The need for a better understanding of the processes involved with swash motion and the topographic response has recently led to numerous theoretical and field investigations. Particular attention has been dedicated to the study of beach cusps. As described in the previous chapter, the nature and origin of these rhythmic shoreline features is still not clear and even observations reported in the literature are sometimes in such disagreement that the definition of a single theory capable of explaining beach cusp formation under every observed circumstance is probably an impossible task. The previous chapter showed in fact that cusps have been observed in both reflective and dissipative environments, under net accretionary or erosional conditions. Their presence has also been associated with sediments ranging from fine sand to boulders and often related to very specific topographic or wave field conditions. In general, however, it appears that the formation and development of a beach cusp morphology is associated with reflective conditions, waves normally approaching the shoreline and well sorted coarse sandy sediments.

The previous chapter also suggested several mechanisms for beach cusp formation but the agreement with field and laboratory data has mainly restricted the debate to two theories that Werner and Fink (1993) consider incompatible. The first theory refers to beach cusps as a result of an instability in the hydrodynamics resulting in the superimposition of standing edge wave motions on the incoming wave field, leading to an alongshore periodic variation of the run-up whose wavelength is related to the cusp spacing (Guza and Inman, 1975). The second theory, the self-organisation mechanism, is described by Werner and Fink (1993) and more generally relates to an approach which depends on a coupling of hydrodynamics and sediment which "self-organises" into regular patterns without any external spatially distributed forcing. It is suggested that complex systems characterised by strongly non-linear and dissipative behaviour (which is the case of the interaction between hydrodynamics and sediment movement) may evolve into patterns through feedback processes.

This chapter deals with an investigation of the self-organisation hypothesis for the swash zone and in particular for beach cusp formation and development, and the possibility of predicting beach cusp spacing by knowing only the value of the swash excursion. The processes involved and relating to the self-organisation hypothesis will be considered through a sensitivity analysis of the parameters in the model. The problem of reaching an equilibrium state, the rate at which it might happen, and the suggestion that the random inputs present in the model may affect cusp formation are discussed. Results obtained by running the model over an initially non-planar topography, characterised by a cusped shoreline or by the presence of non-rhythmic features, are presented. The compatibility between the standing edge wave approach and the self-organisation model will be discussed by means of a series of numerical simulations under a simplified form of standing edge wave forcing. Implications of these model results for the understanding of cusp formation and for future field observations are discussed.

5.2 Model description

A model for beach cusp formation and development has been implemented using Fortran 77 code. The aim of the present work was not to build a self-organisation model competing with the one already proposed by Werner and Fink (1993), but to analyse the processes involved with the formation of cusps, their development, the final spacing and the dependency of these processes on the parameters and the details of the algorithm. The approach used for the simulation of beach cusp evolution refers to a discrete number of particles representing the fluid and causing sediment motion, rather than to the classical differential equations involving the use of continuous variables. Feedback between flow and morphology is modelled in such a way that every time a particle moves, the topography changes and can immediately affect the particle motion. Feedback is then the cause for the formation of these rhythmic patterns as it allows (positive feedback) the evolution of an initial perturbation, generated because of the presence of different random features in the model.

5.2.1 Hydrodynamics

Swash hydrodynamics are described through a defined number of water particles moving under the influence of gravity over an established grid representing the beach slope. Flow motion is described according to the following equations:

$$\frac{\partial u}{\partial t} = -g \frac{\partial h}{\partial x} \quad (5.1)$$

$$\frac{\partial v}{\partial t} = -g \frac{\partial h}{\partial y} \quad (5.2)$$

where x and y are used to distinguish between the cross-shore and alongshore direction, with u and v indicating the respective velocity components, t is time, g is gravity and h is the beach elevation. Friction and percolation are neglected. By integrating Eqs. (5.1) and (5.2) and by adopting a finite-difference approximation one obtains the equations describing the particle position:

$$x_t = x_{t-\Delta t} + u_{t-\Delta t} \Delta t - 0.5g \sin \beta_{x,t-\Delta t} \Delta t^2 \quad (5.3)$$

$$y_t = y_{t-\Delta t} + v_{t-\Delta t} \Delta t - 0.5g \sin \beta_{y,t-\Delta t} \Delta t^2 \quad (5.4)$$

where $\sin \beta$ indicates the beach gradient in the x or y direction. Using a centred difference method and considering, as an example, the cross-shore direction and a point characterised by the (i, j) co-ordinates, the beach gradient is equal to:

$$\sin \beta_{x_i} = \frac{\Delta h_{x_i}}{\sqrt{\Delta h_{x_i}^2 + (2 * \Delta x)^2}} = \frac{h_{i+1} - h_{i-1}}{\sqrt{(h_{i+1} - h_{i-1})^2 + 4 * \Delta x^2}} \quad (5.5)$$

with Δx indicating the cross-shore grid-size.

Seaward of the swash zone, in a region that should resemble the surf zone, water particles are treated in a more simplistic way such that velocities are considered to be constant and the trajectory randomly assigned at the beginning of the swash cycle, or resulting from the motion inside the swash zone, is maintained. At the beginning of each swash cycle, water particles are assigned an alongshore and cross-shore velocity component and a location in the model domain from which they start their motion.

5.2.2 Sediment dynamics

For sediment transport, a parameterisation similar to the one proposed by Werner and Fink (1993) has been used so that the sediment flux gradient between two adjacent grid points “ i ” and “ $i+1$ ” is evaluated through the relationship:

$$\Delta q_s = \alpha (v_{i+1}^m - v_i^m) \quad (5.6)$$

where α is a dimensional coefficient, v_i indicates the velocity at the grid point “ i ” and “ m ” is a coefficient providing the power of the proportionality between sediment flux and flow velocity. In agreement with the majority of the bedload transport theories (Bagnold, 1963; Bailard and Inman, 1981), a value of “ m ” equal to 3 has been adopted in the simulations while the value of “ α ” has been chosen depending on the grid size and bed slope in order

to ensure smooth variations of the bed elevation. A sensitivity analysis towards these parameters has been performed and results will be shown in the next section.

The amount of net erosion or deposition effectively changing the bed elevation results from the difference of the carrying capacity between two consecutive grid points. By considering the kinetic properties of a water particle whose motion is governed only by gravity, carrying capacity is equal to the difference between the elevation of the grid point when the particle was at time “t” and the elevation of the grid point when the particle moved to at time “t + Δt”. In fact, considering the difference between velocities at two consecutive grid points, one obtains:

$$v_i^2 = [v_{i-1}^2 - 2 * g * (h_i - h_{i-1})] \quad (5.7)$$

$$v_{i+1}^2 = [v_i^2 - 2 * g * (h_{i+1} - h_i)] \quad (5.8)$$

$$\Delta C_s = c_s (v_i^2 - v_{i+1}^2) = c_s [v_i^2 - v_i^2 + 2g(h_{i+1} - h_i)] = 2c_s g (h_{i+1} - h_i) \quad (5.9)$$

where:

h_i = elevation of the grid point i;

ΔC_s = amount of net erosion/deposition;

c_s = coefficient for the definition of the carrying capacity.

Because of this parameterisation, inside the swash zone, the run-up is mainly characterised by deposition (water particles are decelerating) while run-down is characterised by erosion (water particles are accelerating). The region seaward of the swash zone is characterised by a carrying capacity that has been arbitrarily considered to be linearly proportional to the elevation, so that it has its maximum value at the bottom of the swash zone. Out of the swash zone, the run-up is characterised by erosion while the run-down by deposition.

The change in the bed elevation, is related to the single locations where a water particle is present. There is obviously the need of “spreading” such change over a wider area. For this reason and also in order to model topographic changes in a more realistic way, two subroutines have been created and will be presented in the next two subsections.

5.2.2.1 Morphological smoothing

At each time step, once the net amount of erosion/deposition has been evaluated, the change in the topography is obtained through the use of a smoothing function, which basically works as a diffusive term. As a result sediment is eroded/deposited around a defined area (usually a five by five matrix surrounding the location of interest), whose scale is much smaller than the final cusp spacing. The smoothing used here accounts for

the pre-existing topography in such a way that differences in the local slopes are limited. In fact, for a defined location, the smoothing operates by evaluating the plane that best fits the elevations of a certain number of surrounding locations and then distributes the sediment in order to minimise differences from that plane.

5.2.2.2 Angle of repose

Because of the erosion and deposition caused by successive waves, it is possible that topography will change in a non-realistic way, an example being the case of two adjacent grid points with a beach gradient superior to the angle of repose of sediment. By considering an angle of repose, for example of 30 degrees, it is possible to establish a limit for the local beach gradient and, if such limit is exceeded, operate another smoothing and change the topography. The way this second kind of smoothing is performed needs to be very efficient in order to overcome possible loops caused by moving the sediment into grid points whose changed elevations will again exceed the limit value. For this reason, before spreading the amount of sediment that is actually exceeding the angle of repose limit, every surrounding point whose elevation would be changed needs to be checked. The criteria adopted consists of measuring the hypothetical new height that each of the surrounding grid points would reach after smoothing, and only if this new elevation is smaller than the one of the point exceeding the angle of repose will smoothing be performed.

5.2.3 Boundary conditions

At the alongshore boundaries of the modelling domain, periodic boundary conditions have been used so that water particles moving over one boundary reappear on the other side of the grid and sediment is rearranged on both sides of the grid allowing for sediment continuity. The use of such boundary conditions necessarily implies the presence of two regions, each of them extending out of the field limits, where the topography needs to be exactly equal to the one present on the other side of the grid field but inside the field limit. For example, if one considers Figure 5.1, a beach is represented through a grid field extending, in the longshore direction, from A to B. It is possible to distinguish three different areas:

- 1) A-B: grid field area (the one where water particles move and interact);
- 2) A'-A (or B-B'): region extending outwards of the grid field area;

- 3) A-A'' (or B''-B): region inside the grid field area whose changes are reflected on the region B-B' (or A'-A) respectively.

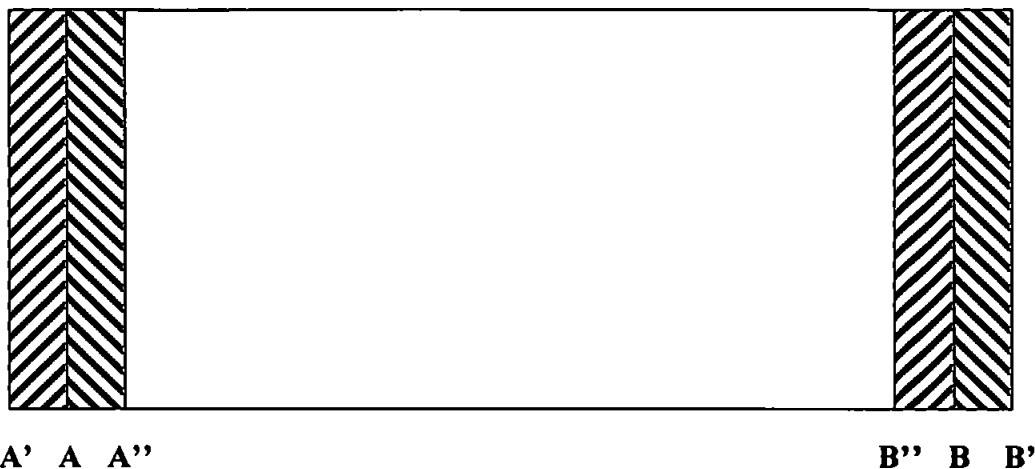


Figure 5.1 Different regions of the grid field as related to the boundary conditions

The presence of these overlapping areas ensures that every time a particle is going out of the grid field, and so it is entering from the other side, the beach gradient present is consistent with the previous topography. The width of the overlapping region is obviously a function of the area affected by the smoothing as, depending on the width of the smoothing, the topography of A-A'' (or B''-B) may change even if the particle is not inside that region. A last consideration regards the importance of the width of the grid field where particles move (region A-B) as it has to be big enough to avoid the “forcing” of any periodicity caused by the use of the boundaries which could eventually result in longshore rhythmic patterns. The size of the region A-B needs to be larger than the longshore excursion of water particles and obviously larger than the predicted cusp spacing. Several simulations, conducted by varying the grid spacing and the length of the alongshore domain, have been run in order to verify that any “numerical” forcing was avoided. As a result, it is possible to conclude that the formation of beach cusps is not influenced by the size of the grid or caused by the spreading of a perturbation from the edges of the grid field towards the centre but it arises from random positions and cusps are all forming simultaneously.

Another assumption related to the boundary limits of the model has been made and concerns the lack of interaction between one wave cycle and the following one. Every generated uprush will be basically unaffected by the outgoing backwash. No boundary is required at the top of the swash zone as particles will automatically invert their velocity and start the backwash.

5.2.4 Random features of the model

At the beginning of each swash cycle, water particles are assigned an alongshore and cross-shore velocity component by random choice from within a fixed range. Water particles are also given a location in the model domain that they occupy at the beginning of the cycle. This starting position on the grid is also randomly assigned for each cycle although a fixed, constant spacing between water particles can be assigned too. In order to understand the influence of these random inputs on cusp formation and development, different random sequences have been considered, and simulations run, by only changing the starting point (seed) of the pseudo-random number generator (results will be presented in the next section). The importance of this analysis lies in the fact that the nature of a self-organisation model is such that morphological evolution is the result of a feedback process rather than of an external forcing. Small variations in the input parameters might therefore significantly influence the rate of growth, or even the final spacing, of the resulting cusps.

5.2.5 Model simulation

An example of the results obtained through the model is given in Figure 5.2 where the changes on a shoreline leading to cusp formation and development are shown. Figure 5.2.a shows the domain being investigated and the division between the swash and the surf zone. The simulation herein presented is characterised by a beach slope equal to 10° (grid sizes in the longshore and cross-shore direction are equal to 10cm) while the water particles are nearly normally (the maximum angle of approach randomly assigned is of the order of $\pm 2^\circ$) approaching the shoreline. The cross-shore velocity at the seaward boundary of the swash zone is of 2.5 m/s (with random variations of the order of 2%) which results in a swash excursion approximately equal to 1.8 m. Figure 5.2.b is a contour plot showing the topographic changes after only 10 cycles. It is already possible to see the presence, around the change between swash and surf zone, of some alongshore distributed rhythmic features which continue to develop, and after 30 swash cycles (Figure 5.2.c) start to develop the characteristic shape of beach cusps with the alternation of horns and embayments. After 50 cycles (Figure 5.2.d) the topography is well pronounced although still not completely stable. In fact (Figure 5.2.e) after 100 cycles two of the horns (respectively the third and the fourth starting from the right) merge into a single one. Still the topography is not stable and, after 150 cycles (Figure 5.2.f), the prominence of the second horn from the left is consistently diminished and completely disappears when a more stable configuration is

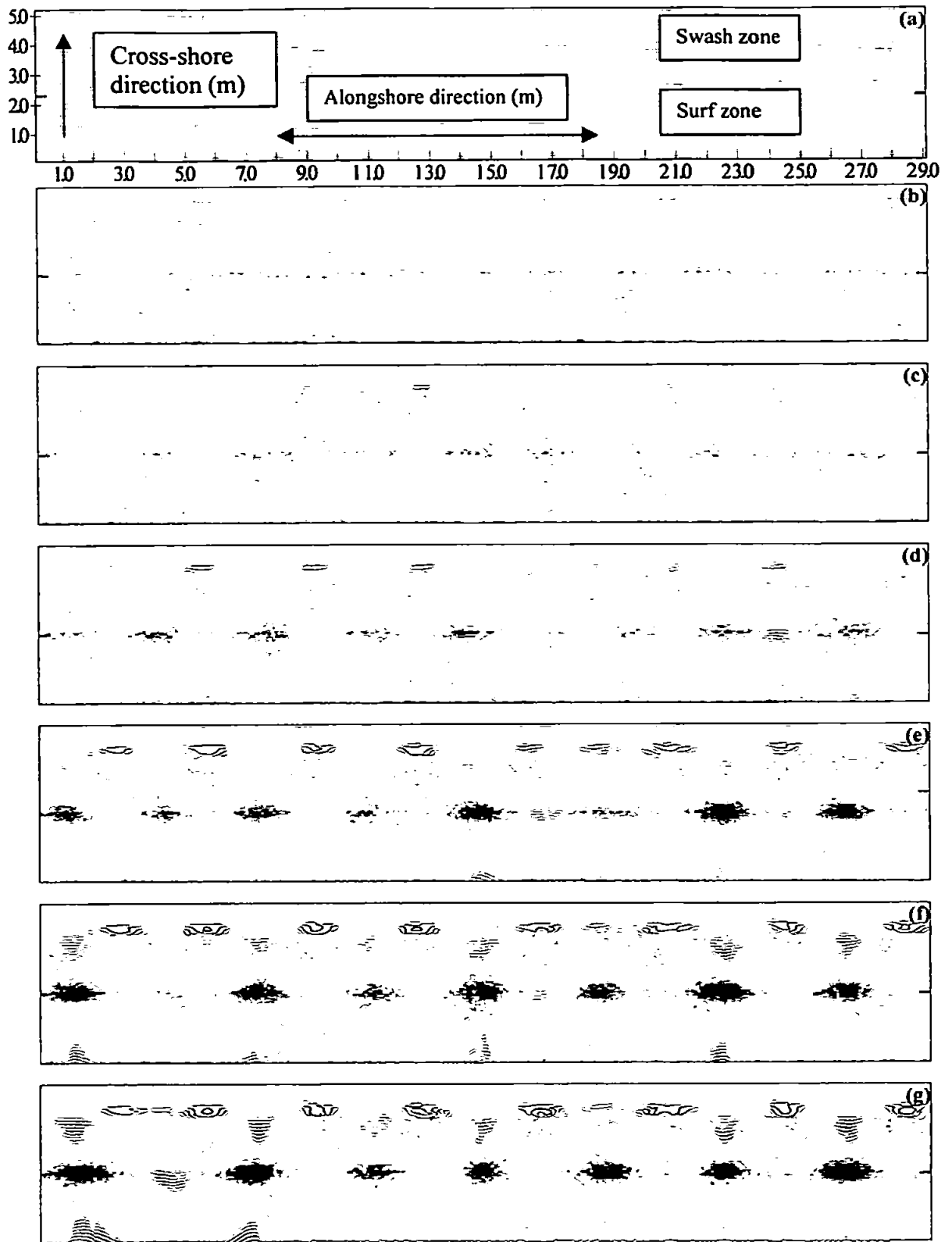


Figure 5.2 Formation and evolution of a cusped beach (see text)

reached after 200 cycles (Figure 5.2.g). Out of the swash zone, as a result of the way the surf zone has been modelled, areas of deposition and erosion can be observed in front of embayments and horns respectively. This morphological feature is also evident on natural beaches where a mirror reflection of the cusped shoreline has often been reported (Kuenen, 1948; Masselink and Pattiaratchi, 1998b). By the configuration shown in Figure 5.2.g, the topography is much more stable and other changes, again a merging or dividing of horns and embayments, appear only after a very large number of cycles; the random element of the model means that a situation of no net erosion/deposition inside a single system horn-embayments is never reached and sometimes water particles manage to overtop from one side of the horn to the other transferring sediment. Considering the morphology developed after 200 cycles (Figure 5.2.g), the cusp spacing is around 3.6 m which corresponds to a swash excursion with a coefficient of about 2.0. Such a value is very close to the values commonly observed, especially when one considers the variability and the difficulty in measuring the swash excursion in the field. In fact the linear regression obtained through the use of most of the available field and laboratory data, as presented in the previous chapter and in Coco et al. (1999), suggests a proportionality coefficient between swash excursion and cusp spacing of around 1.6.

The result obtained for the simulation previously described has been confirmed by several other simulations run over beaches characterised by different slopes or by flows characterised by a different swash excursion. Figure 5.3 shows the result of such simulations and the following correlation between cusp spacing and swash excursion, which, as previously indicated, favourably agrees with field and laboratory measurements.

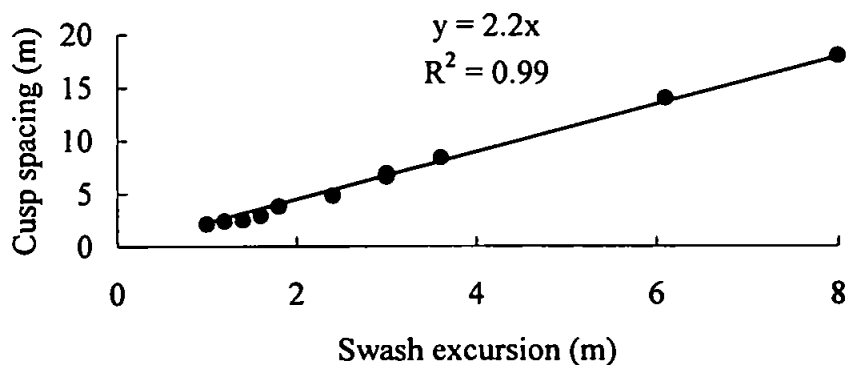


Figure 5.3 Relationship between cusp spacing and swash excursion for numerical simulations

Each point on the plot corresponds to simulations run considering swash excursions obtained by changing both the beach slope and the initial velocity of the incoming swash front with all the other model parameters kept constant.

5.2.6 Physical mechanism

The formation and development of beach cusps is the result of feedback processes. In fact, the presence of non-linearities in the sediment transport parameterisation, combined with the randomness in the trajectory of the water particles, leads to the basic instability. The perturbation starts to develop because of the randomness causing the formation of isolated low or high areas. Such areas affect the flow attracting or diverging water particles more than the surrounding flat areas. The non-linear relationship between flow and sediment flux causes a deepening of the lower areas and the accretion of the higher ones (positive feedback). In fact, a lower area will cause water particles to accelerate and so erosion, with the opposite happening in the higher areas. The morphological smoothing, as often happens in cellular automata models, will spread the perturbation and connect it with those evolving in other areas so that the process of reaching a more regular configuration is facilitated. Once a cusped shoreline is present, water particles will, on average, be driven by the existing topography causing minor changes inside a cusp-embayment-cusp system. Changes will still be possible as a result of the randomness present in the every swash front.

5.3 Sensitivity to model parameterisation

The choice of modelling the swash front through a finite number of water particles has been tested by varying the number of particles and their spacing at the beginning of each swash cycle. Results show that the spacing between water particles, and hence the number of particles present in the domain during each swash cycle, does not affect the final result but only the speed at which the process develops. In fact, if a smaller particle spacing is considered, a higher number of water particles is present in the domain and, with all the other parameters kept the same, this results in a faster development of cusps. An example is given in Figure 5.4 where a beach slope of 10° and water particles with a swash excursion of 1.8 m are considered (the same conditions have been used for all the simulations presented in this section). Each point represents the number of cycles necessary to reach what could be defined as a quasi-equilibrium (it will be shown later that,

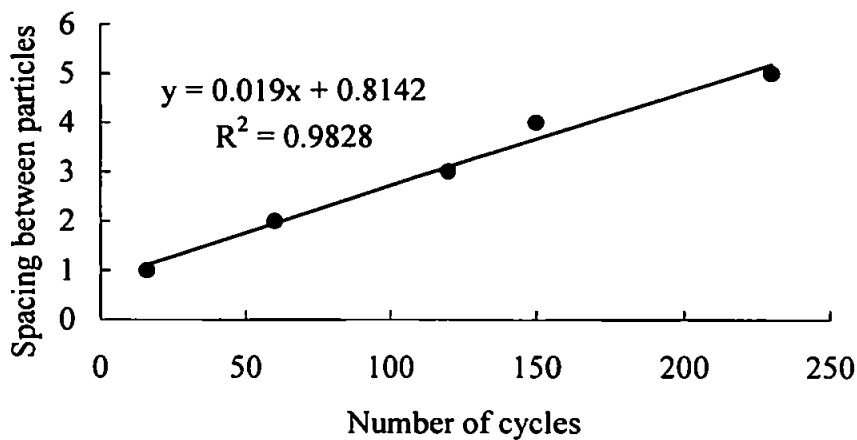


Figure 5.4 Relationship between the number of water particles representing the swash front and the number of cycles required to reach a quasi-equilibrium spacing

even on well-developed cusps, there is always a small amount of net erosion or deposition and a slow evolution of the cusp patterns).

Our simulations show that the exponent “m” in the velocity describing the sediment flux (equation 5.6), is an important parameter of the algorithm, different values resulting in different spacing during the simulations of beach cusp formation (Figure 5.5). Because of the lack of knowledge of the way sediment transport is modelled this result cannot be considered unexpected and in fact other authors have found a similar sensitivity when investigating morphodynamic instabilities (Christensen et al., 1995; Falques et al., 1996). This parameter results in the biggest source of variation in the quasi-equilibrium cusp spacing, but the variation is still small when compared to the scatter present in field measurements (see previous chapter or Coco et al., 1999). Another important result is given by the lack of cusp appearance for the case of $m = 1$ which basically corresponds to a linear relationship between sediment flux and velocity. This result also confirms the importance of non-linearities for the development of instabilities and is also in agreement with similar cellular automata model previously described (Murray and Paola, 1994).

On the other hand, the magnitude of the coefficient “ α ” in the sediment transport parameterisation (equation 5.6) has an effect only on the rate at which beach cusps develop, not on the final spacing. An example of this phenomenon is given in Figure 5.6 where a sediment flux proportional to the cube of the velocity ($m = 3$) has been used. In the limit of an extremely small value of α , no cusp formation occurs as changes in the morphology are so small that the degree of randomness present in the model prevents feedback to the hydrodynamics. The line fitting the data shows the asymptotic increase of

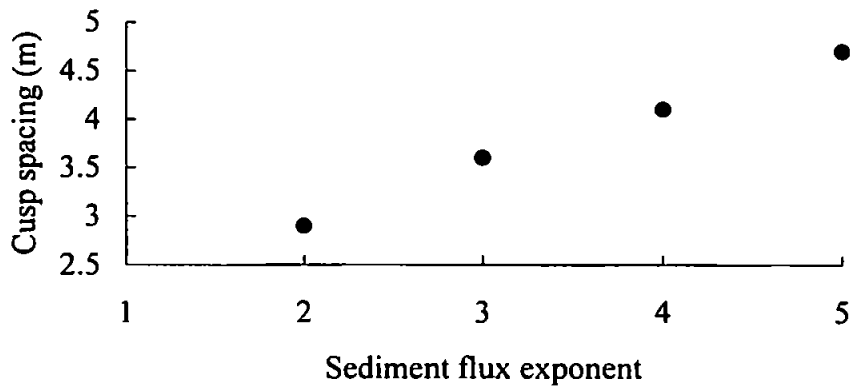


Figure 5.5 Variation of the cusp spacing with the sediment flux exponent

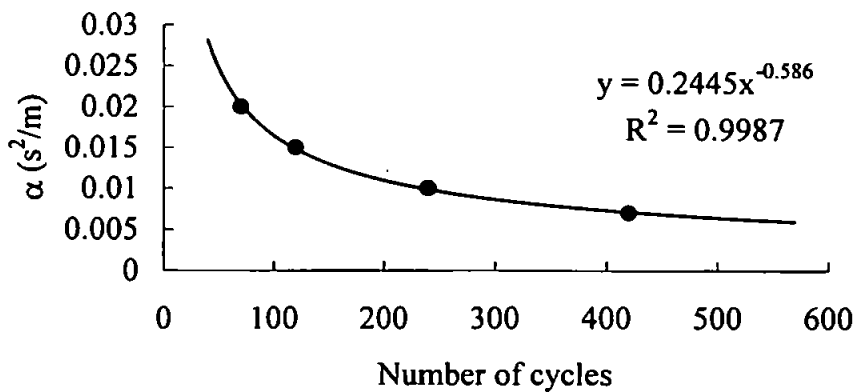


Figure 5.6 Relationship between the “ α ” coefficient (see equation 5.6) and the number of cycles required to reach a quasi-equilibrium spacing

number of cycles necessary to reach quasi-equilibrium as α is reduced. At the upper limit, values of the α coefficient higher than 0.02 result in unrealistic morphological changes of same order of magnitude as the beach slope gradient in a single time step.

The size of the sediment smoothing domain does not influence the cusp spacing, provided of course that it is much smaller than cusp wavelength; for all the runs shown in this chapter the size of the smoothing domain is no more than about 15 % of the final wavelength. However, the nature of the smoothing has an important effect on the process of beach cusp formation. The use of smoothing functions that do not account for the pre-existing topography, for example a constant or pyramidal re-distribution of the evaluated amount of local erosion/deposition, does not result in beach cusp formation. Such a result should not be considered surprising as the nature of the model implies a continuous local interaction and feedback between fluid and sediment and the sediment itself. Spreading the

sediment without accounting for the local pre-existing topography would obviously inhibit such processes.

The choice of different values for the angle of repose, if realistic, does not affect the final cusp spacing but, as expected, only the shape and the rate at which cusps are formed; in effect, smoothing following the exceeding of the angle of repose acts in opposition to the formation of steep slopes and so slows down the feedback process (see Figure 5.7).

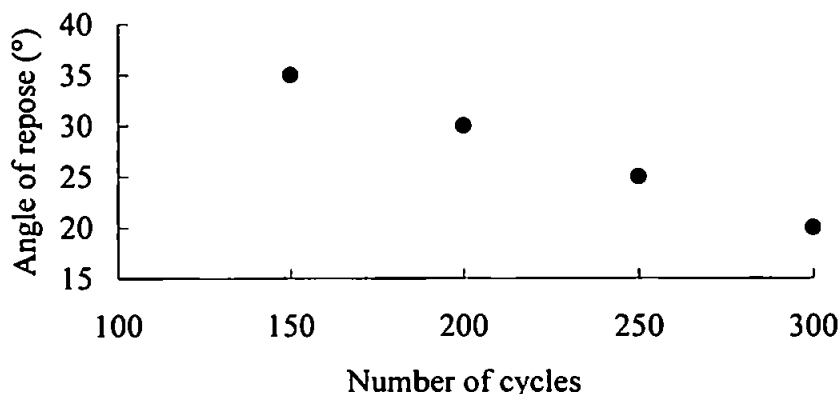


Figure 5.7 Relationship between the angle of repose and the number of cycles required to reach a quasi-equilibrium spacing

The sensitivity of the model results to the addition of a simulated hydrodynamic pressure gradient has also been investigated. Pressure gradients have been modelled in a very simplistic way so that, for each time step, the alongshore component of the velocity of each water particle is affected by other water particles that may be present in a fixed surrounding area. As a result, the water particle can be “driven” by the others. When its alongshore velocity brings it into close proximity with another particle, its alongshore velocity changes sign, with the water particle moving in the opposite direction to the previous time step. Simulations including this effect tend to result in slightly larger final spacing but the magnitude of the change (around 10%) suggests a small importance of pressure gradients in the process of beach cusp formation.

The conclusion of this sensitivity analysis is that cusp spacing is relatively insensitive to realistic changes in input and model parameters, any changes being well within the scatter in observed spacings. In contrast, as expected, these parameters have a strong influence on the rate of cusp development.

5.4 Tests of model behaviour

The present model has been used to investigate the mean circulation patterns over a cusped topography. As shown in the previous chapter, field investigations have considered the possibility of cusps formation with a horn convergent (Kuenen, 1948; Williams, 1973) or divergent (Bagnold, 1940; Dean and Maurmeyer, 1980) circulation pattern. Results obtained through the simulations indicate a horn divergent pattern such that the hydrodynamics, as soon as the topography begins to evolve, are driven by the local slope. This result is shown in Figure 5.8 where the flows averaged over a swash clearly diverge from the horns towards the embayments.

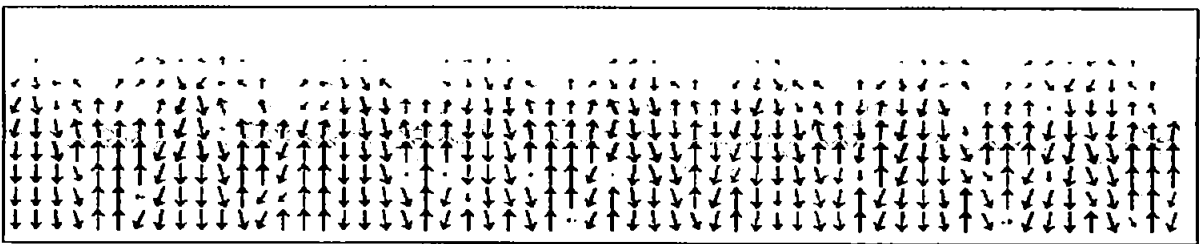


Figure 5.8 Flow pattern over a cusped beach

Some authors have also stressed the relation between the circulation over a developing cusped shoreline and the process, erosive or accretionary, leading to the formation and development of these features. As a result, there is the strong indication (Russell and McIntire, 1965; Masselink et al., 1997) that a horn divergent circulation is related to accretionary conditions. The present numerical model confirms this hypothesis. Figure 5.9 shows the initial and the 100 cycle average (over the whole alongshore domain used in the simulation) cross-shore profiles.

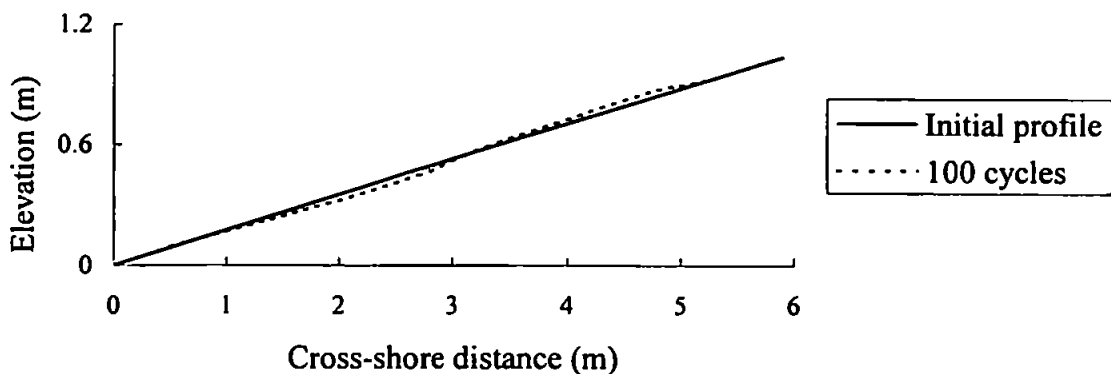


Figure 5.9 Average cross-shore profile at the beginning of the simulation (planar slope) and after 100 cycles (developed cusped morphology)

A similar result is obtained for larger number of cycles and it is clearly comparable to field observations (Guza and Bowen, 1981). It is clearly shown that the cusped morphology developing in the swash zone (region between 3 and 6 m in the cross-shore direction) has an accretionary nature while, as a reflection of sediment continuity, erosion is present seaward of the swash zone.

In order to quantify the development of cusps during formation, evolution and even destruction, the bed elevation on an alongshore grid-line approximately at the centre of the swash zone has been analysed by means of a spectral analysis, with the following parameter indicating the sharpness of the peak of the spectrum (Darras, 1987):

$$Q_p = \frac{2}{m_0^2} \int_0^\infty k \cdot S(k)^2 dk \quad (5.10)$$

where:

Q_p = peakedness factor;

m_0 = spectral density moment of zero order;

k = alongshore wavenumber;

$S(k)$ = spectral density.

This parameter has been used to investigate the influence of a steady longshore current on cusp development. Several observations (Russell and McIntire, 1965; Miller et al., 1989) report that cusp destruction occurs if a change in the wave field causes the presence of a longshore current. In order to investigate such situations a longshore current has been superimposed on the wave motion over a cusped topography and, as expected, cusps are rapidly wiped out. Figure 5.10 shows in fact the evolution of the sharpness of the spectral peak, initially running the model with an approximately normal incident wave field (a random alongshore component of flow around $\pm 2^\circ$ and a cross-shore velocity around 2.5 m/s is considered). After one hundred cycles, beach cusps are already developed and stable (solid line) but if the initial component of the water particle longshore velocity is changed, so as to approximate an oblique wave approach and a resulting longshore current, the sharpness of the peak in the spectrum rapidly decreases (dotted lines). The figure also shows that the destruction of beach cusps is faster for larger angles of approach and results in peakedness values eventually comparable with the ones at the beginning of the process, where a flat beach was present, and no cusp can be identified. The case of a smaller angle of wave approach (around 6°) does not result in the complete destruction of the existing morphology but in very strong changes in the position and spacing of the beach cusps.

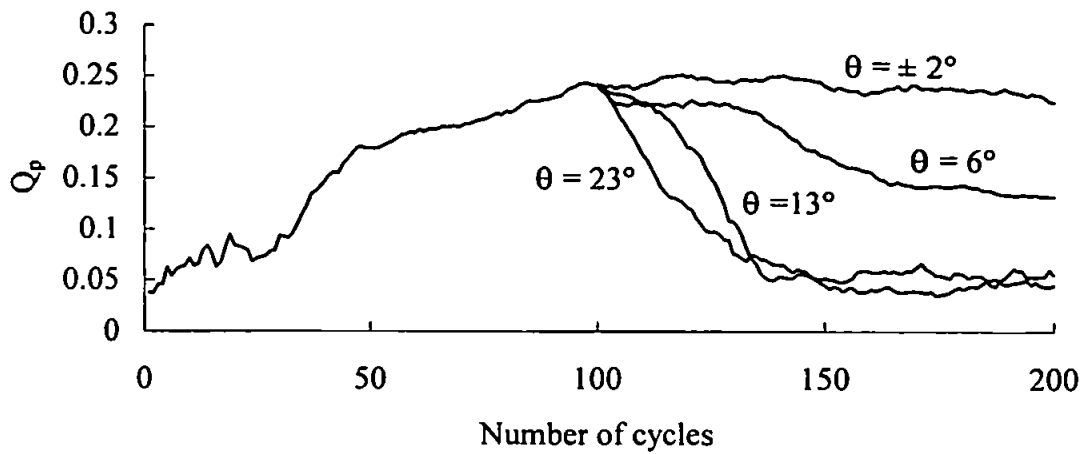


Figure 5.10 Variation of the peakedness (Q_p) for different values of the angle of approach. The first 100 cycles were run with $\theta = \pm 2^\circ$

The presence of an obliquely approaching wave field over an initially planar slope has also been simulated in order to understand its implications on cusp formation. Cusp spacing is not affected by small increases in the alongshore component of the water particles' velocity. On the other hand, and in agreement with field observations (see for example Holland, 1998), if water particles are characterised by an angle of approach bigger than a value around 10° cusps are not formed.

As shown in the previous chapter, many authors (Inman and Guza, 1975; Holland, 1998) consider narrow banded conditions, the so-called "clean conditions", as an important requirement for beach cusp formation. The model herein developed allows for testing such a requirement by increasing, for example, the randomness in the cross-shore component of the input velocities. By considering increasing values of randomness, feedback processes are prevented and cusps do not develop. Figure 5.11 shows the results of simulations of such processes and, as a measure of cusp formation, the spectrum peakedness after 200 cycles has been used (results show exactly the same trend if the maximum value of Q_p over the whole simulation is considered). This result again confirms the consistency between self-organisation modelling and field observations.

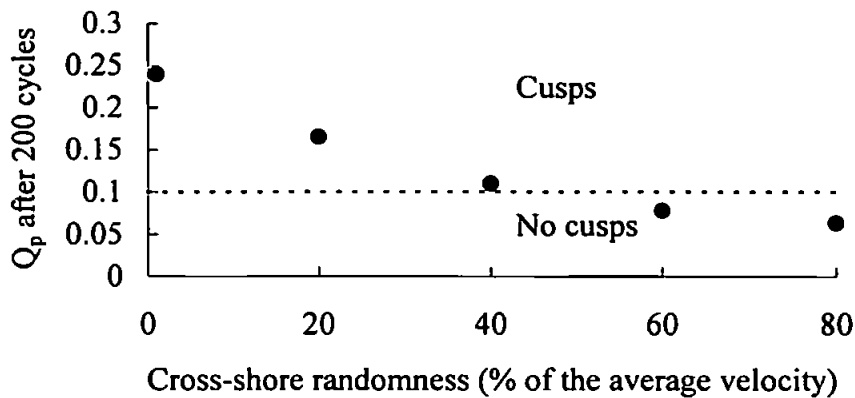


Figure 5.11 Cusp existence and randomness in swash excursion

One of the criticisms of the self-organisation approach concerns the time necessary for beach cusp formation. It is argued (Komar, 1998) that natural irregular waves would require a much longer time to develop cusps than that suggested by the Werner and Fink (1993) model, which is between 6 min and 3 hrs (for 10 sec waves) depending on the parameters chosen.

An analysis of the present model suggests that such a time cannot be uniquely established. Figure 5.12 shows results obtained when running the model with the same parameters but changing the random seed for the determination of the water particle position over the starting grid line and the respective initial velocity components (cross-shore and alongshore). The value of the cusp spacing for each of the two runs, respectively indicated by the letters a and b, is shown through contour plots of the spectrum of an alongshore grid-line approximately at the centre of the swash zone. It is possible to see that, in the first case, a final spacing of 4 m is reached after about 400 cycles while the second case reaches the same condition only after running the model for more than 800 cycles. Figure 5.13 shows results obtained analysing the same runs in terms of the peakedness factor (Q_p). Run 5.13.a presents a very sharp increase of the peakedness quickly reaching a value around 0.2 (such value could be considered as indicative of a well-developed cusped shoreline). Run 5.13.b develops a cusped shoreline at a much slower rate and reaches such values of peakedness only after 400 cycles. Furthermore, the peak reached by run 5.14.a after 200 cycles rapidly decreases because of the re-organisation of the shoreline into a slightly wider spacing while run 5.14.b experiences the same changes, in the cusp spacing and, as a reflection, in the peakedness, only after 700 cycles. It is thus clear that, with this kind of self-organisation models, the time necessary for beach cusp formation is not unique. That the process of beach cusp formation and development is sensitive to the random input

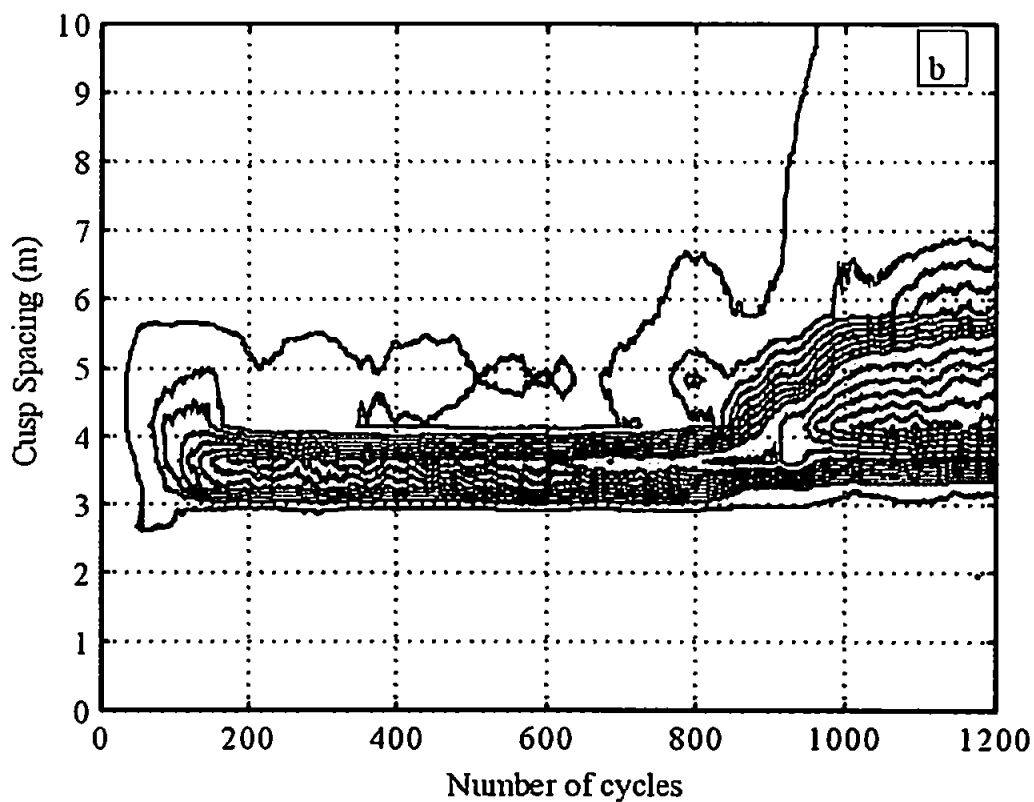
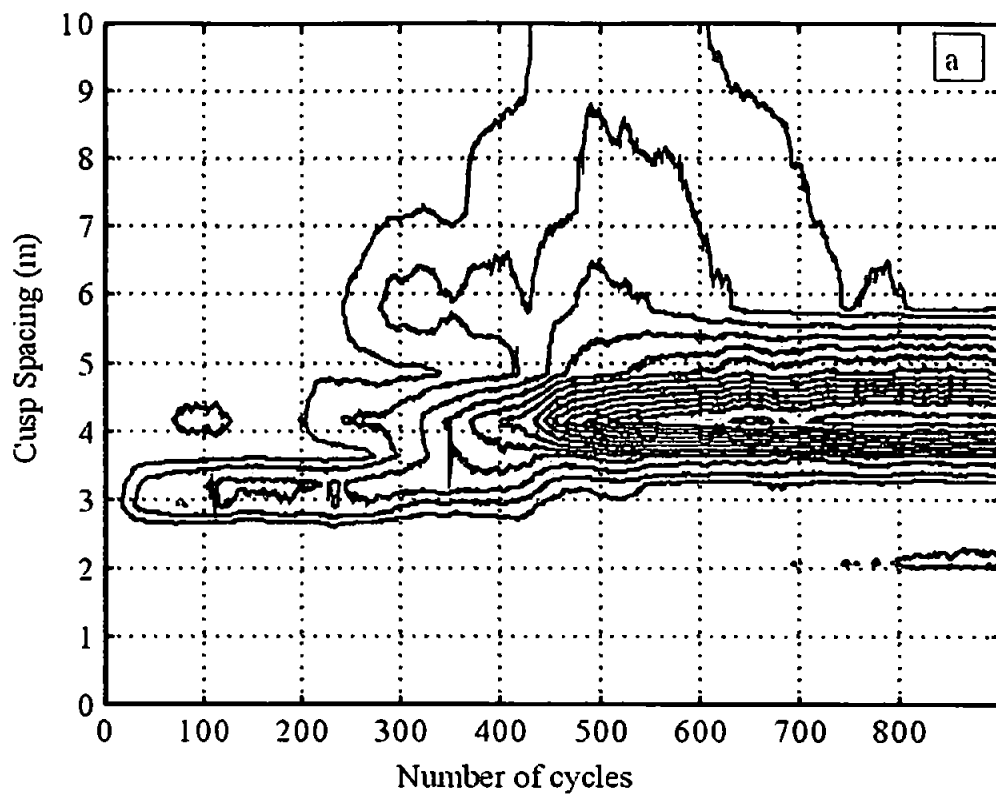


Figure 5.12 Comparison between spectra of an alongshore gridline inside the swash region during cusp formation and development (swash excursion is around 1.8 m). The two samples differ only in the random seed used

should not be considered as a shortcoming of the model. Other studies underline the importance and the effect of wave chronology upon a beach morphology which non-linearly responds to an input characterised by a combination of systematic and stochastic hydrodynamic driving forces (Southgate, 1995). Although this model works on a much smaller time-scale than the one suggested by Southgate (1995), the idea that different sets of random inputs, characterised by the same statistical properties, unpredictably characterise the development of a shoreline agrees with those earlier findings.

The conclusion that such differing growth rates for cusp formation can occur simply due to different random conditions may explain why beach cusps are often observed in isolated patches or with a non uniform spacing (see Plate 5.1) on a beach exposed to apparently uniform incident waves. Although our sensitivity analysis suggests we must be cautious in interpreting absolute growth rates from the model, nevertheless the longer timescales indicated by these simulations are of the order of hours. This imply that, on a tidal beach or under changing wave conditions, these timescales may be too long to form beach cusps.

5.5 Long-term model behaviour

Some interesting conclusions on the model behaviour can be drawn when simulations are run for very large number of cycles. As an example, we consider a domain characterised (Figure 5.14.a) by a longshore distance equal to about 30 m and a cross-shore distance approximately equal to 6 m. The beach is subject to a wave front represented by water particles positioned at every third grid point on the starting grid-line (a grid size of 0.1 m in both the alongshore and the cross-shore direction has been used also in this simulation). The particles are characterised by a cross-shore initial velocity component ranging randomly between 2.50 and 2.48 m/s while the alongshore component of the velocity ranges randomly between plus and minus 0.1 m/s. The beach is initially characterised by an uniform slope equal to 10° and the resulting swash excursion is around 1.8 m. After a short number of cycles (around 50) cusps are already present (Figure 5.14.b). At this stage, although the spacing is not exactly regular and cusps are still very small, the circulation pattern (horn divergent) is strongly influenced by the topography and so reinforces the development of cusps. After 200 cycles (Figure 5.14.c) a regular cusped beach is present with an equally spaced sequence of horns and embayments. This configuration of the shoreline, whose only difference with Figure 5.2.g is in the random seed, seems to be stable and the circulation pattern is driven by the existing topography. By running the model further on it is then possible to see that after 400 cycles (Figure 5.14.d) some

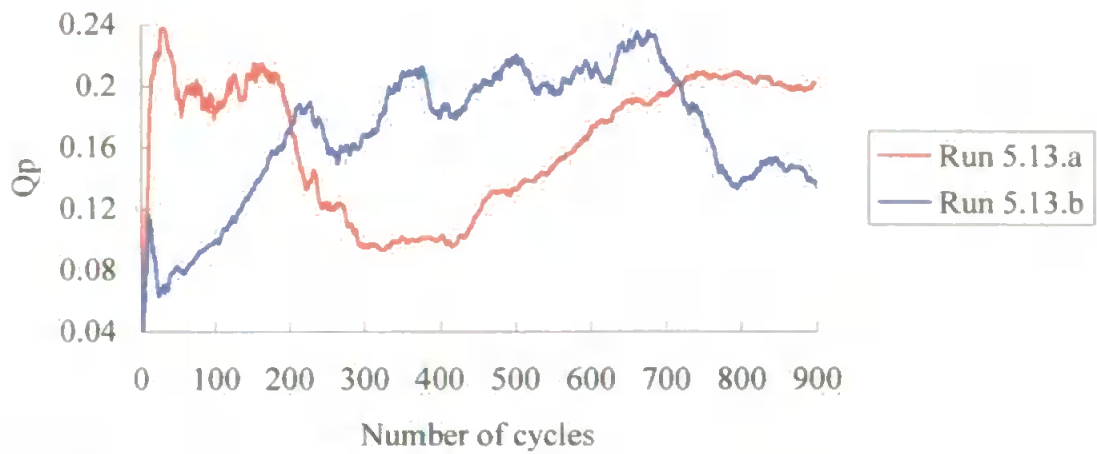


Figure 5.13 Variation in the peakedness factor (Q_p) for the runs considered in Figure 5.12.a and 5.12.b



Plate 5.1 Cusp formation with a non-uniform spacing (smaller spacings are around 4m, courtesy of Gerd Masselink, Loughborough University, U.K.)

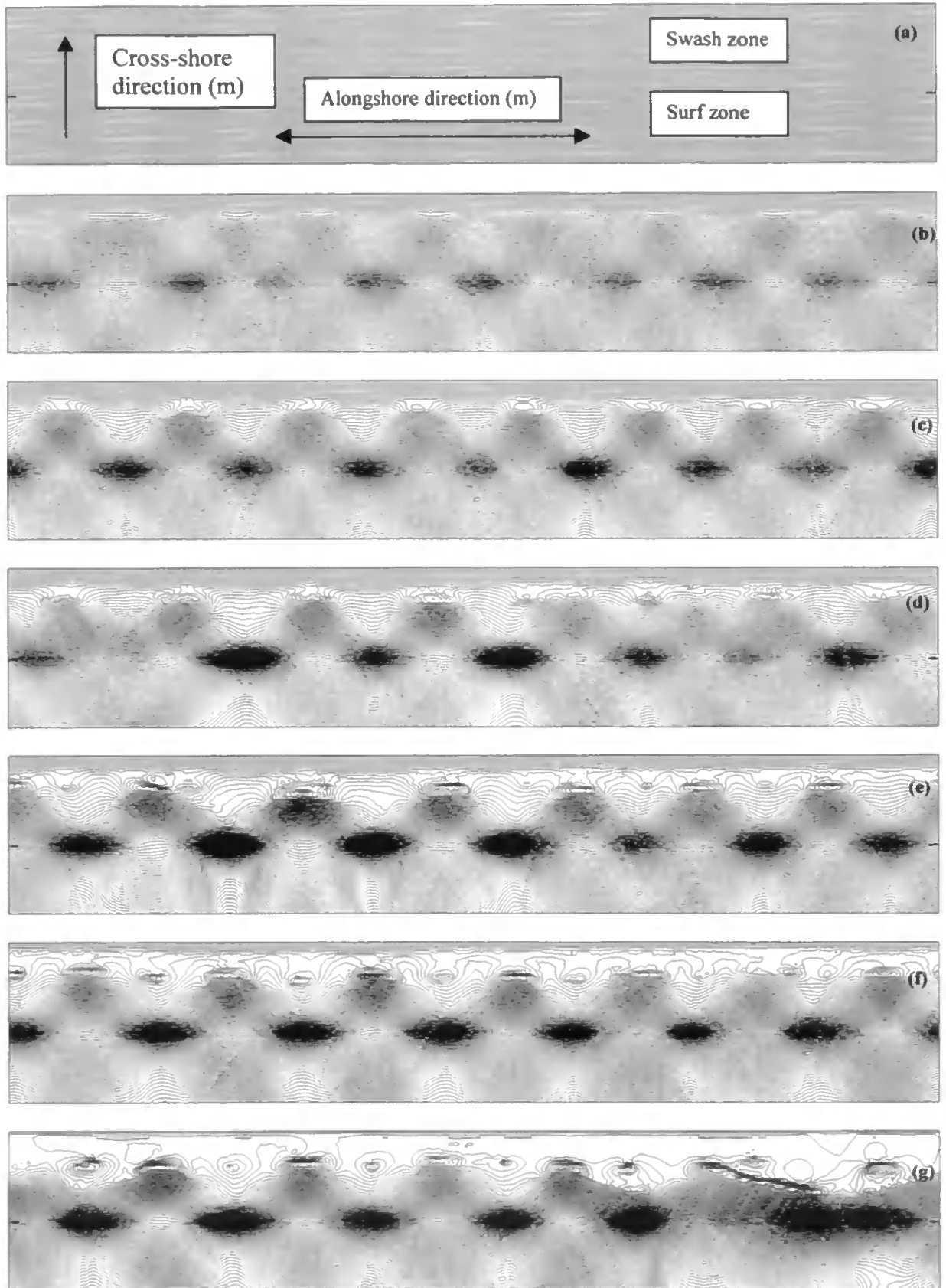


Figure 5.14 Formation and long term evolution of a cusped beach (see text)

significant modifications begin to occur. Cusp spacing is not so regular anymore; some of the horns are getting bigger while others are slowly disappearing. The shoreline is moving towards a different configuration and in fact, after 800 cycles (Figure 5.14.e) a new beach cusp spacing has been achieved. The beach has reorganised into a different configuration characterised by a larger spacing (from 3.5 m to approximately 4 m). This configuration seems to very dynamical and in fact after 1400 cycles (Figure 5.14.f) it is possible to notice a displacement in the horns' locations (compare the position of the horns in this contour plot with the one of Figure 5.14.e) due to merging and separation of the features. Further running of the model results again in a merging and separation of the horns (the beginning of this process is shown in Figure 5.14.g which represents the morphology after 2000 cycles) and the topography becomes less clear, although the presence of cusps is still easily identified.

As shown in the previous sections, the circulation pattern observed during our simulations is the horn divergent one on both developing and well-developed cusps although, probably because of the random input, an equilibrium situation with no net sediment movement is never reached. There is the suggestion that the horn divergent circulation pattern could initially enhance cusp development but only until a certain point after which the horns are so steep that the same circulation pattern begins to be disruptive and cause movement of sediment from the horns to the bays. Our simulations show sediment flux gradients within a single cusp which vary on long timescales, with periods of relatively low and constant gradient broken by periods where the flux gradient doubles and changes in cusp location and shape occur. Clearly, even for well-developed cusps, the feedback between flow and topography can be disrupted by randomness in the wave field. The highly dynamic nature of cusps shown by these observations needs to be verified through field investigations.

5.6. Results over a non-planar topography

One of the shortcomings of the edge wave model has always been considered to be the fact that the dispersion relationship used for the prediction of the beach cusp spacing has been derived assuming the presence of a planar beach. Edge wave motions can obviously be found over non-planar cross-shore topographies, each characterised by a different dispersion relationship. Analytical solutions have been found for a beach topography characterised by an exponential slope (Ball, 1967) while for more complex cross-shore beach profiles, numerical schemes have been proposed (Darbyshire, 1978; Holman and Bowen, 1979; Oltman-Shay and Howd, 1993). As a result, there is the strong suggestion

that a linear slope approximation could lead to significant errors in the wavelength estimation (Holman and Bowen, 1979; Oltman-Shay and Howd, 1993) and so in the cusp spacing prediction. Moreover, the lack of a model describing the changes occurring to edge waves because of the topographic modifications does not allow for a complete and satisfactory description of the process(es) involved with beach cusp formation. Only the model proposed by Guza and Bowen (1981) studies the interaction between edge waves and already developed beach cusps and, as a result, a de-tuning of the edge waves is suggested. Their model could explain why standing edge waves, whose alongshore variations would suggest a cusp spacing similar to the measured one, are not found on well-developed cusped shorelines even though they could be responsible for the initial interaction leading to beach cusp formation. In contrast, the self-organisation approach does not require any specific initial condition. It is therefore of some interest to investigate how the self-organisation might interact with some pre-existing cusp spacing resulting, for example, from standing edge wave motion.

Initial simulations have been run by considering the effect of isolated features for example the presence of a bar (Figure 5.15) or of a non-rhythmic feature (like the bump shown in Figure 5.16). These features are found not to affect the process of beach cusp formation and after a number of cycles (depending on the size and shape of the feature) they are destroyed and a regular cusped shoreline appears. In these cases, the spacing at which beach cusp “organise” is the same as would have been obtained by running the model on a linear slope, and so is related to the swash excursion. This result shows the strength of the self-organisation mechanism and underlines, as already indicated by the work of different authors (Dean and Maurmeyer, 1980; Werner and Fink, 1993), the strong relationship between cusp spacing and swash excursion.

The model has also been run with initial conditions representative of pre-existing developed cusped topography with a spacing different to that obtained when the simulation starts with a planar topography. In this way, it is possible to test the strength of the self-organisation mechanism under topographic conditions which could potentially induce a circulation pattern similar to the one(s) observed in the field, but without the predicted relationship between cusp spacing and swash excursion. The cusped shoreline has been idealised through the use of the expression already suggested by different authors (Dean and Maurmeyer, 1980; Masselink and Pattiaratchi, 1998b):

$$h(x, y) = x \tan \beta \left(1 + \epsilon \sin \frac{2\pi y}{\lambda} \right) \quad (5.11)$$

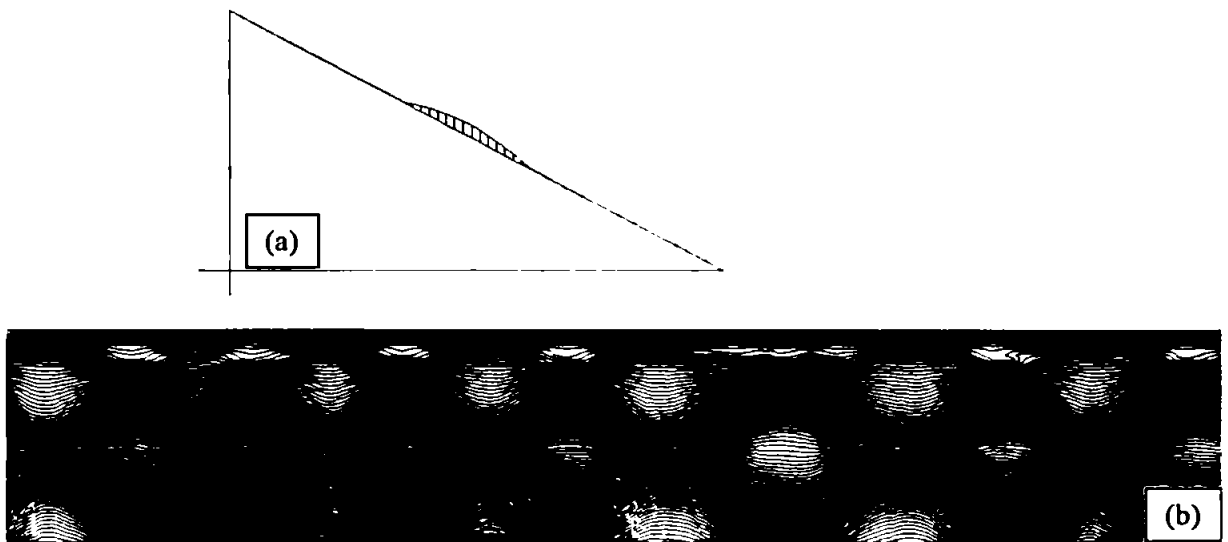


Figure 5.15 Cross-shore profile of an initially barred topography (a) and beach cusp formation after 200 cycles (b)

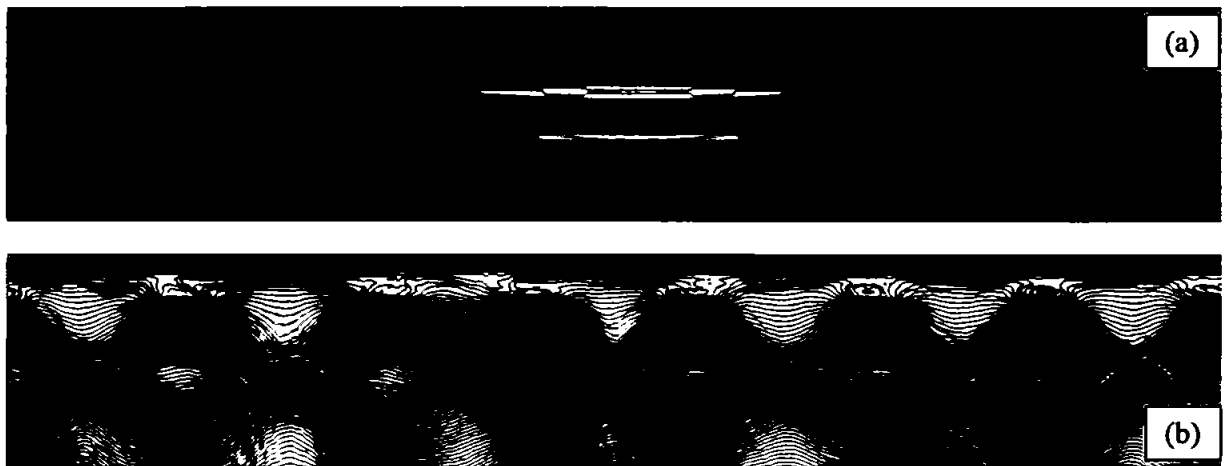


Figure 5.16 Formation of beach cusps on a topography initially characterised by the presence of a bump (a). Figure (b) shows the topography developed after 200 cycles

where λ represents the cusp spacing and ε is a parameter providing a measure of the difference in the horn and bay steepness and so of the cusp prominence:

$$\varepsilon = \frac{\tan \beta_{\text{horn}} - \tan \beta_{\text{bay}}}{\tan \beta_{\text{horn}} + \tan \beta_{\text{bay}}} \quad (5.12)$$

Different authors have reported measures of ε and it generally ranges between values very close to 0 and reaching 0.3 (Komar, 1973; Dubois, 1978; Dean and Maurmeyer, 1980; Dubois, 1981; Masselink and Pattiaratchi, 1998b). It might be expected that the response of

pre-existing cusps to the self-organisation model will depend on their prominence, ϵ , and also on the degree to which their wavelength differs from the expected self-organisation wavelength, related to the swash excursion. The latter can be parameterised as:

$$\Lambda = \frac{\lambda_{\text{initial}}}{\lambda_{\text{s.-o.}}} \quad (5.13)$$

where the symbols λ_{initial} and $\lambda_{\text{s.-o.}}$ refer respectively to the superimposed initial spacing and to the spacing obtained when running the self-organisation model over a planar slope. Results are shown in Figure 5.17.

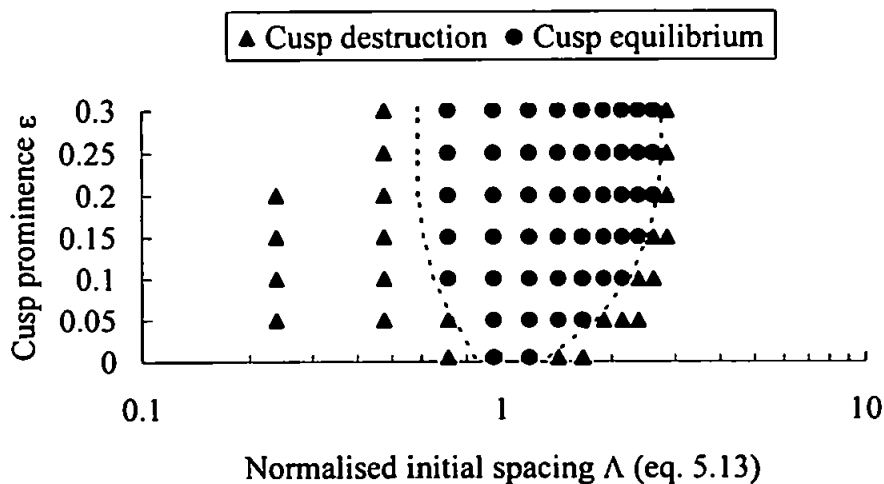


Figure 5.17 Self-organisation process over an initially cusped shoreline

It is clear that increasing the parameter ϵ for the initial topography, cusps are more stable and able to “drive” the water particle motion in such a way that the self-organisation mechanism is prevented. The smallest value used for ϵ has been equal to 0.005 but even in that case the pre-existing topography has a relevant influence on the processes and two different spacings can coexist with the hydrodynamics considered. Results indicate that even large amplitude cusps are destroyed if their spacing is more than a factor of two different from the spacing obtained when the self-organisation model is run on a planar slope. On the other hand, for spacing differing less than a factor of two, if the topography is so well developed that feedback processes are prevented or limited to negligible values, no change can occur and the initial topography remains stable (to a certain extent the opposite situation to the one already described regarding the use of small values of the coefficient α in the sediment transport parameterisation).

5.7 Numerical simulations of compatibility between edge wave and self-organisation

In order to try to better understand the possibility of coexistence between the two mechanisms, several simulations have been run by using the self-organisation model under a simplified form of standing edge wave input. The presence of standing edge waves has been simulated in the model by considering an alongshore sinusoidal variation in the cross-shore velocity of the water particles representing the incoming swash front. The alongshore component of the water particles has been considered equal to zero so as to simulate waves normally approaching the shoreline. The presence of both synchronous and subharmonic standing edge waves has been considered with the latter being simulated through a change of sign in the sinusoidal component of the velocities between successive swash cycles so that nodes and antinodes could be generated. All the results herein presented concern simulations run over a 10° slope with cross-shore velocities ranging between 2.2 and 2.8 m/s (average swash excursion around 1.8 m). The only randomness present in these simulations concerns the possibility that water particles, although equally spaced, may start from different grid points than the ones of the previous swash cycle. For the modelling of the hydrodynamics and sediment transport in the swash and surf zone, the same parameterisation as the simulations discussed in the previous sections has been applied. With such a parameterisation, the maximum swash period is around 3.2 sec and the ϵ parameter (equation 4.13) is equal to 2.45 which is very close to the values measured or theoretically derived (see Chapter 4).

As the model herein presented does not include any kind of interaction between incoming and outgoing waves there is no explicit period of the incoming wave. By assuming that the incident wave period is equal to the swash period, it is possible to evaluate, through the use of equation (4.5) and (4.6), the cusp spacing associated with eventually present subharmonic or synchronous standing edge waves respectively. By using such spacing, the sinusoidal variation of the input velocities in the alongshore direction has been evaluated and the standing edge wave effect on the swash run-up simulated.

Figure 5.18 shows the resulting topography when a subharmonic edge wave forcing is considered, with the resulting run-up maxima indicated in the plot, not to scale, through the use of a continuous line. This plot clearly indicates the correspondence of horns and embayments to antinodes (defined as locations where the run-up alternates maxima and minima for successive swash cycles) and nodes (defined as locations where the run-up maximum does not change between successive swash cycles) respectively. Such a pattern

shows an opposite behaviour to the one obtained by Guza and Inman (1975) through a series of laboratory experiments where sand was spread in the swash zone after the excitation of subharmonic standing edge waves. According to the experiment by Guza and Inman (1975), conducted in prevalent erosive conditions, horns correspond to standing edge wave nodes and embayments to antinodes. The possibility that accretionary conditions may lead to an opposite behaviour, and so in agreement with the one observed through the present model, has already been reported (Russell and McIntire 1965). The process of cusp development here is that decelerating water particles, usually during the swash run-up, cause deposition. As a consequence, and because of the continuous feedback between morphology and hydrodynamics, during the backwash the flow will be diverted from areas of deposition. Backwash flow is also accelerating under the effect of gravity and so will cause erosion.

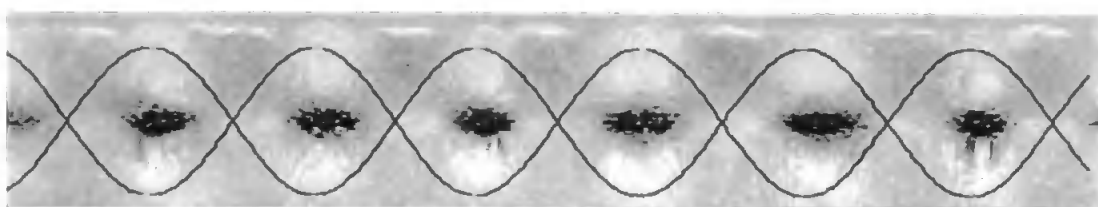


Figure 5.18 Formation and evolution of a cusped beach under subharmonic standing edge wave forcing

Different results are obtained when synchronous standing edge wave motions are simulated and, in order to obtain a stable cusp configuration, the sinusoidal variation of the velocities needs a wavelength close to the self-organisation (or subharmonic) expected spacing (Figure 5.19) rather than the one resulting from equation (4.6). Even in this case the horns appear in correspondence with the run-up maxima while the embayments correspond to the run-up minima and, because the backwash is concentrated in such area, deposition occurs immediately out of the swash zone.

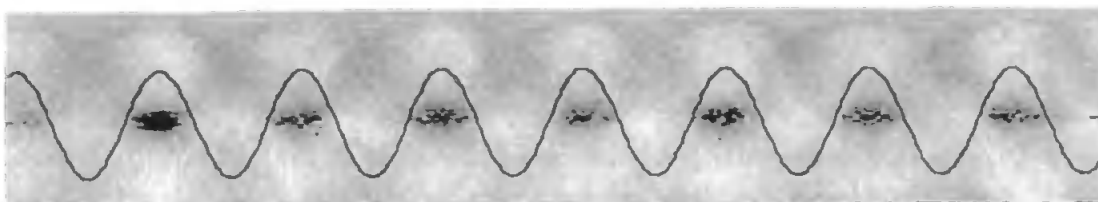


Figure 5.19 Formation and evolution of a cusped beach under synchronous standing edge wave forcing

Significantly different results are obtained when the condition that swash period equals incident wave period is relaxed. For example, simulated incoming standing edge waves can be characterised by an alongshore wavelength much smaller than the ones shown in the previous cases. Figure 5.20 shows results obtained with a subharmonic standing edge wavelength less than half the self-organisation predicted one. Such sinusoidal input would be related to a very small incident wave period (around 2 sec) but this simulation is presented only to clearly show the effect of the interaction between an external forcing and the self-organisation mechanism. In fact, the pattern resulting from such a simulation still displays some cusped features but it is definitely less regular than previous simulations and clearly not related to node-antinode sequence.

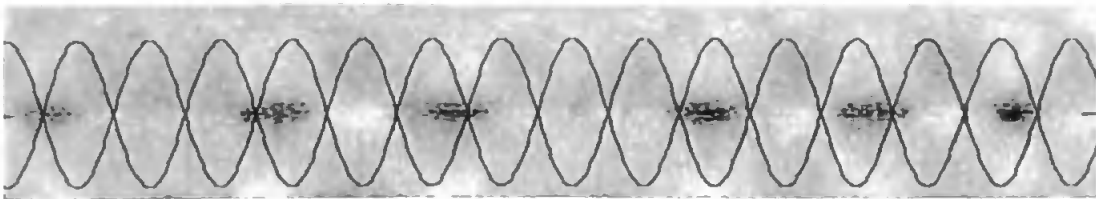


Figure 5.20 Formation and evolution of a cusped beach under sub-harmonic standing edge wave forcing

Some other interesting results are shown in Figure 5.21 where synchronous standing edge wave motions, with a wavelength equal to the one resulting from considering equation (4.6), are simulated. As a result, after 50 cycles (Figure 5.21.a), a cusped shoreline develops with a correspondence between run-up maxima and horns. If the simulation is run further (Figure 5.21.b) it is easy to identify a halving of the spacing in the cusped shoreline with the disappearance of every other feature and the readjusting of the topography into a spacing closer to the self-organisation one (which means only related to the swash excursion). A similar behaviour, a halving of the beach cusp spacing in only few hours, has been reported by the accurate topographic measurements of Masselink and Pattiaratchi (1998b). Unfortunately no detailed measurement of the hydrodynamics (wavelength of eventually present standing motions) was taken by Masselink and Pattiaratchi (1998b) so that no definitive comparison or conclusion on this phenomenon can be drawn.

The intriguing morphological changes shown in Figure 5.21, have also been studied with a different approach. A series of simulations has been run by considering an initially non-planar topography and a randomly generated swash excursion (like the one used for the simulation showed in Figure 5.2). This approach could be considered as a simulation of the theoretical work proposed by Guza and Bowen (1981) where it is shown that well-

developed cusps are capable of detuning and suppressing edge wave motions. Figure 5.22 shows the topography resulting after running the model over a cusped topography produced with a synchronous standing edge wave forcing (the one showed in Figure 5.21.a). By comparing the two plots it can be seen that, once sinusoidal motion is not forcing the morphology, the shoreline re-organises into a different spacing with horns and embayments in different positions than at the beginning of the simulation. The final spacing is exactly the same as the one obtained in Figure 5.2 (same parameters have been applied to the two simulations) which testifies to the robustness of the self-organisation mechanism against pre-existing topography (a feature the standing edge wave approach does not possess). As discussed in the previous sections, different results are obtained when running the model over a more prominent cusped topography (like the one showed in Figure 5.21.b). As a confirmation, Figure 5.23 shows that the initial topography is so prominent and well-developed that no change in the spacing is allowed but only an enlargement of the already present features. These observations confirm to the possibility of a “topographic threshold” such that a less prominent morphology would allow for the beginning of feedback processes, and so of the self-organisation mechanism, while more prominent features would control and affect the hydrodynamics so strongly that no relevant change is allowed.

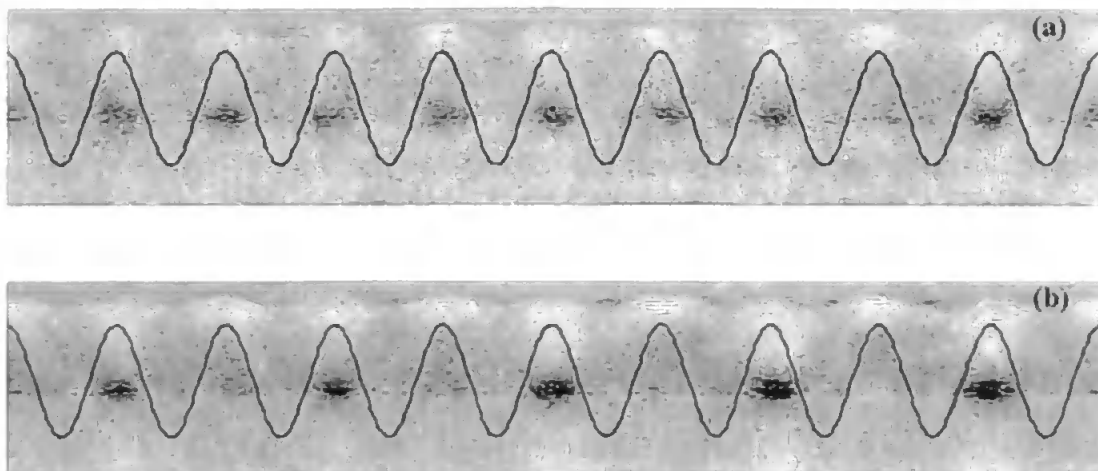


Figure 5.21 Formation and evolution of a cusped beach under synchronous standing edge wave forcing (see text)

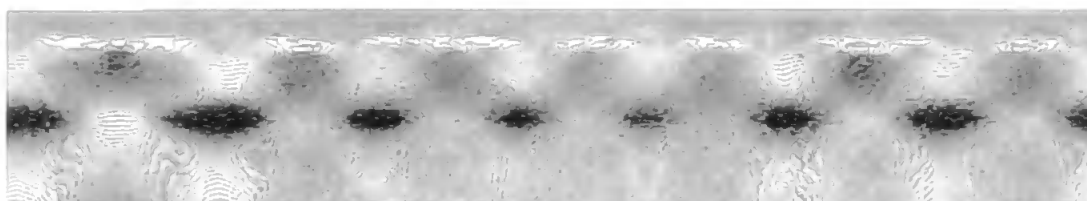


Figure 5.22 Development of a cusped beach over a pre-existing topography




Figure 5.23 Development of a cusped beach over a pre-existing topography

A final comment needs to be made in order to describe the difference between the simulations with a standing edge wave forcing and those characterised by a random input. In fact, it has been suggested by different authors (see for example Seymour and Aubrey, 1985; Inman and Guza, 1982) that standing edge waves can be important only during the initial stages of cusp formation providing the initial alongshore instability that, reinforced by flow patterns, would then grow into finite amplitude cusps without any need of a standing edge wave forcing. This being the case, cusps forming under a standing edge wave forcing should grow faster than cusps resulting from a self-organisation process. Simulations for the two cases have been run and results compared through the use of the peakedness parameter (equation 5.10). Results, shown in Figure 5.24, clearly indicate that, from the very first cycles, the presence of a hydrodynamic forcing with a structure in the longshore direction would cause a faster growth of beach cusps. Simulations have also been run by considering a standing edge wave input only for a limited initial number of cycles and then a normal approaching wave field. Because of the parameterisation considered, even only 10 cycles of standing edge wave forcing are sufficient to define the final structure of the pattern that exactly corresponds (spacing and horn-embayment locations) to the simulation performed under a continuous standing edge wave forcing. The small differences in Q_p found after 100 cycles indicate the minor role of the randomness not allowing for a clear shape of the cusps as compared to the case of continuous standing edge wave forcing. Such a result is not unexpected because a careful analysis of Figure 5.24 reveals that after 10 cycles the value of Q_p is already well above 0.1 which indicates the presence of a clear alongshore structure in the morphology. Much more intriguing is the simulation with a standing edge wave forcing present only for the first 2 swash cycles. In such a case, the value of Q_p indicates a very small structure in the topography and the whole process of beach cusp formation is much slower. Nevertheless, cusps form at the same spacing and with horns and embayments exactly at the same locations as the run under a continuous standing edge wave forcing. The simulation run with no longshore structure in the hydrodynamic forcing follows a completely different path and, although the growth appears to be faster than the case of initial standing edge wave input, the final pattern shows a slightly different spacing and a completely different positioning of horns and embayments.

It is clear that the previous results have important implications in terms of the possibility of detecting which mechanism is responsible for beach cusp formation. Very accurate, nearly swash cycle by swash cycle, field measurements would in fact be needed in order to verify whether an alongshore structure is present in the runup or not. The problem of accurate field measurements is also complicated by the possibility that, as soon as an alongshore structure in the topography develops, edge waves could be affected by resonant scattering and so leading to the growth of edge waves characterised by the same or different longshore wavenumber (Chen and Guza, 1998; Chen and Guza 1999).

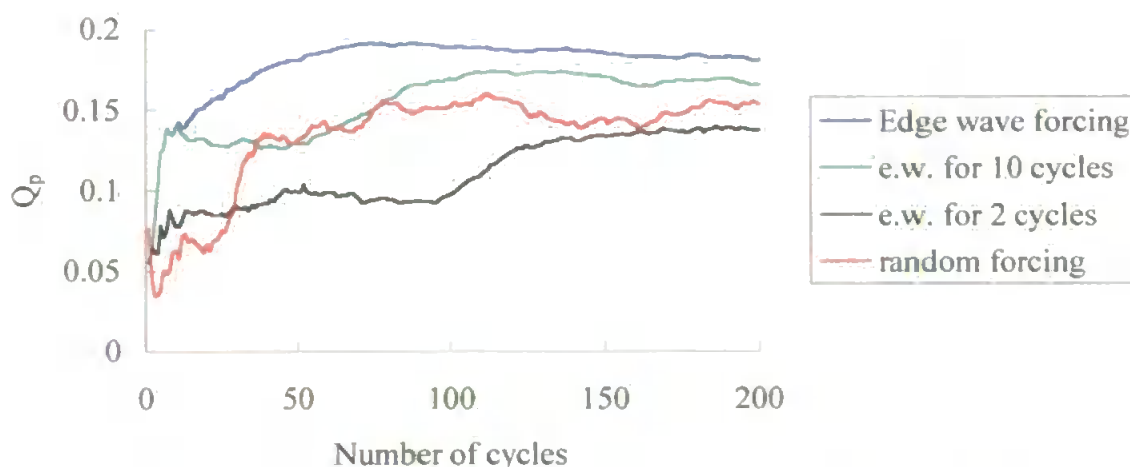


Figure 5.24 Variation in the peakedness under different hydrodynamic inputs

5.8 Discussion

A model for beach cusp formation and development has been implemented on the basis of the work proposed by Werner and Fink (1993) where beach cusps are the result of the feedback interaction between flow and morphology. Interaction between incoming and outgoing waves, infiltration and refraction have all been neglected but cusp formation is still evident and the shoreline adjusts to a spacing in agreement with field measurements. A sensitivity analysis of the parameters involved in the simulations indicates that most of the input and model parameters (like sediment transport, angle of repose, randomness) primarily affect the rate of beach cusp formation and have only a small influence on the final spacing. Cusp spacing linearly scales with the swash excursion, the proportionality coefficient being in agreement with field and laboratory data (see Chapter 4).

In addition to the prediction of cusp spacing, several other features of the simulations are in good agreement with field observations. As generally observed, the process of beach cusp

formation is found to be of a depositional nature within the swash zone, and is associated with a flow pattern over the cusped shoreline which is clearly horn divergent. Also as observed, the presence of an alongshore current is found to destroy cusps; the quantitative prediction that cusps are destroyed if the swash runs up the beach at an angle greater than about 6° seems to be confirmed by field testing.

The relevance of other features of model behaviour can only be assessed through more detailed field observations. Changes in the initial random seed and runs for large numbers of swash cycles reveal a highly dynamic system with significant unpredictable behaviour. Cusp spacing tends to change with time and cusp regularity shows large long-term variations. Even after a quasi-equilibrium pattern has developed, cusps can be destroyed and reformed in different locations. The rate of initial formation of cusps is also found to be highly variable and dependent on initial random input; it is suggested that this might account for the patchy occurrence of cusps on relatively uniform beaches.

In addition, the possibility of beach cusp formation on a non-planar beach has been investigated. Results confirm the strength of the self-organisation process and imply a mechanism which is not simply the result of feedback from a topographically driven steady-flow. Unless of very high prominence, pre-existing topography is usually destroyed and beach cusps reform with a spacing in accord to the self-organisation prediction. However, very prominent pre-existing cusps do persist if their spacing is no more than a factor of two different from that expected by self-organisation.

The possibility of coexistence between the standing edge wave model and the self-organisation one has been investigated through a series of simulations under a simplified standing edge wave input. Results seem to indicate the possibility of cusps of co-existence between the two models at least under a subharmonic standing edge wave forcing whose spacing prediction, as shown in section 4.4 (eq. 4.22), is very similar to the one obtained with the present self-organisation model. It is then possible to argue that beach cusp might well be the result of either a hydrodynamical instability (but only under conditions that are able to ensure topographic equilibrium) or a coupled flow-sediment instability driven by feedback processes.

Chapter 6: Comparison between model results and field data using a non-linear technique

6.1 Introduction

The usual assumption, when dealing with coastal evolution, is that shoreline changes are the direct consequence of a change in the hydrodynamic forcing which tends to move the system away from the previous equilibrium and brings it towards a new equilibrium state. In the first place, it is important to underline that the forcing is not unique but is the result of different components acting at different time-scales (waves, tides), subject to random variations, that can become dominant for certain conditions (storms) or locations (under the wave breaking) or simply because of human action (breakwaters, beach nourishment, etc.). As a result, the response of the system can simply “mirror” the forcing conditions or interact and, usually for weak forcing conditions, even affect it to the point where the whole system is governed by feedback processes and by the non-linear relationship(s) between forcing and response. As a consequence, the suggestion that a non-linear system, like the coastal one, can freely respond to the forcing needs to be analysed as well as the possibility of a chaotic response resulting in self-organised patterns. This approach has already been applied to natural sciences (Hastings and Sugihara, 1993; Bak, 1997), including long-term coastal morphodynamics (Southgate and Beltran, 1995; Southgate and Beltran, 1996), providing evidence for the primary role of self-organisation in the evolution of complex systems. Applying this concept to short-term morphological changes is a difficult task because of the intrinsic interaction between forced and free responses although, as outlined in chapter 2, coastal morphodynamics are characterised by many of the features associated with non-linear dissipative dynamical systems.

Several techniques have been developed in recent years in order to analyse data obtained from complex systems and only recently their application into environmental sciences has been considered. Most of these techniques, which have proved to be useful in describing the system’s behaviour and in some cases even in forecasting the system evolution, require very long data series so that the application to coastal morphodynamics is possible only in very few data sets and only for some of such techniques (Southgate et al., 1999). The application of non-linear techniques is a very useful tool also when comparisons between field data and model results are made. In fact, most of the non-linear techniques provide a qualitative description of the processes through a parameter (for example the fractal dimension or the Lyapunov exponent). The characterisation of a system’s behaviour

through a parameter can then allow, if the same parameter can be extracted, comparisons with numerical models.

This chapter deals with the use of nonlinear techniques in order to compare results of a non-linear model with field measurements performed during beach cusp formation. The possibility that nearshore processes are the result of a self-organisation process and that morphological changes in the topography follow a fractal distribution will also be analysed. In order to give evidence of fractal behaviour different techniques will be applied to beach elevations deriving from field measurements and from the results of the previously described self-organisation numerical model for beach cusp formation. Separate time series of beach elevations will be considered in order to prove that the same physical process is occurring over the different locations surveyed or in the numerical model.

6.2 Analysis of time series through non-linear techniques

Several techniques have been proposed in the last years in order to improve the understanding of the role of non-linearities in complex systems like coastal morphodynamics. Before briefly reviewing some of them, it is important to underline that most of these techniques do not necessarily perform better than the linear ones especially when applied to forecasting or to reducing the number of variables in a data set. For example, transforming the data using a linear technique like Empirical Orthogonal Eigenfunction analysis has already proved to be very successful in its coastal environment applications (see for example Winant et al., 1975; Hsu et al., 1994; Wijnberg and Terwindt, 1995) as well as spectral analysis which is still one of the most effective tools used to detect periodicity and trends. The main purpose for using non-linear techniques is the characterisation of the system (Southgate et al., 1999). This means understanding whether the system is “attracted” towards an equilibrium state (which can also be periodic or chaotic), the time scale at which different behaviours may occur and the influence of the forcing conditions on the system’s response.

The most common non-linear analysis techniques are those related to the concept of “time-delay embedding” where the overall dynamics of a system (for example the fractal dimension or the Lyapunov exponent) are reflected into the response of a single variable. Such technique is used to find the number of independent variables describing the system and has been successfully applied into oceanographic studies (Jaffe and Rubin, 1996; Frison et al., 1999; Holland et al., 1999). It does not seem to be applicable to

measurements of bed levels because of the large amount of data required for the analysis, a condition hardly satisfied by any of the existing data sets (Southgate, 1997). A similar procedure (Forecasting Signature Method), although based on the comparison between results obtained from “trial models”, has also been proposed and proved to be successful for the analysis of a two-dimensional pattern (Rubin, 1992). It still requires very long time series (several hundreds) but offers a very interesting prospective as it can be used to analyse images like those obtained through remote sensing systems.

An innovative approach to the analysis of time series is given by the use of artificial neural networks. This technique involves the use of a “training” set of data and consists of a series of layers of nodes connecting inputs and outputs. Each node, in each layer, has got a different weight, previously determined through the “training” set, and output values are obtained through a combination of linear and non-linear transformation of values at each node. Although this technique is a typical example of “black box” modelling and so does not allow for an understanding of the underlying physical processes, recent applications in the oceanographic field (Kingston and Davidson, 1999; Tsai and Lee, 1999) indicate the strength and validity of this approach.

Another technique that begins to find applications also in the oceanographic field (Babovic and Abbott, 1997b; Davidson et al., 1999) is related to the evolutionary concept as established by Darwin in the 19th century. Selection, mutation and reproduction on a population undergoing an evolutionary process are the basis of a mechanism that allows the “most fitting” variable to reproduce more often and the evolutionary process to proceed (Babovic and Abbott, 1997a). Several techniques follow this basic concept (Genetic Algorithms, Genetic programming, Evolution Strategies, Evolutionary Programming), are capable of producing very accurate results and allow for an understanding of the fundamental variables and so of the mechanisms involved in the processes analysed.

The fractal technique is basically a statistical approach and is considered to be particularly suitable when high dimensional systems (like coastal morphodynamics) are studied and the length of the time series available is limited. This technique will be described in much more detail in the next section as it will be applied to field measurements and model results. The same approach has been considered in different fields of environmental sciences by Hastings and Sugihara (1993) and has already been applied to coastal morphodynamics by Southgate and Beltran (1995, 1996) and Southgate and Möller (1999).

6.3 The fractal approach

Fractals can be defined as scale-invariant (or self-similar) geometric objects. Following such a definition, fractal (or self-similar) processes can be described through the use of the fractal dimension D which is the variable controlling the regularity of the phenomenon. The hypothesis related to considering a fractal distribution is that a process can be repeated on different scales in the same way. This idea has usually been applied to describe spatial patterns but can also be applied to fractal (or self-similar) processes in time.

The characterisation of a fractal process can be obtained by generalising the axioms defining a so-called Brownian motion or random walk (Mandelbrot, 1982). As a result, a continuous process $y(t)$ can be defined as a continuous (in time) fractal process if, for any time step dt , the increments $dy(t) = y(t+ dt)-y(t)$ have a variance proportional to a power of dt . Such power is then related to the Hurst exponent (H) and can be evaluated, as shown later, through different techniques. The importance of the Hurst exponent also lies in its relationship to the previously defined fractal dimension, so that, for most of the processes: $D = 2 - H$. The value of H is of primary importance as a pure fractal process is characterised by a constant value, with time, of H . Such occurrence, although possible, is not the most common while much more often it is possible to divide the time domain into regions of constant H and so discern between different processes happening at different time scales. The application of valid limits to the fractal distribution could be a great help in the understanding of the system's behaviour (Southgate and Möller, 1999). Moreover, the value of H can vary between 0 and 1 with the value $H=0.5$ indicating a random walk. Values of the Hurst exponent higher than 0.5 suggest persistence in the behaviour of the time series such that each increment dy is positively correlated to the previous one. On the other hand, a value of the Hurst exponent lower than 0.5 indicates anti-persistence. A very simple and idealised example can be made in order to explain the meaning of persistence and anti-persistence and to show the possible applicability of such concepts. It is in fact possible to hypothesise the existence of a time series of beach elevation for a location where a beach nourishment intervention is needed. Suppose the application of the fractal analysis for such time series and the evaluation of the global Hurst exponent results in a short term behaviour (around 6 months) indicating persistence (a period of erosion/accretion would be followed by an equally long period of erosion/accretion) and in an anti-persistent long term behaviour (a period of erosion/accretion would be followed by an equally long period of accretion /erosion). Then, the frequency of beach nourishment interventions could be evaluated using such information so that the maximum efficiency

would be obtained if the quantity of material laid on the beach exceeds the amount of erosion expected over 6 months. Laying less material would result in the possibility of immediate loss of the material (persistent periods of erosion of 6 months) while exceeding the 6 months amount would avoid any short-term risk and allow for the possibility that a sort of cycle accretion/erosion is established.

In order to evaluate the Hurst exponent three different established techniques have been considered (Hastings and Sugihara, 1993): the growth of variance, the growth of range (global Hurst exponent) and a correlation technique (local Hurst exponent). The choice of such techniques relies on the methods giving independent results and so allowing for comparisons.

The growth of variance technique is applied by selecting a time interval dt , evaluating all the increments Δy and then the corresponding variance. This operation can be repeated for subsequent time intervals and, if the process is fractal, a logarithm plot of the variance against time step will result in a straight line characterised by a $2H$ value of the slope. As for fractal processes the Hurst exponent is independent of the time interval, if long time series are available, it is also possible to apply this procedure by considering general time intervals or windows of data.

The growth of range technique suggests a similar procedure and the sum of the ranges (difference between maximum and minimum values of the increments) related to a chosen time step is associated to the time step itself. If the process is fractal, a logarithm plot of ranges and time intervals should result again in a straight line with slope equal to H . This second approach requires particular attention when applied to small time intervals as the value of H can be overestimated so much that a random walk would be characterised by $H=0.63$ rather than 0.5. North and Halliwell (1994) analyse the generation of synthetic data and show the existence of an initial biased zone that could affect the final evaluation of the Hurst exponent. Unfortunately for natural time series the end of such a transient zone is not unequivocally determined and North and Halliwell (1994) suggest that such value could change depending on the nature of the time series.

The two techniques previously described provide a measure of the fractal character of the time series over the whole range of time increments dt and so are usually indicated as global Hurst exponent (the value of the Hurst exponent is obtained through a regression of the variance/range over all the time intervals dt considered). It is also possible to evaluate

the Hurst exponent for each single time interval (local Hurst exponent H_{loc}) so that information can be deduced on the time range over which fractal behaviour is observed. This technique is based on the evaluation of the correlation coefficient between successive increments which has the form:

$$\rho_H = \frac{[y(t + 2dt) - y(t + dt)] * [y(t + dt) - y(t)]}{\{[y(t + 2dt) - y(t + dt)]^2 * [y(t + dt) - y(t)]^2\}^{1/2}} \quad (6.1)$$

The local Hurst exponent is then given by the formula:

$$H_{loc} = \log(2 + 2\rho_H) / \log 4 \quad (6.2)$$

The initial stage of the procedure adopted is the same as the one suggested by Southgate and Beltran (1995, 1996) and data are treated according to the following sequence:

- a) evaluate goodness of fit of the beach elevations to a Gaussian distribution
- b) create the cumulative time series (with the beach levels expressed in terms of the time-mean value)
- c) evaluate the global and local Hurst exponent

The need to use a cumulative series of the increments rather than the actual beach elevations is due to the nature of the physical process studied (every beach level is bound to the one measured at the previous time step) and to the nature of the hypothesis being tested (whether beach levels represent the increments of a fractal process or not). North and Halliwell (1994) and Southgate and Möller (1999) also indicate other factors that have to be considered before starting the analysis and that could sensibly affect the accuracy in the evaluation of the global Hurst exponent (H). It has already been stressed that the growth of range technique is very sensitive to the length of the time series but also other problems, common to all the different techniques, have to be considered. In fact, there is the suggestion that also the use of large dt can bias the estimation of H . For such reason, and in accordance with Hastings and Sugihara (1993), the maximum time interval considered in any analysis is always equal to 1/3 of the total number of measurements constituting the time series. On the other hand, a periodic component in the time series can potentially reduce the value of H while a non-stationarity of the means (revealed by comparing mean values for different “windows” of the time series) can sensibly increase the value of H to the point of even exceeding 1. Another source of bias could derive from the need of data interpolation (in time or space) as such an operation can alter the statistical properties of the whole time series.

Attention must also be paid to the data distribution as disagreement exists in the literature on the importance that data fit a Gaussian distribution. Hastings and Sugihara (1993) clearly indicate that fractal behaviour requires Gaussian distribution of the data. On the other hand, Southgate and Möller suggest that if the data fits a Gaussian distribution and if the time series are fractal, H should be equal (or at least close) to 0.5. A non-Gaussian distribution of the data should result in a significantly persistent ($H > 0.5$) or anti-persistent process ($H < 0.5$).

6.4 Data available

A field survey was conducted by Masselink et al. (1997) from 3rd to 9th March on City Beach, Perth, Western Australia. Such coastline, characterised by a mean slope around 6°, experiences low wave energy and a microtidal regime with spring tide ranges less than 1m. Prior to the field survey City Beach was characterised by the presence of a pronounced cusped morphology that was considered during selection of the survey transects. Seven shore-normal transects were established across the beach face, with an alongshore spacing of 7.5m, the resulting measurements spanning two cusp horns and adjacent embayments. Each of the seven transects consisted of 19 steel pegs which were inserted at 1m cross-shore intervals. Transects extended from landward of the berm crest to the base of the beach face. The height of the exposed pegs was manually measured every hour for the duration of the field study with accuracy around $\pm 0.03\text{m}$. Examples of three-dimensional changes in the morphology are shown in Figure 6.1 where "T" indicates the hour at which measurements have been taken (T=1 corresponds to the initial morphology while T=145 is the result of the last survey). Because of the spatial (beach levels were measured always at the same locations) and temporal (beach levels were measured every hour) resolution, no interpolation of the data is needed.

The 133 beach level series obtained through the field measurements have been transformed into cumulative time series by first deducting the time-mean value and then adding the successive increments. Figures 6.2, 6.3, 6.4 show examples of the measured beach levels, referred to the time mean, and of the cumulative series. Time series have been numerated according to their position with the first number indicating one of the nineteen cross-shore locations (from top to bottom of the swash) and the second one the seven alongshore transects (from left to right).

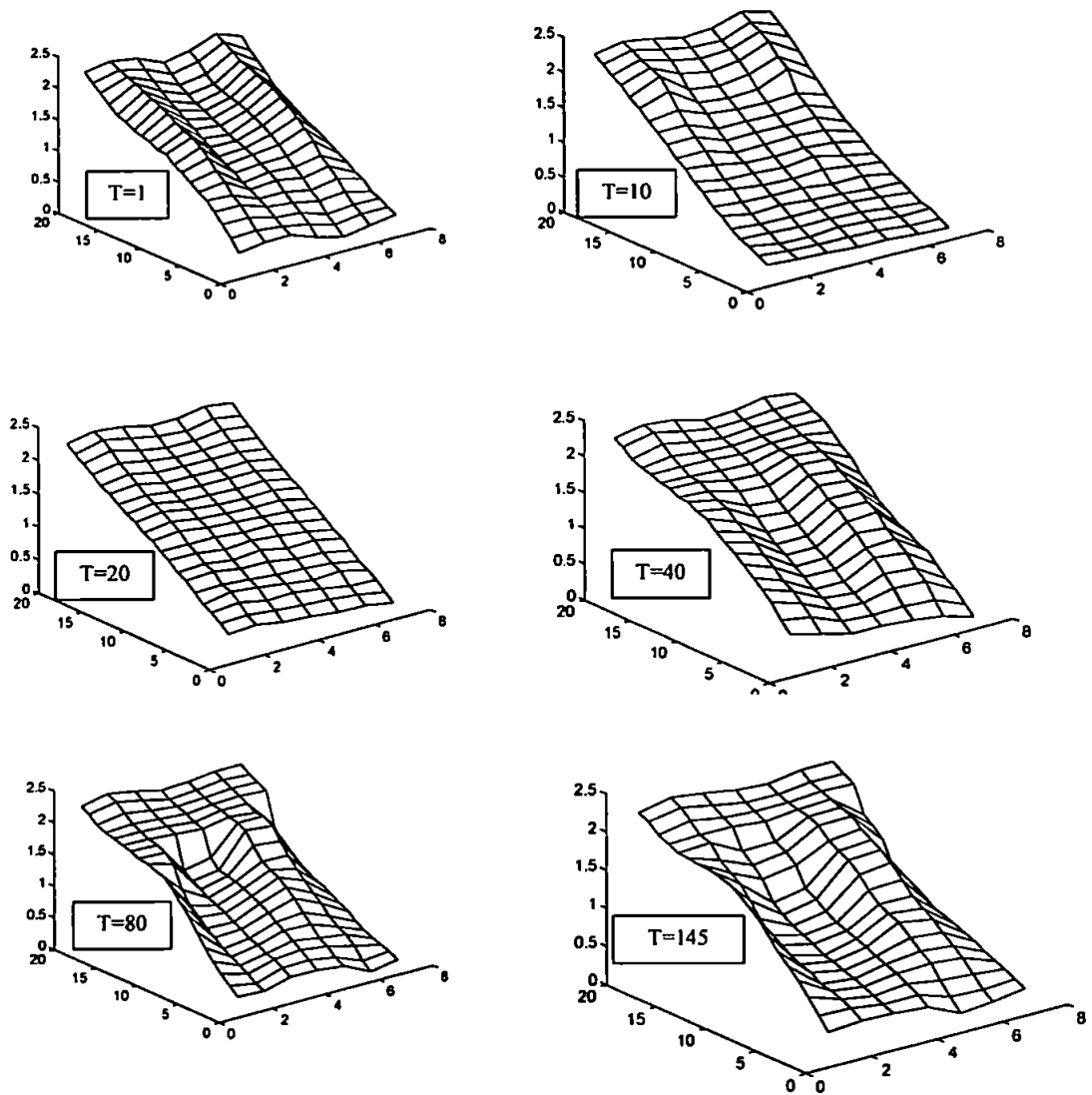


Figure 6.1 Cusp evolution during the field experiment (T=1 indicates the initial topography while T=145 corresponds to the last survey)

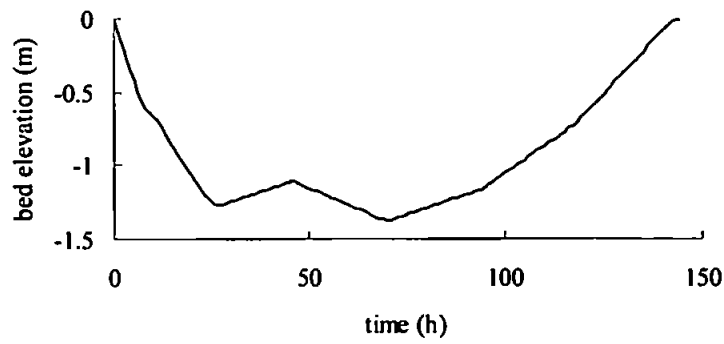
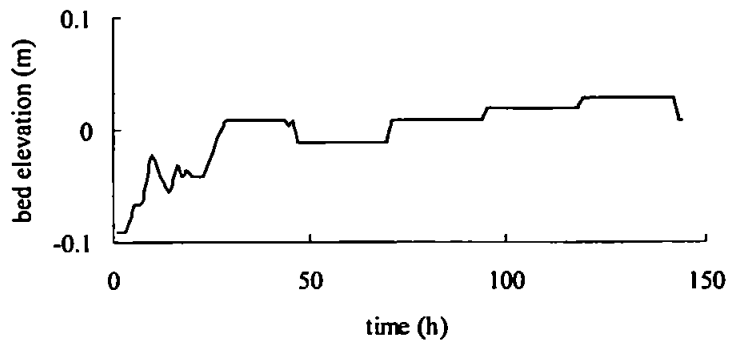


Figure 6.2 Actual and cumulative beach levels at the top of the swash zone (location 4-7)

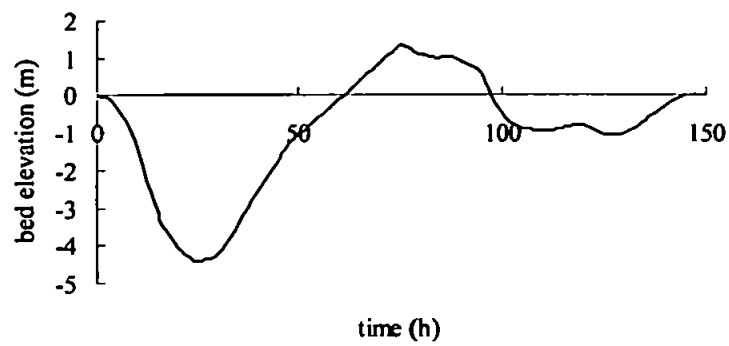
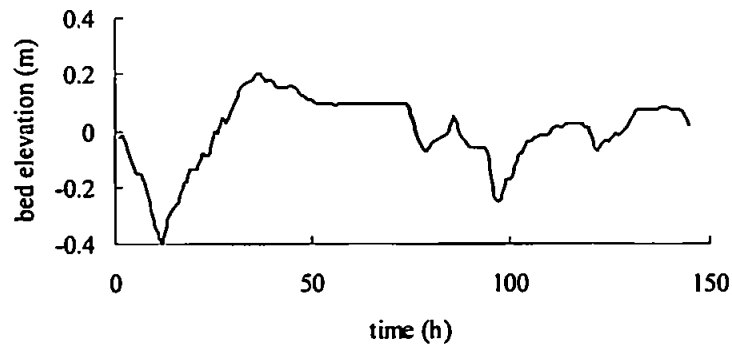


Figure 6.3 Actual and cumulative beach levels at the centre of the swash zone (location 10-3)

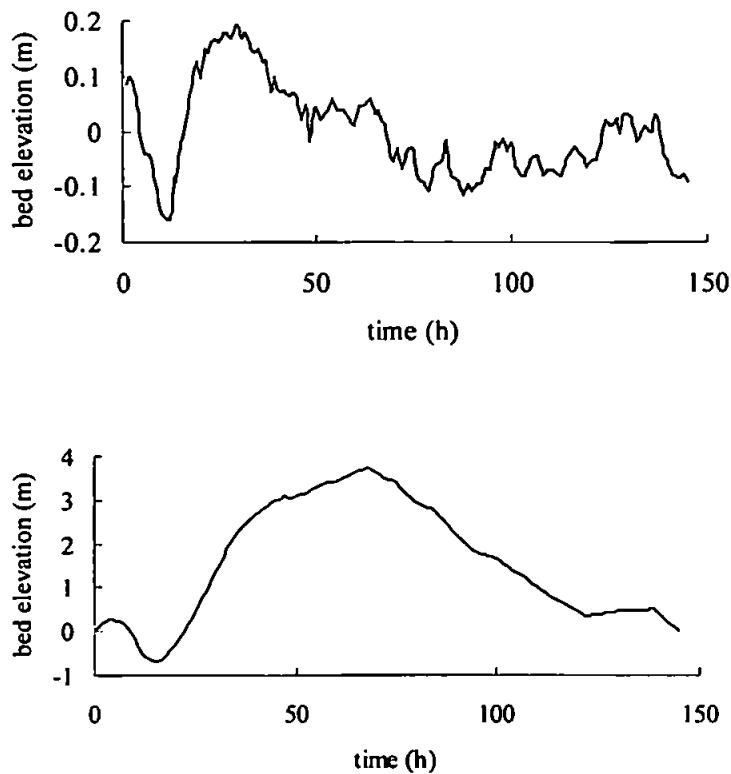


Figure 6.4 Actual and cumulative beach levels at the bottom of the swash zone (location 14-5)

The hydrodynamic conditions, constituting the external forcing acting on the topography, wave heights varied considerably during the field experiment and three different phases have been observed:

- a) an initial period (approximately the first 24 surveys) of rising wave heights associated with a storm system resulting in the presence of strong longshore currents and so in beach cusp destruction
- b) falling wave energies following the passage of the storm (roughly corresponding to the following 65 surveys)
- c) a period of three distinct sea breeze cycles (corresponding to the last 56 surveys) which were associated with an increase in wave height, decrease in period and obliquely approaching wind waves

Data deriving from numerical simulations of the self-organisation model presented in chapter 5 have been used in order to test the hypothesis of fractal distribution and to compare the values of the Hurst exponent with the field measurements. Results from such a numerical model will be here analysed by applying the previously described fractal analysis techniques to bed elevations inside the swash zone. Also in this case, no time or space interpolation of the data is needed. The use of a numerical model also allows for

longer time series and simulations of different length or different forcing conditions have been run. Figures 6.5 and 6.6 show examples of the time-mean beach levels and of the cumulative series for a simulation 600 cycles long. In such simulation, after cusp appearance (around 100 cycles), a strong oblique wave approach has been “forced” and, once cusps had been wiped out (around cycle 200), a normal approach has been considered again until the end of the simulation.

6.5 Results

The 133 points surveyed during the field experiments (7 transects of 19 points each) have been analysed by firstly checking the goodness of fit to a Gaussian distribution. Results from chi-square tests indicate poor fit with less than 10% of the beach level time series following a Gaussian distribution. Table III and IV show the value of the Hurst exponent for each of the locations (the seven columns of the table refer to the seven field transects) evaluated through the growth of variance and range technique respectively. In both cases the maximum time interval adopted is equal to 50 hours. The average value of the Hurst exponent for the growth of variance case is equal to 0.76 with a standard deviation equal to 0.1 while for the growth of range case the mean value is 0.78 with a standard deviation of 0.1. The maximum difference between values of the Hurst exponent for a single location, evaluated with the two different techniques, is equal to 0.15 while the average difference (absolute values have been considered) between single locations is less than 0.05. Examples of the results obtained are given for 3 arbitrarily chosen locations at the top, centre and bottom of the swash zone respectively (Figure 6.7, 6.8, 6.9 for the growth of variance and Figure 6.10, 6.11, 6.12 for the growth of range). Such plots seem to give evidence of a fractal distribution for the field measurements analysed with a straight line reasonably well fitting the points for both the growth of variance and growth of range technique. The values of the Hurst exponent, consistently above 0.5, clearly indicate the persistency of the process. A better indication of the possibility of fractal behaviour, including the time scale at which the process is present, is given by the local Hurst exponent (Figure 6.13, 6.14, 6.15). Such coefficient appears to be less stable than the global measures of H and is never constant over all the time intervals analysed. Only in some of the cases H_{loc} seems to indicate the possibility of fractal behaviour but even then the time scale suggested is not clearly related to any physical process. Instead, it is possible to analyse the behaviour of the single cross-shore locations. In fact, at the top of swash zone very few changes happen (see Figure 6.1 and 6.2) and they are obviously related to the movement of the shoreline induced by the tide.

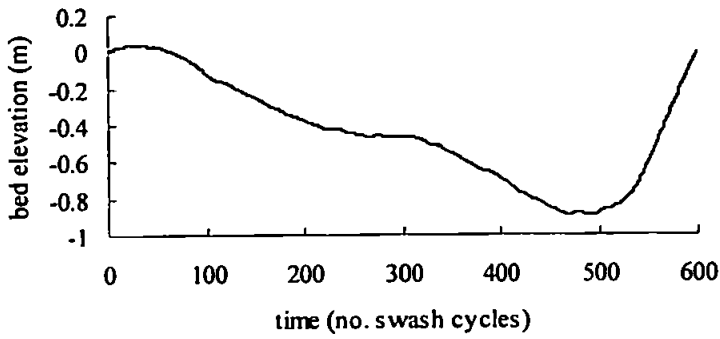
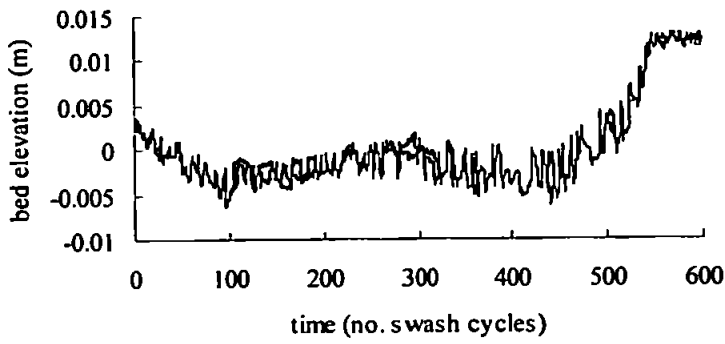


Figure 6.5 Actual and cumulative bed elevations for a model simulation (bottom of the swash zone)

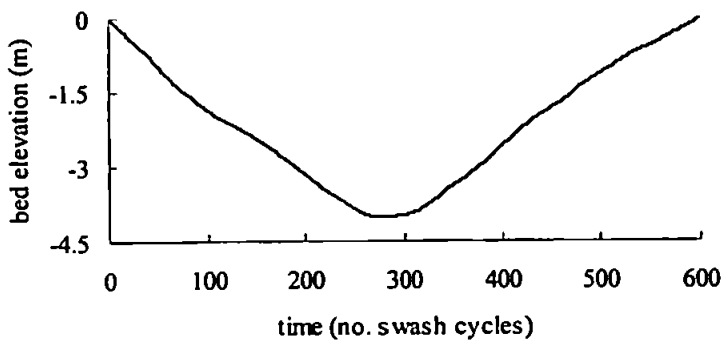
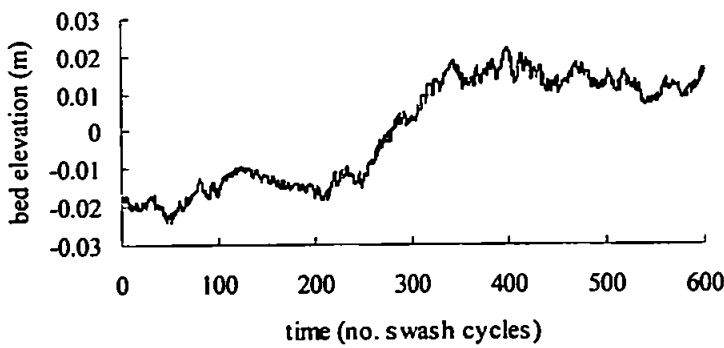


Figure 6.6 Actual and cumulative bed elevations for a model simulation (inside the swash zone)

Table III Value of the Hurst exponent for field data using the growth of variance method
(offshore direction goes from top to bottom of the table)

0.77	0.82	0.48	0.53	0.78	0.67	0.87
0.66	0.69	0.70	0.59	0.78	0.75	0.81
0.69	0.66	0.69	0.68	0.76	0.80	0.81
0.90	0.67	0.73	0.70	0.71	0.74	0.76
0.96	0.69	0.72	0.75	0.90	0.56	0.72
0.95	0.69	0.73	0.88	0.90	0.80	0.74
0.95	0.69	0.80	0.91	0.95	0.86	0.74
0.93	0.71	0.81	0.89	0.95	0.87	0.74
0.91	0.69	0.79	0.88	0.95	0.92	0.76
0.88	0.68	0.74	0.84	0.93	0.92	0.75
0.85	0.65	0.68	0.81	0.92	0.91	0.75
0.81	0.64	0.68	0.77	0.91	0.89	0.74
0.78	0.67	0.68	0.71	0.89	0.87	0.72
0.70	0.63	0.68	0.73	0.87	0.86	0.72
0.71	0.63	0.72	0.66	0.83	0.86	0.75
0.63	0.65	0.73	0.54	0.79	0.83	0.76
0.63	0.62	0.76	0.63	0.80	0.84	0.78
0.71	0.65	0.77	0.66	0.69	0.83	0.82
0.73	0.70	0.80	0.76	0.74	0.87	0.87

Table IV Value of the Hurst exponent for field data using the growth of range method
(offshore direction goes from top to bottom of the table)

0.73	0.97	0.55	0.54	0.77	0.61	0.99
0.71	0.82	0.64	0.69	0.85	0.71	0.75
0.73	0.52	0.72	0.72	0.66	0.80	0.73
0.88	0.63	0.70	0.73	0.74	0.86	0.63
0.97	0.61	0.70	0.72	0.88	0.68	0.71
0.98	0.66	0.75	0.91	0.90	0.75	0.68
0.97	0.76	0.81	0.97	0.97	0.82	0.63
0.95	0.72	0.83	0.99	0.98	0.82	0.60
0.93	0.69	0.80	1.00	0.97	0.91	0.64
0.91	0.67	0.76	0.95	0.95	0.94	0.68
0.89	0.64	0.69	0.92	0.93	0.94	0.75
0.85	0.60	0.71	0.87	0.92	0.91	0.75
0.81	0.65	0.71	0.80	0.91	0.90	0.70
0.69	0.61	0.71	0.80	0.89	0.90	0.73
0.71	0.60	0.75	0.75	0.87	0.93	0.78
0.62	0.65	0.75	0.63	0.83	0.90	0.78
0.63	0.64	0.80	0.71	0.83	0.92	0.83
0.69	0.68	0.81	0.77	0.71	0.92	0.87
0.69	0.79	0.85	0.85	0.80	0.99	0.92

The global Hurst exponent (Figure 6.7 and 6.10) simply indicates persistent fractal behaviour while H_{loc} (Figure 6.13) indicates that persistent fractal behaviour is possible only at time intervals around 15-30 hours which basically means only when the tide allows the runup to reach such an area. At the centre of the swash the situation, although the global H still indicates persistence (Figure 6.8 and 6.11), is "less fractal" as changes in the topography are mainly a reflection of the hydrodynamic forcing. Figure 6.3 clearly shows the erosive effect of the storm (after 10 hours), subsequent accretion and the erosive effect due to the sea breeze. As a result, H_{loc} (Figure 6.14) is never close to a constant and for

large time intervals even assumes negative values. At the bottom of the region analysed (Figure 6.4) changes in the morphology due to the external forcing, apart from the effect of the initial storm, are less evident and the results provided by the global H (Figure 6.9 and 6.12) are in some way confirmed by H_{loc} (Figure 6.15) that is nearly constant over a range of time intervals going from 10 to 25 hours. The behaviour suggested by the time series here showed is confirmed by the analysis of the other time series available.

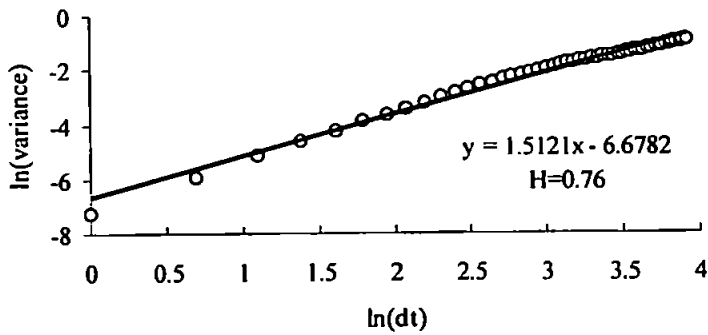


Figure 6.7 Growth of variance at the top of the swash zone (Location 4-7)

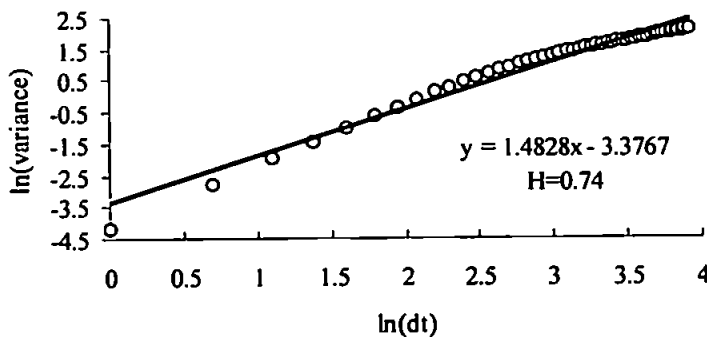


Figure 6.8 Growth of variance at the centre of the swash zone (Location 10-3)

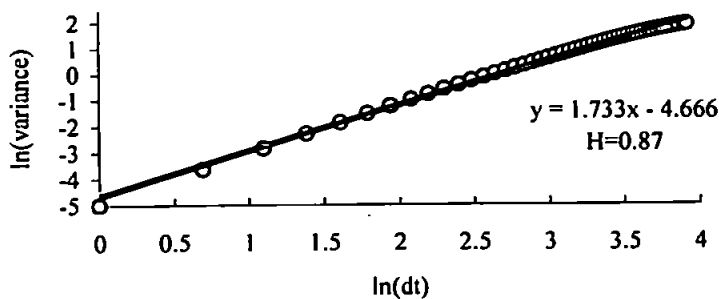


Figure 6.9 Growth of variance at the bottom of the swash zone (Location 14-5)

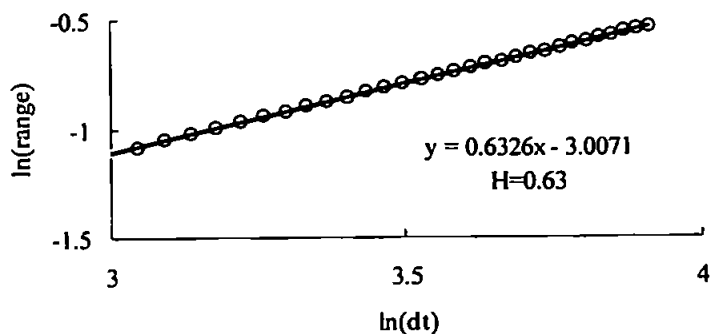


Figure 6.10 Growth of range at the top of the swash zone (Location 4-7)

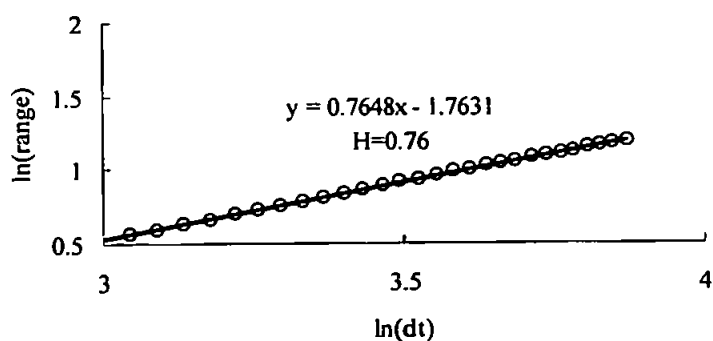


Figure 6.11 Growth of range at the centre of the swash zone (Location 10-3)

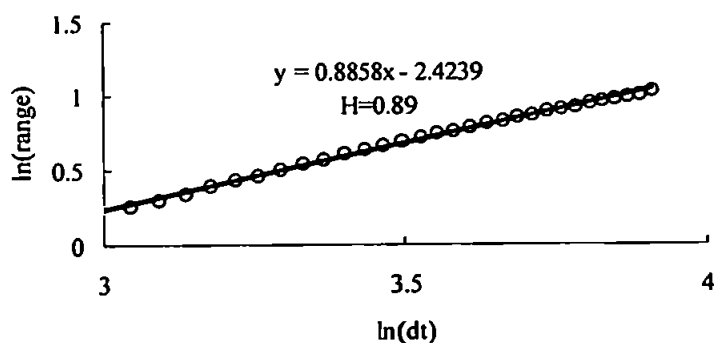


Figure 6.12 Growth of range at the bottom of the swash zone (Location 14-5)

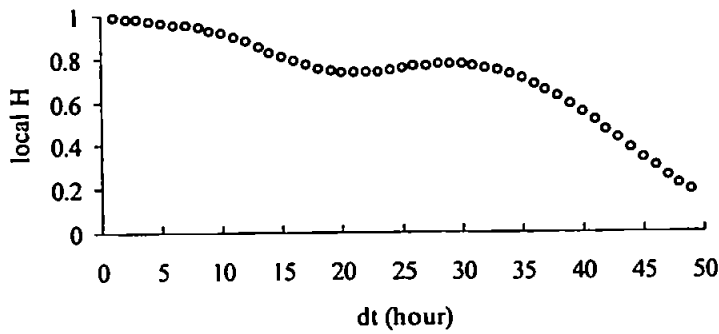


Figure 6.13 Local Hurst exponent at the top of the swash zone (Location 4-7)

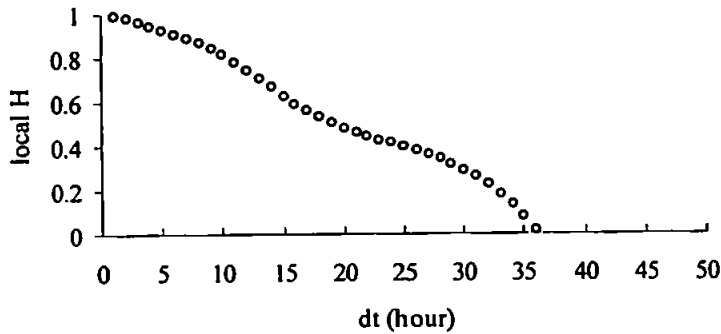


Figure 6.14 Local Hurst exponent at the centre of the swash zone (Location 10-3)

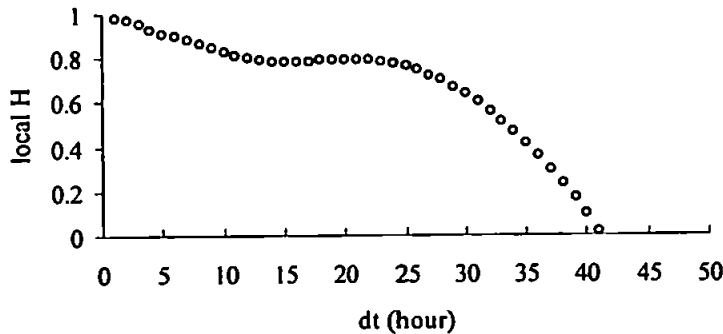


Figure 6.15 Local Hurst exponent at the bottom of the swash zone (Location 14-5)

Bed elevation time series deriving from the numerical simulations show again a very poor fit to a Gaussian distribution. Simulations of different length and with different forcing conditions have been run. Results do not seem to be sensitive to the input (forcing) conditions. On the other hand, for long time series and for certain locations not subject to relevant changes (for example a horn remaining in a fixed position for the whole simulation), the problem of non-stationarity of the means occurs and no fractal behaviour can be detected (global Hurst exponent higher than 1). Results obtained for the simulation

described in section 6.5, when applying the growth of variance and growth of range technique for the evaluation of the global Hurst exponent, indicate mean values of 0.85 and 0.81 for the growth of variance and growth of range respectively (450 time series have been considered). Standard deviations are in both cases below 0.1 and the maximum difference (absolute value) between Hurst values calculated with the two techniques over a single time series is around 0.15. Such results (shown in Figures 6.16, 6.17, 6.18, 6.19), confirmed by the analysis of time series at other locations and for other simulations, indicate again the possibility of fractal behaviour and indicate persistency of the process. Examples of the results obtained through the local Hurst exponent technique are shown in 6.20, 6.21. As for the field time series, H_{loc} provides a better understanding for the physical processes occurring and the time-scaling region at which they happen. In fact, Figure 6.20 clearly shows that, at the bottom of the swash zone, in an area where the random element in the forcing is still very strong (the topography has not the possibility to influence the particle motion), fractal behaviour can be detected at different time scales ($1 < dt < 20$, $90 < dt < 125$, $180 < dt < 200$). On the other hand, well inside the swash zone (Figure 6.21) the effect of the developing topography is much more important in controlling the behaviour and the possibility of a fractal process is detected only at very small time intervals ($dt < 30$).

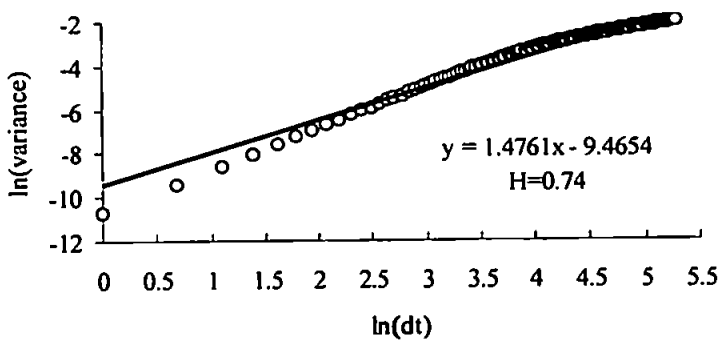


Figure 6.16 Growth of variance for a model simulation (bottom of the swash zone)

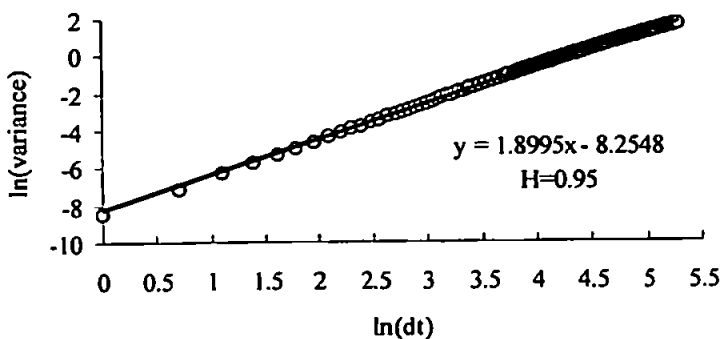


Figure 6.17 Growth of variance for a model simulation (inside the swash zone)

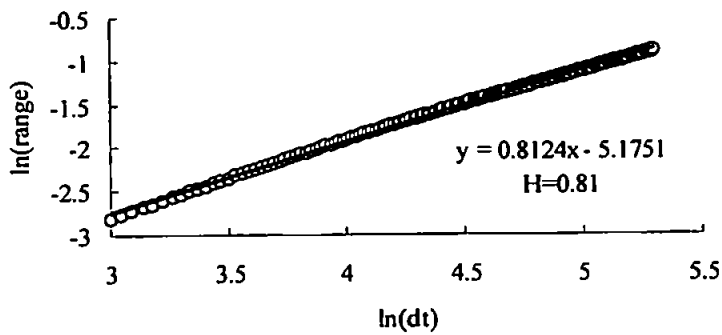


Figure 6.18 Growth of range for a model simulation (bottom of the swash zone)

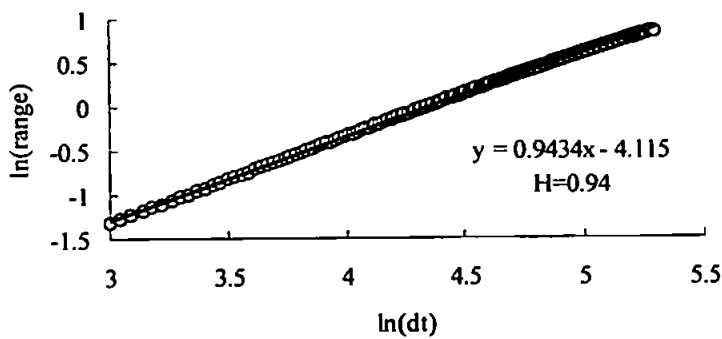


Figure 6.19 Growth of range for a model simulation (inside the swash zone)

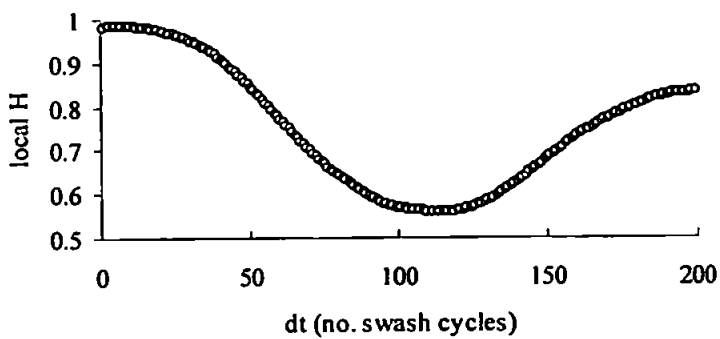


Figure 6.20 Local Hurst exponent for a model simulation (bottom of the swash zone)

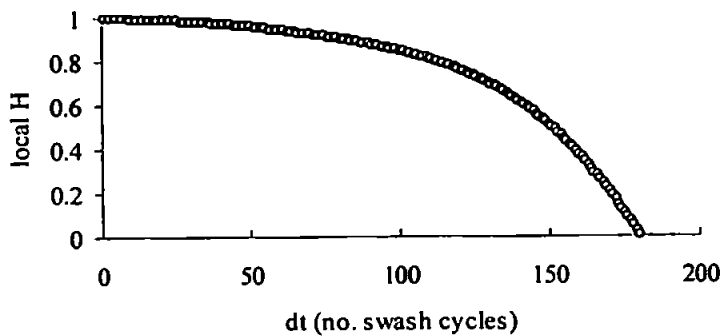


Figure 6.21 Local Hurst exponent for a model simulation (inside the swash zone)

6.6 Discussion

Before a comparison between the field measurements and the model data can be made, it is necessary to raise some relevant points concerning the fractal approach including its sensitivity, strength and shortcomings. First of all, it is important to underline that this technique is probably the only one available for the analysis of “short” time series (of the order of 100 measurements). Still, even longer time series can be not entirely representative of the physical process and the indication of fractal distribution may be derived from one of the various sources of error previously described rather than being a property of the system. For example, the indication given by the global Hurst exponent can be biased by the use of a logarithm plot and, in the case of the growth of range, by the evaluation of a parameter (H) whose formulation is characterised by an intrinsic monotonic increase with the time interval. For this reason it is important to couple the indication given by the global Hurst exponent with the more efficient local Hurst coefficient that also provides a measure of the time scaling region. The use of separate time series also allows for a statistically more reliable parameter although choosing locations which are too close may result in similar value of H only because time series are measuring exactly the same process.

The biggest uncertainty of this analysis is still given by the necessity of satisfying the hypothesis of Gaussian distribution for the data of each time series. As previously stated, there is no agreement on such a hypothesis that in this study has not been satisfied by both the field measurements and the numerical model results. For this reason, it is probably better to consider the results of this analysis as an indication of the system’s response to the (hydrodynamic) forcing and of the importance of non-linearities without implications for fractal or chaotic behaviour. Such indication, and its time scale, is obviously measured with much more accuracy by the local Hurst exponent rather than by the global Hurst

exponent. The hypothesis of chaotic or fractal behaviour in the swash region is probably a conclusion that cannot be fully demonstrated (at least with the data available) but the fact that self-organising processes are relevant, at certain time scales, is still strongly indicated.

The use of non-linear analysis, like the fractal approach, for comparing field measurements and model data provides useful results. Such comparison can be made only on a qualitative basis as recreating the forcing conditions observed in the field is nearly an impossible task. But this analysis provides more information than a mere correspondence between cusp spacing for a defined swash excursion. In fact, by comparing the results given by the measure of the local Hurst exponent inside the swash zone (Figure 6.14 and 6.21) it is clear that, if the forcing is dominant (be it due to the topography controlling the flow circulation or to the hydrodynamic conditions) the role of self-organisation is negligible. Self-organisation is instead important at locations where the forcing conditions are less effective (Figure 6.15 and Figure 6.20).

Chapter 7: Conclusions and future directions

The possibility that commonly observed morphological patterns in the nearshore region are the result of free behaviour rather than being related to a template in the hydrodynamic forcing conditions has been investigated. Current research follows two main approaches in order to model non-linear dynamical systems (like the coastal one): stability analysis and cellular automata. Such approaches have already been proven to successfully describe the appearance and, in some cases, the evolution of morphological patterns at different scales (from ripples to sand ridges). In this work the two different techniques have been considered in order to simulate pattern formation in the surf and swash zone respectively.

The concept of linear stability analysis has been considered for the simulation of pattern formation in the surf zone. The model (MORFO13) used for the solution of the governing equations and of the eigenproblem resulting from assuming a perturbation of the basic state has been developed by Prof. Albert Falqués and in this study further developments have been introduced for sediment transport parameterisation. Nearshore patterns arise because, in a saturated surf zone, topographic disturbances can cause a perturbation in the radiation stress of the incoming waves. Such perturbations drive cellular flows that result in the growth of bedforms. The use of different cross-shore stirring functions for the suspended sediment transport parameterisation seems to play a key role in the formation of large-scale bedforms. The use of a stirring function increasing with water depth until the breaking line results in the formation of a crescentic bar pattern. On the other hand, if the stirring function decreases towards the breaking point or is constant throughout the surf zone, then a giant cusp pattern is observed. The two different distributions of suspended sediment, and so of the stirring function, have already been observed in the field. The off-shore decreasing distribution refers to low wave conditions while constant or off-shore increasing distributions are more likely to happen under high wave conditions, when long-period motions become significant.

Such results, obtained by linearising the governing equations, will need to be tested, in particular for the sediment transport parameterisation, with field measurements. Other features of the model might be improved so that some of the restrictive hypotheses in the hydrodynamics can be removed. For example the use of a regular incoming wave field and of a fixed breaking point could have a significant effect and alter the growth rates of the patterns. Introducing wave refraction and a non-linear relationship between flow and

sediment transport are necessary steps in order to study the finite amplitude development of such features.

The modelling of the swash zone and the formation of beach cusps has been considered by developing an original cellular automata model based on the work by Werner and Fink (1993). Here it was chosen to model beach cusp formation and development because for such features a purely hydrodynamic instability approach capable of explaining their formation already exists. The hydrodynamic approach refers to standing edge waves as an external forcing with beach cusps being a reflection of the sediment moved by such forcing. The hypothesis tested through the numerical model herein developed is that beach cusps form because of the interaction between sediment and flow. Model simulations show that beach cusps effectively develop because of feedback processes between flow and topography. The physical process allowing for the formation and development of the features is a combination of positive and negative feedback. Positive feedback is induced through the non-linear relationship between sediment transport and flow that enhances the growth of high areas and deepens the low ones. The topography then develops a favourite wavelength that is proportional to the swash excursion. A sensitivity analysis of the model behaviour indicated that only the sediment transport parameterisation can affect the final cusp spacing while the other parameters only influence the rate at which cusps develop. In agreement with field observations, the model suggests that cusps can form only under a narrow banded normal incident wave field, and can be destroyed by the presence of waves obliquely approaching the shore (angles bigger than 10°). Simulations performed by changing the random seed in the initial input, indicate high variability in the growth rates and, in general, a very dynamical system evolving even at long time scales. The influence of a non-planar topography has also been investigated. The importance and strength of the self-organisation mechanism is again shown and the pre-existing features, unless so prominent as to completely drive the flow circulation, are wiped out allowing for cusp formation. Specific fieldwork, combining flow and sediment transport measurements in the swash zone during cusp formation, is needed in order to ratify some of these results. On the other hand, it is evident that the model herein developed can be still improved by introducing other features (infiltration, exfiltration, friction, refraction) that would allow for more realistic simulations and possibly for a link with more traditional approaches.

The use of the existing field and laboratory data proved that, apart from the standing edge wave theory and the self-organisation approach, none of the other mechanisms proposed in the literature are capable of explaining the mechanism responsible for beach cusp

formation. Furthermore, if the possibility that swash saturates is accepted (evidence is given analytically and through the use of field and laboratory experiments), cusp spacing prediction through the subharmonic standing edge wave model and the self-organisation approach are indistinguishable. The possibility of coexistence of the two models has been investigated by running a series of simulations of the self-organisation model with a standing edge wave (subharmonic or synchronous) forcing. Results indicate the possibility of coexistence of the two models in the case of incoming standing edge waves characterised by a wavelength similar to that suggested by the self-organisation approach. As a result, the only conclusion that can be drawn is that the formation of beach cusps is the result of an instability process and that such instability can be purely hydrodynamic or the result of a sediment-flow interaction. In order to discern between the two hypotheses more field tests are required. Interesting results could be given by an experiment on the same lines as the one conducted by Sato et al. (1992) where a cusped beach has been flattened and the subsequent cusp reformation observed. Although the flattening of the beach is a difficult task, in this way it would be possible to adequately place an alongshore array of instruments (in correspondence to previous horns and embayments which should reflect nodes and antinodes) and carefully monitor the presence and wavelength of standing edge wave motions.

The formation of features in the nearshore region as the result of “free” behaviour has been investigated by using two models that are conceptually different, so that a brief comparison can be made. The stability approach offers the advantage of a more traditional modelling technique in that the relevance of each single term (friction, viscosity, etc.) in the growth of the bedforms can be evaluated. On the other hand, such an approach is computationally heavy especially if a non-linear analysis is required. The self-organisation approach is much simpler to implement and allows for the analysis of the non-linear evolution of the features. Another important aspect that differentiates the two approaches is that the linear stability analysis results in the determination of a single growth rate of the preferred wavelength while the self-organisation model questions the possibility of a unique growth rate and indicates its dependency on the initial input randomness.

Detailed comparisons between available field measurements of beach cusp formation and development (Masselink et al., 1997) and the self-organisation model are possible only on a qualitative basis and the use of non-linear techniques for data analysis is suggested here. Most of the techniques have been developed only in recent years and their application usually requires very long time series. For this reason, other than a simple comparison

between measured and modelled cusp spacing under certain swash conditions, a fractal analysis of time series of bed elevations obtained through field measurements and model results has been performed. Different techniques have been used in order to evaluate the Hurst exponent, which is a statistical measure of the data distribution that can be related to the fractal dimension. Some of these techniques, the ones related to the evaluation of the global Hurst exponent, do not seem to provide useful information as they describe with a single parameter the data behaviour over the whole time-scale considered. On the other hand, the local Hurst exponent provides more interesting results as it relates a measure of the possibility of fractal behaviour, and of the importance of non-linearities, to the “local” time-scale considered. Time series obtained from model simulations or field measurements are in qualitative agreement as they both indicate the possibility of self-organising behaviour at locations and time-scales where the forcing conditions are clearly less dominant. A shortcoming of this analysis is that it has been performed over series of data that do not follow a Gaussian distribution, but other authors (Southgate and Beltran, 1996; Southgate and Möller, 1999) have considered this hypothesis of secondary importance. More field testing is required in order to provide longer time series. This would allow for the possibility of studying non-linear processes, like beach cusp formation and development, through these innovative data analysis techniques, and would allow for comparisons with numerical models.

A further evolution of the nearshore modelling presented herein could be given by the development of a self-organisation model for the hydrodynamics in the swash zone. The possibility that subharmonic motions can develop inside the swash zone without being the reflection of incident wave patterns or the result of bathymetric variations in the alongshore direction needs to be explored. A similar study has been recently proposed for the surf zone and indicates in the non-linear interaction between incoming waves and longshore current the initial mechanism for the formation of rip channels (Murray and Reydellet, 1999). The intriguing possibility that the interaction between incoming and outgoing swash can result in an “organised” longshore flow structure needs to be investigated, as well as its implications for the formation of periodic features in the swash region.

References

- Allen, J.R.L., 1984. *Sedimentary structures*. Elsevier.
- Allen, J.R., Putsy, N.P., Bauer, B.O., and Carter, R.W.G., 1996. A field data assessment of contemporary models of beach cusp formation. *Journal of Coastal Research*, **12**(3): 622-629.
- Anderson, R.S., 1990. Eolian ripples as examples of self-organization in geomorphological systems, *Earth-Science Reviews*, **29**: 77-96.
- Anderson, R.S., and Bunas, K.L., 1993. Grain size segregation and stratigraphy in aeolian ripples modelled with a cellular automaton. *Nature*, **365**: 740-743.
- Ann, H., 1979. *An experimental study on the formation of rhythmic topography on sandy beaches*. Unpublished M.Sc. Thesis, Department of Civil Engineering, Tokyo University (cited in Takeda and Sunamura, 1983).
- Antia, E.E., 1987. Preliminary field observations on beach cusp formation and characteristics on tidally and morphodynamically distinct beaches on the Nigerian coast. *Marine Geology*, **78**: 23-33.
- Antia, E.E., 1989. Beach cusps and beach dynamics: a quantitative field appraisal. *Coastal Engineering*, **13**: 263-272.
- Antsyferpv, S., and Kos'yan, R., 1990. Study of suspended sediment distribution in the coastal zone. *Coastal Engineering*, **14**: 147-172.
- Babovic, V., and Abbott, M.B., 1997a. The evolution of equations from hydraulic data. Part I: Theory. *Journal of Hydraulic Research*, **35**(3): 397-410.
- Babovic, V., and Abbott, M.B., 1997b. The evolution of equations from hydraulic data. Part II: Application. *Journal of Hydraulic Research*, **35**(3): 411-430.
- Bagnold, R.A., 1940. Beach formation by waves: some model experiments in a wave tank. *Journal of the Institution of Civil Engineers*, **15**: 27-52.
- Bagnold, R.A., 1963. An approach to the sediment transport problem from general physics. *U.S. Geol. Survey*, Washington D.C., Prof. Paper 422-1, 37 pp.
- Bailard, J.A., 1981. An energetics total load sediment transport model for a plane sloping beach. *Journal of Geophysical Research*, **86**: 10938-10954.
- Bailard, J.A., and Inman, D.L., 1981. An energetics bedload model for a plane sloping beach: local transport. *Journal of Geophysical Research*, **86**: 2035-2043.
- Bak, P., 1997. *How nature works: the science of self-organised criticality*. Oxford University Press.
- Baldock, T.E., and Holmes, P., 1999. Simulation and prediction of swash oscillations on a steep beach, *Coastal Engineering*, **36**(3): 219-242.
- Ball, F.K., 1967. Edge waves in ocean finite depth. *Deep sea research*, **14**: 79-88.

- Barcilon, A.I., and Lau, J.P., 1973. A model for the formation of transverse bars. *Journal of Geophysical Research*, **78**: 2656-2664.
- Battjes, J.A., 1975. Surf similarity. *Proceedings of the 14th Conference on Coastal Engineering*, ASCE, New York, 466-480.
- Blondeaux, P., 1990. Sand ripples under sea waves. Part 1. Ripple formation. *Journal of Fluid Mechanics*, **218**: 1-17.
- Bowen, A.J., 1969. Rip currents 1: Theoretical investigations. *Journal of Geophysical Research*, **74**: 5467-5478.
- Bowen, A.J., 1972. Edge waves and the littoral environment. *Proceedings of the 13th Conference of Coastal Engineers*, ASCE, 1313-1320.
- Bowen, A.J., 1980. Simple models of nearshore sedimentation; beach profiles and longshore bars. In *The Coastline of Canada*, S.B. McCann editor; Geological Survey of Canada, Paper 80-10: 1-11.
- Bowen, A.J., and Guza, R.T., 1978. Edge waves and surf beat. *Journal of Geophysical Research*, **83**(C4): 1913-1920.
- Bowen, A.J., and Holman, R.A., 1989. Shear instabilities of the mean longshore current 1. Theory. *Journal of Geophysical Research*, **94**: 18023-18030.
- Bowen, A.J., and Inman, D.L., 1969. Rip currents 2: Laboratory and field observations. *Journal of Geophysical Research*, **74**: 5479-5490.
- Bowen, A.J., and Inman, D.L., 1971. Edge waves and crescentic bars. *Journal of Geophysical Research*, **76**: 8662-8671.
- Calvete, D., 1999. *Morphological stability models: shoreface-connected sand ridges*. Ph.D. Thesis. Universitat Politècnica de Catalunya, Barcelona, Spain.
- Chafetz, H.S., and Kocurek, G., 1981. Coarsening-upward sequences in beach cusp accumulations. *Journal of Sedimentary Petrology*, **51**: 1157-1161.
- Chen, Y., and Guza, R.T., 1998. Resonant scattering of edge waves by longshore periodic topography. *Journal of Fluid Mechanics*, **369**: 91-123.
- Chen, Y., and Guza, R.T., 1999. Resonant scattering of edge waves by longshore periodic topography: finite beach slope. *Journal of Fluid Mechanics*, **387**: 255-269.
- Christensen, E., Deigard, R., and Fredsøe, J., 1995. Sea bed stability on a long straight coast. *Proceedings of the 24th Int. Conf. Coastal Engineering*, ASCE, 1865-1879.
- Cloud, P.E., 1966. Beach cusps: response to Plateau's rule? *Science*, **154**: 890-891.
- Coco, G., O'Hare, T.J., and Huntley, D.A., 1999. Beach cusps: a comparison of data and theories for their formation. *Journal of Coastal Research*, **15**(3): 741-749.
- Cowell, P.J., and Thom, B.G., 1995. Morphodynamics of coastal evolution. In R.W.G. Carter and C.D. Woodruffe, *Coastal evolution*, Cambridge University Press, 33-86.

- Darbyshire, J., 1977. An investigation on beach cusps in Hell's Mouth Bay. In Angel M., *A voyage of discovery*, Pergamon Press Oxford & New York.
- Darlymple, R.A., and Lanan, G.A., 1976. Beach cusps formed by intersecting waves. *Geological Society of America Bulletin*, 87, 57-60.
- Darras, M., 1987. List of sea state parameters. *Supplement to bulletin n.52*, IAHR.
- Davidson, M.A., Kingston, K.S., and Huntley, D.A., 1999. A new parametric solution for directional wave analysis in reflective wave fields. *Journal of Waterways, Port, Coastal and Ocean Engineering*, in press.
- De Vriend, H.J., 1991. Mathematical modelling and large-scale coastal behaviour, Part 1: Physical Processes. *Journal of Hydraulic Research*, 29(6): 727- 740.
- Dean, R.G., and Maurmeyer, E.M., 1980. Cusps at Point Reyes and Drakes Bay beaches, California. *Proceedings of the 13th International Conference on Coastal Engineering*, ASCE, New York, 863-884.
- Deigaard, R., Drønen, N., Fredsøe, J. Jensen, J.H., Jørgesen, M.P., 1999. A morphological stability analysis for a long straight barred coast. *Coastal Engineering*, 36: 171-195.
- Dolan, R., 1971. Coastal landforms: crescentic and rhythmic. *Geological Society of America Bull.*, 82: 177-180.
- Dolan, R., and Ferm, J.C., 1968. Crescentic landforms along the Atlantic coast of the United States. *Science*, 159: 627-629.
- Dubois, R.N., 1978. Beach topography and beach cusps. *Geological Society of America Bulletin*, 89: 1133-1139.
- Dubois, R.N., 1981. Foreshore topography, tides, and beach cusps, Delaware. *Geological Society of America Bulletin*, 92: 132-138.
- Dyer, K.R., 1977. *Estuarine oceanography*. McGraw Hill Yearbook Science and Technology, McGraw Hill Book Company.
- Eckart, C., 1951. Surface waves in water of variable depth. *Wave Rep.* 100, S10 Ref. 51-12, 99 pp., Univ. Calif. Scripps Inst. Oceanogr.
- Falqués, A., 1991. A note on the Barcelon and Lau model for transverse bars. *Rev. de Geofísica*, 47: 191-195.
- Falqués, A., Montoto, A., and Iranzo, V., 1996. Bed-flow instability of the longshore current. *Continental Shelf Research*, 16(15): 1927-1964.
- Falqués, A., Montoto, A., and Iranzo, V., 1997. Coastal morphodynamic instabilities. *Proceedings of the 25th Int. Conf. Coastal Engineering*, ASCE, vol.3, 3560-3573.
- Falqués, A., Ribas, F., Larroudé, P., and Montoto, A., 1999. Nearshore oblique bars. Modelling versus observations at the Truc Vert Beach. *Proceedings of River, Coastal and Estuarine Morphodynamics*, I.A.H.R. Symposium, Genova, Italy, 207-216.

- Forbes, D.L., Orford, J.D., Carter, R.W.G., Shaw, J., and Jennings, S.C., 1995. Morphodynamic evolution, self-organisation, and instability of coarse-clastic barriers on paraglacial coasts. *Marine Geology*, **126**: 63-85.
- Forrest, S.B., and Haff, P.K., 1992. Mechanics of wind ripple stratigraphy. *Science*, **255**: 1240-1243.
- Fredsøe, J., 1974. On the developments of dunes on erodible channels. *Journal of Fluid Mechanics*, **64**: 1-16.
- Fredsøe, J., and Deigaard, R., 1992. *Mechanics of coastal sediment transport*. World Scientific.
- Frisch, U., Hasslacher, B., and Pomeau Y., 1986. Lattice-gas automata for the Navier-Stokes equation. *Physical Review Letters*, **56**(14): 358-361.
- Frison, T.W., Abarbanel, H.D.I., Earle, M.D., Schultz, J.R., and Scherer, W.D., 1999. Chaos and predictability in ocean water levels. *Journal of Geophysical Research*, **104**(C4): 7935-7951.
- Galvin, C.J. Jr., 1968. Breaker type classification on three laboratory beaches. *Journal of Geophysical Research*, **73**(12): 3651-3659.
- Gorycki, M.A., 1973. Sheetflood structure: mechanism of beach cusp formation and related phenomena. *Journal of Geology*, **81**: 109-117.
- Guza, R.T., and Bowen, A.J., 1975. The resonant instabilities of long waves obliquely incident on a beach. *Journal of Geophysical Research*, **80**: 4529-4534.
- Guza, R.T., and Bowen, A.J., 1976. Finite amplitude edge waves. *Journal of Marine Research*, **34**: 269-293.
- Guza, R.T. and Bowen, A.J., 1976. Resonant interactions for waves breaking on a beach. *Proceedings of the 15th International Conference on Coastal Engineering*, ASCE New York, 560-579.
- Guza, R.T. and Bowen, A.J., 1981. On the amplitude of beach cusps. *Journal of Geophysical Research*, **80**(21): 4125-4132.
- Guza, R.T. and Davis, R.E., 1974. Excitation of edge waves by waves incident on a beach. *Journal of Geophysical Research*, **86**: 1285-1291.
- Guza, R.T. and Inman, D.L., 1975. Edge waves and beach cusps. *Journal of Geophysical Research*, **80**(21): 2997-3012.
- Guza, R.T. and Thornton, E.B., 1982. Swash oscillations on a natural beach. *Journal of Geophysical Research*, **87**: 483-491.
- Hallet, B., 1990. Spatial self-organization in geomorphology: from periodic bedforms and patterned ground to scale-invariant topography. *Earth-Science Reviews*, **29**: 57-75.

- Hastings, H.M., and Sugihara, G., 1993. *Fractals: a user's guide for the natural sciences*. Oxford University Press.
- Hino, M., 1975. Theory formation of rip-current and cuspidal forms. *Proceedings 14th Conference of Coastal Engineers*, ASCE, 901-919.
- Holland, K.T., 1998. Beach cusp formation and spacings at Duck, USA. *Continental Shelf Research*, **18**: 1081-1098.
- Holland, K.T. and Holman, R.A., 1996. Field observations of beach cusps and swash motions. *Marine Geology*, **134**: 77-93.
- Holland, K.T., Vincent, C.L., and Holman, R.A., 1999. Statistical characterisation of nearshore morphodynamic behavior. *Proceedings of Coastal Sediments '99*, Long Island, 2176-2189.
- Holman, R.A. and Bowen, A.J., 1979. Edge waves on complex beach profiles. *Journal of Geophysical Research*, **84**: 6339-6346.
- Holman, R.A. and Bowen, A.J., 1982. Bars, bumps, and holes: models for the generation of complex beach topography. *Journal of Geophysical Research*, **87**: 457-468.
- Horikawa, K. (Ed.), 1988. *Nearshore dynamics and coastal processes*. University of Tokio Press.
- Hsu, T.W., Ou, S.H., and Wang, S.K., 1994. On the prediction of beach changes by a new 2-D empirical eigenfunction model. *Coastal Engineering*, **23**: 255-270.
- Hulscher, S.J.M.H., 1996. Tidal-induced large-scale regular bed form patterns in a three-dimensional shallow water model. *Journal of Geophysical Research*, **101**(C9): 20727-20744.
- Hulscher, S.J.M.H., De Swart, H.E., and De Vriend, H.J, 1993. The generation of offshore tidal sand banks and sand waves. *Continental Shelf Research*, **13**(11): 1183-1204.
- Hunt, I.A., 1959. Design of seawalls and breakwaters. *Proc. Amer. Soc. Civil Eng.*, **85**: 123-152.
- Hunter, R.E., Clifton, H.E., and Phillips, R.L., 1979. Depositional processes, sedimentary structures, and predicted vertical sequences in barred nearshore systems, southern Oregon coast. *Journal of Sedimentary Petrology*, **49**(3): 711-726.
- Huntley, D.A., 1980. Edge waves in a crescentic bar system. In *The Coastline of Canada*, S.B. McCann editor; Geological Survey of Canada, Paper 80-10: 111-121.
- Huntley, D.A. and Bowen, A.J., 1973. Field observations of edge waves. *Nature*, **243**: 160-162.
- Huntley, D.A. and Bowen, A.J., 1979. Beach cusps and edge waves. *Proceedings of the 16th International Conference on Coastal Engineering*, ASCE New York, 1378-1393.

- Huntley, D.A., Davidson, M., Russell, P.E., Foote Y., and Hardisty, J., 1993. Long waves and sediment movement on beaches: recent observations and implications for modelling. *Journal of Coastal Research*, **15**: 215-229.
- Huntley, D.A., Guza, R.T., and Bowen, A.J., 1977. A universal form for shoreline run-up spectra? *Journal of Geophysical Research*, **82**(18): 2577-2581.
- Huthnance, J.M., 1982a. On one mechanism forming linear sand banks. *Estuarine, Coastal and Shelf Science*, **14**: 79-99.
- Huthnance, J.M., 1982b. On the formation of sand banks of finite extend. *Estuarine, Coastal and Shelf Science*, **15**: 277-299.
- Hwang, C., Tsai, L., Lin, P., and Tsai, C., 1996. Studies on the suspended concentration in the surf zone. *Proceedings of Coastal Engineering 1996*, ASCE: 4088-4097.
- Inman, D.L., and Guza, R.T., 1982. The origin of swash cusps on beaches. *Marine Geology*, **49**: 133-148.
- Iribarren, C.R., and Nogales, C., 1949. Protections des ports. *17th Int. Nav. Congr.*, Lisbon, Portugal, sect. 2, comm. 4: 31-80.
- Jaffe, B.E., and Rubin, D.M., 1996. Using nonlinear forecasting to learn the magnitude and phasing of time-varying sediment suspension in the surf zone. *Journal of Geophysical Research*, **101**(C6): 14283-14296.
- Kaneko, A., 1985. Formation of beach cusps in a wave tank. *Coastal Engineering*, **9**: 81-98.
- King, C.A.M., 1972. *Beaches and Coasts*. London: Arnold, 570p.
- Kingston, K.S., and Davidson, M.A., 1999. Artificial neural network model of sand bar location for a Macro-Tidal Beach, Perranporth, U.K. *Proceedings of River, Coastal and Estuarine Morphodynamics*, I.A.H.R. Symposium, Genova, Italy, 227-236.
- Komar, P.D., 1971. Nearshore circulation and the formation of giant cusps. *Geological Society of America Bull.*, **82**: 2643-2650.
- Komar, P.D., 1973. Observations of beach cusps at Mono lake, California. *Geological Society of America Bulletin*, **84**: 3593-3600.
- Komar, P.D., 1998. *Beach processes and sedimentation* (second edition). Prentice Hall, Englewood Cliffs, N.J.
- Krumbein, W.C., 1947. Shore processes and beach characteristics. *Beach Erosion Board Technical Memorandum*, No.3. (cited in TAKEDA and SUNAMURA, 1983).
- Kuenen, P.H., 1948. The formation of beach cusps. *Journal of Geology*, **56**: 34-40.
- Landau, L.D., and Lifshitz, E.M., 1959. *Fluid mechanics. Vol.6 of Course of theoretical physics*. London. Pergamon Press.

- Landry, W., and Werner, B.T., 1994. Computer simulations of self-organized wind ripple patterns. *Physica (D)*, **77**: 238-260.
- Lippmann, T.C., and Holman, R.A., 1990. The spatial and temporal variability of sand bar morphology. *Journal of Geophysical Research*, **95(C7)**: 11575-11590.
- Longuet-Higgins, M.S. and Parkin, D.W., 1962. Sea waves and beach cusps. *Geographical Journal*, **128**: 194-201.
- McKenzie P., 1958. Rip-current systems. *Journal of Geology*, **66(2)**: 103-113.
- Mandelbrot, B.B., 1982. *The fractal geometry of nature*. Freeman, San Francisco.
- Masselink, G., 1999. Alongshore variation in beach cusp morphology in a coastal embayment. *Earth Surface Processes and Landforms*, **24(4)**: 335-348.
- Masselink, G., Hegge, B.J., and Pattiaratchi, C.B., 1997. Beach cusp morphodynamic. *Earth Surface Processes and Landforms*, **22**: 1139-1155.
- Masselink, G., and Pattiaratchi, C., 1998a. Morphodynamic impact of sea breeze activity on a beach with beach cusp morphology. *Journal of Coastal Research*, **14(2)**: 393-406.
- Masselink, G., and Pattiaratchi, C.B., 1998b. Morphological evolution of beach cusp morphology and associated swash circulation patterns. *Marine Geology*, **146**: 93-113.
- Mei, C.C., 1989. *The applied dynamics of ocean surface waves*. World Scientific.
- Miche, A., 1951. Exposés a l'action de la houle. *Ann. Ponts Chaussees*, **121**: 285-319.
- Miller, J.R., Miller, S.M.O., Torzynski, C.A., and Kochel, R.C., 1989. Beach cusp destruction, formation, and evolution during and subsequent to an extratropical storm, Duck, North Carolina. *Journal of Geology*, **97(6)**: 749-760.
- Mulrennan, M.E., 1992. Ridge and runnel beach morphodynamics: an example from the central east coast of Ireland. *Journal of Coastal Research*, **8(4)**: 906-918.
- Murray, A.B., and Paola, C., 1994. A cellular model of braided rivers. *Nature*, **371**: 54-57.
- Murray, A.B., and Reidellet, G., 1999. Rip currents in the absence of bathymetric forcing. *Proceedings of River, Coastal and Estuarine Morphodynamics*, I.A.H.R. Symposium, Genova, Italy, 405-413.
- Niederoda, A.W., and Tanner, W.F., 1970. Preliminary study on transverse bars. *Marine Geology*, **9**: 41-62.
- Nishimori, H., and Ouchi, N., 1993. Formation of ripple patterns and dunes by wind-blown sand. *Physical Review Letters*, **71(1)**: 197-200.
- Nolan, T.J., Kirk, R.M., and Shulmeister, J., 1999. Beach cusp morphology on sand and mixed sand and gravel beaches, South Island, New Zealand. *Marine Geology*, **157**: 185-198.

- North, C.P., and Halliwell, D.I., 1994. Bias in estimating fractal dimension with the rescaled range (R/S) technique. *Mathematical Geology*, 26(5): 531-555.
- Oltman-Shay, J., and Howd, P.A., 1993. Edge waves on nonplanar bathymetry and alongshore currents: a model and data comparison. *Journal of Geophysical Research*, 98: 2495- 2507.
- Orford, J.D., and Carter, R.W.G., 1984. Mechanism to account for the longshore spacing of overwash throats on a coarse clastic barrier in southeast Ireland. *Marine Geology*, 56: 207-226.
- Parker, G., 1976. On the cause and the characteristic scales of meandering and braiding in rivers. *Journal of Fluid Mechanics*, 76: 457-480.
- Phillips, J.D., 1992. Nonlinear dynamical systems in geomorphology: revolution or evolution. *Geomorphology*, 5: 219-229.
- Plateau, J., 1864. *Ann. Rept. Board Regents Smithsonian Inst. 1863*: 207-285.
- Rayleigh, Lord, 1892. On the instability of cylindrical fluid surfaces. *Phil. Mag.* 34: 177-180.
- Rausch, M., Nielsen, J. and Nielsen, N., 1993. Variations of spacings between beach cusps discussed in relation to edge wave theory. *Geografisk Tidsskrift*, 93: 49-55.
- Reynolds, O., 1883. An experimental investigation of the circumstances which determine whether the motion of water shall be direct or sinuous, and of the law of resistance in parallel channels. *Phil. Trans. Roy. Soc.*, 174: 935-982.
- Richards, K.J., 1980. The formation of ripples and dunes on an erodible bed. *Journal of Fluid Mechanics*, 99: 597-618.
- Russell, P.E., 1993. Mechanisms for beach erosion during storms. *Continental Shelf Research*, 13(11): 1243-1266.
- Russell, R.J., and McIntire, W.G., 1965. Beach cusps. *Geological Society of America Bull.*, 76: 307-320.
- Sallenger, A.H., 1979. Beach cusp formation. *Marine Geology*, 29: 23-37.
- Sasaki, T., Horikawa, K., and Hotta, S., 1976. Nearshore currents on a gently sloping beach. *Proceedings of the 15th Int. Conf. Coastal Engineering*, ASCE: 626-644.
- Sato, M., Kuroki, K., and Shinohaura, T., 1992. A field experiment on the formation of beach cusps. *Proceedings of Coastal Engineering 1992*, ASCE: 2205-2218.
- Schwartz, M.L., 1972. Theoretical approach to the origin of beach cusps. *Geological Society of America Bulletin*, 83: 1115-1116.
- Science, 1999. Insert on "Complex systems". *Science*, 284: 79-109.
- Seymour, R.J., and Aubrey, D.G., 1985. Rhythmic beach cusp formation: a conceptual synthesis. *Marine Geology*, 65: 289-304.

- Shepard, F.P., 1963. *Submarine geology*. New York, Harper and Row, 557 p.
- Sherman, D.J., Orford, J.D., and Carter, R.W.G., 1993. Development of cusp-related, gravel size and shape facies at Malin Head, Ireland. *Sedimentology*, **40**: 1139-1152.
- Sleath, J.F.A., 1984. *Sea bed mechanics*. Wiley.
- Smith, D.D., and Dolan, R.G., 1960. Erosional development of beach cusps along the outer banks of North Carolina. *Geological Society of America Bull.*, **71**: 1979.
- Sonu, C.J., 1969. Collective movement of sediment in littoral environment. *Proceedings of the 11th Int. Conf. Coastal Engineering*, ASCE: 373-400.
- Southgate, H.N., 1995. The effects of wave chronology on medium and long term coastal morphology. *Coastal Engineering*, **26**: 251-270.
- Southgate, H.N., 1997. Non-linear methods of analysis for long-term beach and nearshore morphology. *Proceedings of the 27th IAHR Congress*, Theme A, San Francisco, USA.
- Southgate, H.N., and Beltran, L.M., 1995. Time series analysis of long-term beach level data from Lincolnshire, UK. *Proceedings of Coastal Dynamics '95*: 1006-1017.
- Southgate, H.N., and Beltran, L.M., 1996. Self-organisational processes in beach morphology. In: *Physics of Estuarine and Coastal Seas*, Ed. By J. Dronkers and M.B.A.M. Scheffers, p. 409-416.
- Southgate, H.N., and Möller, I., 1999. Fractal properties of coastal profile evolution at Duck, North Carolina, USA. submitted to the *Journal of Geophysical Research*.
- Southgate, H.N., Wijnberg, K.M., Larson, M., Capobianco, M., and Jansen, H., 1999. Analysis of field data of coastal morphological evolution over yearly and decadal timescales. Part 2: non-linear techniques, *Journal of Coastal Research* (accepted).
- Stølum, H.H., 1996. River meandering as a self-organization process. *Science*, **271**: 1710-1713.
- Sunamura, T., Mizuguchi, M., and Ann, H., 1977. An experiment on rhythmic pattern of sandy beaches using a small three dimensional wave tank. Report for Science Research Fund of Ministry of Education: "*Dynamical study on nearshore problems in relation to wave breaking*", Tokyo University (cited in TAKEDA and SUNAMURA, 1983).
- Takeda, I., and Sunamura, T., 1983. Formation and spacing of beach cusps. *Coastal Engineering in Japan*, **26**: 121-135.
- Takeda, I., Terasaki, T., and Sunamura, T., 1986. Formation and spacing of beach cusps on a laboratory beach. *Ann. Rep. Inst. Geosci.*, Univ. Tsukuba, **12**: 55-58

- Tamai, S., 1980. *A study on beach cusps and a prediction of beach change*. Doctoral Thesis, Department of Civil Engineering, Kyoto University (cited in Takeda and Sunamura, 1983).
- Tsai, C., and Lee T., 1999. Back-propagation neural network in tidal-level forecasting. *Journal of Waterways, Port, Coastal and Ocean Engineering*, 125(4): 195-202.
- Trowbridge, J.H., 1995. A mechanism for the formation and maintenance of shore-oblique sand ridges on storm-dominated shelves. *Journal of Geophysical Research*, 100(C8): 16071-16086.
- Ursell, F., 1952. Edge waves on a sloping beach. *Proceedings of the Royal Society of London*, series A, 214: 79-97.
- Van Dorn, W.G., 1978. Breaking invariants in shoaling waves. *Journal of Geophysical Research*, 83: 2981-2988.
- Van Rijn, L.C., 1993. *Principles of sediment transport in rivers, estuaries and coastal seas*. Aqua Publications, Amsterdam.
- Vittori, G., and Blondeaux, P., 1990. Sand ripples under sea waves. Part 2. Finite-amplitude development. *Journal of Fluid Mechanics*, 218: 19-39.
- Vittori, G., De Swart, H.E. and Blondeaux, P., 1999. Crescentic bedforms in the nearshore region. *Journal of Fluid Mechanics*, 381: 271-303.
- Werner, B.T., 1995. Eolian dunes: Computer simulations and attractor interpretation. *Geology*, 23: 1107-1110.
- Werner, B.T., 1999. Complexity in natural landform patterns. *Science*, 284: 102-104.
- Werner, B.T., and Fink, T.M., 1993. Beach cusps as self-organized patterns. *Science*, 260: 968-971.
- Werner, B.T., and Hallet, B., 1993. Numerical simulation of self-organized stone stripes. *Nature*, 361:142-145.
- Wijnberg, K.M., and Terwindt, H.J., 1995. Extracting decadal morphological behaviour from high-resolution, long-term bathymetric surveys along the Holland coast using eigenfunctions analysis. *Marine Geology*, 126: 301-330.
- Williams, A.T., 1973. The problem of beach cusp development. *Journal of Sedimentary Petrology*, 43: 857-866.
- Winant, C.D., Inman, D.L., and Nordstrom, C.E., 1975. Description of seasonal beach changes using empirical eigenfunctions. *Journal of Geophysical Research*, 80(15): 1979-1986.
- Wolfram, S., 1986. Cellular automaton fluids: Basic theory. *Journal of Statistical Physics*, 45(3/4): 471-526.

- Worrall, G.A., 1969. Present-day and subfossil beach cusps on the West African coast. *Journal of Geology*, 77: 484-487.
- Wright, L.D., and Thom, B.G., 1977. Coastal depositional landforms: a morphodynamic approach. *Progress in Physical Geography*, 1: 412-459.
- Zenkovitch, V.P., 1967. *Processes of coastal development*. Oliver & Boyd Ed., Edinburgh-London.